

BIGDOCS: AN OPEN AND PERMISSIVELY-LICENSED DATASET FOR TRAINING MULTIMODAL MODELS ON DOCUMENT AND CODE TASKS

Anonymous authors

Paper under double-blind review

ABSTRACT

Multimodal AI has the potential to significantly enhance document-understanding tasks, such as processing receipts, understanding workflows, extracting data from documents, and summarizing reports. Code generation tasks that require long-structured outputs can also be enhanced by multimodality. Despite this, their use in commercial applications is often limited due to limited access to training data and restrictive licensing, which hinders open access. To address these limitations, we introduce BigDocs-7.5M, a high-quality, open-access dataset comprising 7.5 million multimodal documents across 30 tasks. We use an efficient data curation process to ensure our data is high-quality and license-permissive. Our process emphasizes accountability, responsibility, and transparency through filtering rules, traceable metadata, and careful content analysis. Additionally, we introduce BigDocs-Bench, a benchmark suite with 10 novel tasks where we create datasets that reflect real-world use cases involving reasoning over Graphical User Interfaces (GUI) and code generation from images. Our experiments show that training with BigDocs-Bench improves average performance up to 25.8% over closed-source GPT-4o in document reasoning and structured output tasks such as Screenshot2HTML or Image2Latex generation. Finally, human evaluations showed a preference for outputs from models trained on BigDocs over GPT-4o. This suggests that BigDocs can help both academics and the open-source community utilize and improve AI tools to enhance multimodal capabilities and document reasoning.

1 INTRODUCTION

Visually-Rich Document (VRD) data containing text and structured elements (such as charts, infographics, diagrams, sketches, tables, etc.) are essential cues for users to efficiently understand complex information holistically. To facilitate this understanding, foundation models for VRDs must process these structured documents and subsequently extract key insights, identify patterns, and generate concise summaries and responses from user requests with reasoning (Landeghem et al., 2023; Zhu et al., 2022). Recent advances in multimodal AI (Yang et al., 2023; Team et al., 2024b) have demonstrated impressive capabilities, including generating functional web pages (Zheng et al., 2024), automating document understanding workflows (Wang et al., 2023b), and extracting detailed information from documents to produce comprehensive reports (Borchmann, 2024). However, the datasets used to train these models remain closed-source, with undisclosed details and restrictive licensing, which hampers their broader adoption in research and the advancement of open-source model development. In contrast, current open-source models and datasets (Chen et al., 2023; Liu et al., 2023b; 2024) primarily focus on basic document understanding tasks, such as optical character recognition (OCR), e.g., DocStruct4M (Hu et al., 2024), or basic question-answering and mathematical problems, e.g., Cambrian-7M (Tong et al., 2024). These efforts do not sufficiently address the complexity of processing intricate visual documents or generating long-structured outputs, such as JSON and HTML, which are valuable in real-world applications.

^aFirst Author Equal contribution.

^bSecond Author Equal contribution.

054
055
056
057
058
059
060
061
062
063
064
065
066
067
068
069
070
071
072
073
074
075
076
077
078
079
080
081
082
083
084
085
086
087
088
089
090
091
092
093
094
095
096
097
098
099
100
101
102
103
104
105
106
107

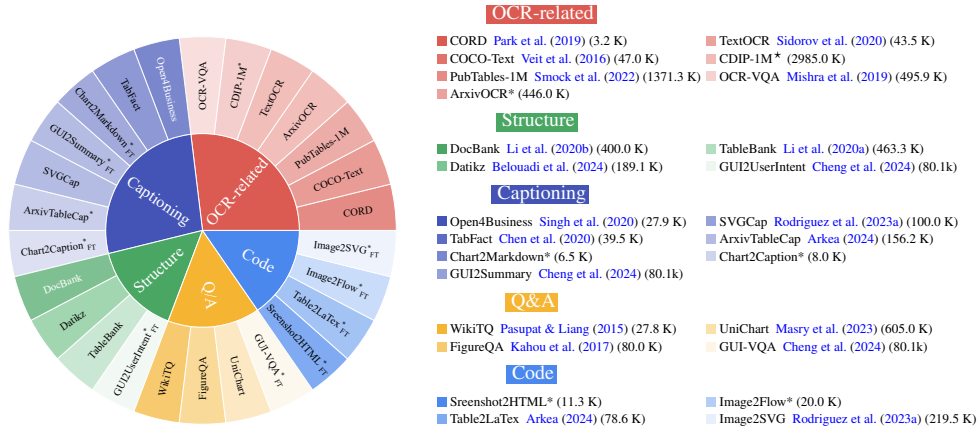


Figure 1: BigDocs: A Large-Scale Structured Continual Pretraining and Finetuning Dataset. The inner circle represents the distribution of BigDocs, detailing the categories. The outer circle displays the specific datasets compiled to form 7 million image-text pairs. Datasets with * denotes our contribution.

In this work, we present BigDocs, a large-scale and open *dataset*, *benchmark suite*, and *models* specifically designed for user-facing document-related tasks. BigDocs aims to bridge existing gaps by enabling open-source models to meet the rising demand for sophisticated document understanding technologies. Comprising 7.5 million image-text pairs, BigDocs is carefully curated to support three core areas: (1) **Document Information Extraction**, which includes enhanced OCR for diverse document types, named entity recognition, layout analysis, and table detection; (2) **Document Understanding**, covering semantic comprehension tasks such as document classification, question answering, and analysis of diagrams; and (3) **Document Creation and Manipulation**, which involves converting visual data into structured formats like HTML, LaTeX, and JSON.

Our survey of 133 existing datasets revealed that 80% of them (i.e., around 100 datasets) have either non-permissive licenses (Jaume et al., 2019; Štěpán Šimsa et al., 2023) or no clear licensing information (Chaudhry et al., 2019; kleister Charity, 2021), creating barriers to reuse and transparency. In response, BigDocs prioritize datasets with permissive licenses (e.g., CC-BY-4.0, MIT) and document-related information, ultimately retaining 16 fully accessible datasets. To further support accessibility, we developed the BigDocs Toolkit, which offers modular tools for data preprocessing, filtering, and consolidation. Additionally, we introduced a unified metadata framework to enhance dataset traceability (e.g., properties, sources, licenses), including detailed documentation of transformations applied by us to the original data. We also conduct a data contamination analysis on downstream tasks data, showing that BigDocs-7.5M has lower contamination rates than previous datasets.

To further advance document intelligence, BigDocs-Bench offers 10 novel downstream tasks, each with four splits: train, validation, test, and hidden test (with 329k training samples, 11k validation samples, 10k testing samples). These tasks focus on structured output generation, including code formats such as HTML, LaTeX, SVG, and Markdown. Our experimental results demonstrate that models trained on the BigDocs suite outperform those trained on existing datasets like DocStruct4M (Hu et al., 2024) on standard document benchmarks. Additionally, automatic and human evaluations on the novel tasks introduced in BigDocs-Bench highlight the advanced capabilities of these models in generating long-format, structured outputs. User evaluations reveal a preference for our models’ outputs 88% of the time over Phi3.5 Instruct and 63% over GPT-4.

Built with a commitment to accountability, responsibility, and transparency (ART) (Bommasani et al., 2023; Vogus & Llansóe, 2021), BigDocs will be open-sourced (upon acceptance), including datasets, models, and documentation to foster responsible AI development. In summary, BigDocs contributions include:

1. **BigDocs-7.5M**, a large-scale, license-permissive dataset designed for continual pretraining (further training from a pretrained foundation model checkpoint) and downstream finetuning (e.g., to follow instructions or task formats) of multimodal models on document-related tasks. It includes traceable *metadata* and curated licensing drawing from document-rich *multiple* data sources, ensuring full public accessibility.

2. **BigDocs-Bench**, a set of 10 new benchmarks, including test datasets as well as corresponding innovative evaluation metrics for multimodal models to generate long-structured code outputs from images, including formats such as HTML, LaTeX, Markdown, and SVG.
3. **BigDocs Toolkit**, unified tools supporting open-source efforts. These tools allow efficient data curation, filtering, formatting, and preparation for training models generating structured outputs.
4. **BigDocs Models**: We conduct extensive experiments using four state-of-the-art public models, demonstrating the advantages of training with BigDocs over alternative datasets and enabling the models to learn novel tasks through our dataset suite.

2 RELATED WORK

Multimodal Datasets. General-purpose vision-language datasets like COCO Caption (Chen et al., 2015) and SBUCaption (Ordonez et al., 2011) primarily feature photographic content, lacking visually-rich document (VRD) data (Sharma et al., 2018; Changpinyo et al., 2021). In contrast, our focus is on text-heavy datasets including PDFs, tables, and invoices (Veit et al., 2016; Mishra et al., 2019; Singh et al., 2021; Li et al., 2020b;a; Soboro, 2022), which are crucial for tasks like information extraction and parsing (Masry et al., 2022; Rodriguez et al., 2023c;b). While datasets like DocStruct4M (Hu et al., 2024) and Cambrian7M (Tong et al., 2024) partially address these needs, they often lack permissive licenses or are not open-source. Kosmos-2.5 (Lv et al., 2023) focuses on building a large document dataset; however, the authors did not make it public. BigDocs fills these gaps by providing 7.5M permissively licensed image-text pairs from 16 academic datasets and other open platforms, supporting diverse document understanding tasks.

Responsible Data and Licensing. Enterprise models like GPT-4 (OpenAI, 2023) and Claude (Anthropic, 2024) are often closed-source, lacking transparency in training data (Bommasani et al., 2024). Foundational works (Geburu et al., 2021; Bender & Friedman, 2018) emphasize the importance of open access and transparency in dataset documentation. Previous works promoting open-access such as StarCoder (Li et al., 2023), The Stack (Kocetkov et al., 2022), FineWeb (Penedo et al., 2024), and LLaMA (Dubey et al., 2024), have addressed this by releasing data or models for language models pretraining. Our work builds on these efforts by creating a curated, well-documented resource for open access (Laurençon et al., 2023), addressing licensing complexities ranging from permissive licenses (e.g., Apache 2.0, MIT (Hu et al., 2024; Gadre et al., 2023)) to restrictive ones like CC BY-SA (Foundation, 2024; Zhang et al., 2024) and CC BY-NC-SA (Wang et al., 2024b). Compound datasets, like Cambrian-7M (Tong et al., 2024), face mixed licensing issues, while some datasets, such as DocVQA (Mathew et al., 2021b), have different licenses for images and annotations. In developing BigDocs, we prioritized permissive licensing in data curation and contributed to new datasets that adhere to open-access principles, ensuring transparency at all stages of development.

Multimodal Document Understanding Models. Recent advancements have introduced several general-purpose multimodal models (Liu et al., 2023b;a; 2024; Bai et al., 2023b; Laurençon et al., 2024; Tong et al., 2024). For example, LLaVA (Liu et al., 2023b) integrates a vision encoder with a language model, with later versions enhancing reasoning and OCR capabilities (Liu et al., 2023a; 2024). Qwen2-VL (Bai et al., 2023b) processes images at native resolutions, while Phi 3.5 Vision (Abdin et al., 2024) offers a lightweight model for reasoning tasks. Specialized models for visually-rich documents, like DocOwl1.5 (Hu et al., 2024) and DocLLM (Wang et al., 2023a), have also gained traction, particularly for commercial applications. However, the datasets for training these models are often not publicly available or have restrictive licenses (Hu et al., 2024). Our work, BigDocs, addresses this by consolidating existing permissive datasets to support the development of reproducible, commercially viable document understanding models.

3 BIGDOCS-7.5M

BigDocs-7.5M is a large-scale, license-permissive, and carefully curated dataset for visual document understanding designed to train foundational models across various document types and tasks. It consolidates public datasets and newly crawled data with permissive licenses by preprocessing, cleaning, and filtering them into a unified collection of 7.5 million image-text pairs. All curated

162
163
164
165
166
167
168
169
170
171
172
173
174
175
176
177
178
179
180
181
182
183
184
185
186
187
188
189
190
191
192
193
194
195
196
197
198
199
200
201
202
203
204
205
206
207
208
209
210
211
212
213
214
215

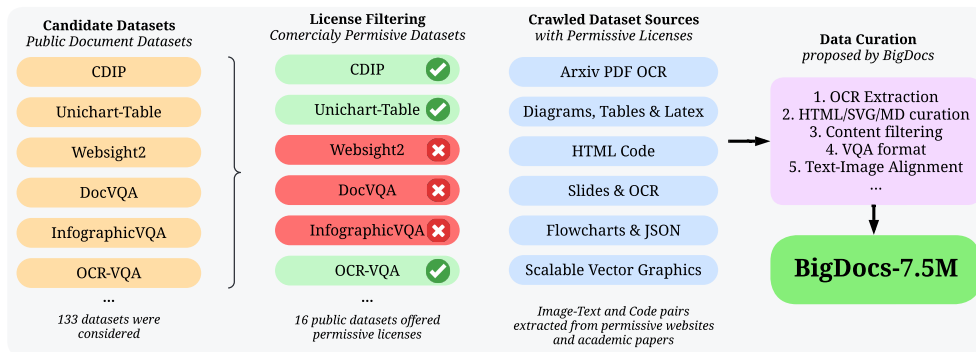


Figure 2: BigDocs-7.5M Dataset Curation. The figure illustrates the extraction, filtering, and curation process of BigDocs-7.5M, which emphasizes maintaining permissive licensing. To build BigDocs-7.5M, we first gather publicly-available vision-language datasets, particularly those centered on document analysis, and apply a rigorous filtering process. We then augment these datasets with our own crawled data. Finally, we standardize all samples and tasks into a unified format to produce BigDocs-7.5M.

datasets and related artifacts will be openly released to foster community collaboration (Bender & Friedman, 2018). The curation process is illustrated in Figure 2 and detailed below.

3.1 DATASET CURATION PROCESS

Existing Dataset Acquisition. The authors, along with domain experts and researchers, guided the collection strategy, assessing dataset relevance, quality, and diversity. We gathered 133 public vision-language datasets by searching academic repositories, open data platforms, and research papers. The collection focused on tasks like image captioning (Chen et al., 2015; Sidorov et al., 2020), OCR (Park et al., 2019; Smock et al., 2022), visual question answering (Mishra et al., 2019; Mathew et al., 2021b), scene-text recognition (Veit et al., 2016; Singh et al., 2021), and document layout analysis (Li et al., 2020a;b), resulting in a diverse multimodal dataset repository.

Datasheets for Datasets. During data acquisition, we compiled detailed datasheets for each dataset, capturing metadata such as ownership, status, size, references, source type, annotations, licensing, and specific observations. We filtered datasets based on licensing compatibility and relevance to our document-related tasks, then extended the datasheets of selected datasets for better categorization. This extension organized datasets by attributes such as medium type (e.g., digital, scanned), document type (e.g., articles, infographics), sourcing method, text type (e.g., computer-generated, handwritten), structure, language, timeframe, and licensing. For licensing, we documented both the image licenses and annotation licenses separately, as these often differed and impacted the overall permissiveness and usability of each dataset. This structured approach aligned datasets with specific use cases (e.g., OCR, structured parsing) and grouped them for pretraining, finetuning, and evaluation, ensuring effective integration into our visual document understanding pipeline.

License Filtering. A key criterion for dataset selection was ensuring permissive licenses (e.g., CC-BY, MIT, Apache 2, CC0) for both images and annotations, suitable for open access and commercial use (more details on various of licenses in Appendix A.7). Datasets with non-permissive licenses, like DVQA (Kafle et al., 2018) (CC-BY-NC 4.0) or DocILE (Štěpán Šimsa et al., 2023) (non-commercial use), or with no license information, like DeepForm (Svetlichnaya, 2020), were excluded. Ultimately, we prioritized permissive licenses for both text and images, resulting in 20% being kept, while 7.5% moderately restrictive and 72.5% non-permissive were discarded. Some included datasets still have images under less clear terms, such as “Fair Use” (e.g., OCR-VQA), documented in the metadata.

3.2 BIGDOCS TOOLKIT: DATA PREPROCESSING, FILTERING, AND CONSOLIDATION

The BigDocs Toolkit provides modular tools for preprocessing, filtering, contamination management, metadata management, and dataset loading. These components work in unison to streamline the integration of large-scale document datasets, ensuring quality and ease for efficient model training.

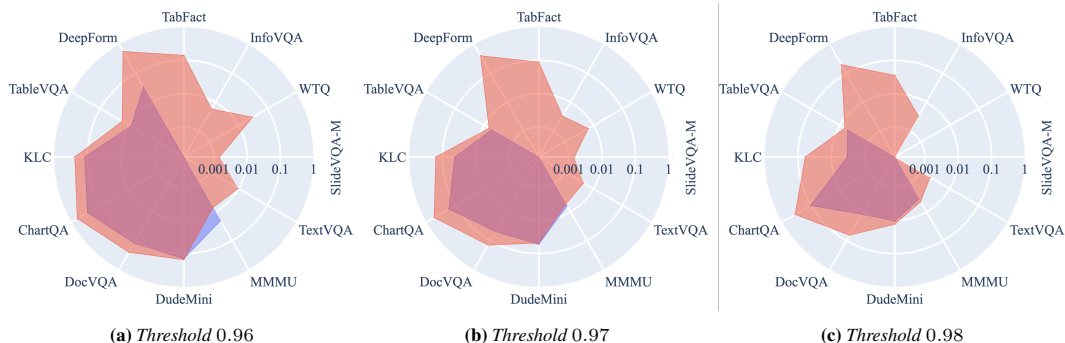


Figure 3: Assessing data contamination (smaller is better). The radial axis (log scale) indicates the proportion of images from the evaluation dataset that exhibit similarity to a training sample beyond a given threshold according to CLIP. Human evaluations indicate that most instances captured at a threshold of 0.98 are problematic, and most problematic samples are identified at a threshold of 0.96. Except for MMMU and DudeMini, BigDocs-7.5M (blue/darkred) is less contaminated compared to DocStruct4M (red).

🔧 Datamaker Module. The BigDocs Toolkit offers a modular framework for dataset curation, focusing on standardization, quality control, and metadata management. Its core *DataMaker* class acts as a template for handlers that extract annotations and convert raw data into a standardized format. A universal function processes tasks like OCR, VQA, and code generation, ensuring consistency. Bounding boxes are standardized, and corrupted samples are filtered. The Toolkit also generates metadata to enhance transparency, covering licensing and processing details (see Appendix A.9).

🔗 Unified Metadata Framework. We propose a unified metadata framework for BigDocs to ensure transparency and traceability. This framework thoroughly examines each raw data source, extracts fine-grained license information, and documents transformations applied to the data (e.g., different sources may have distinct licenses). Each data sample includes a metadata attribute detailing its properties, licenses, sources, and transformations (see Appendix A.9 for an example in Figure 13 and structure details). To our knowledge, this is the first systematic approach to track metadata for visually rich documents, advancing transparency in multimodal dataset curation.

Assessing Contamination. The presence of downstream evaluation data in training datasets can significantly affect the accurate measurement of a model’s effectiveness (Magar & Schwartz, 2022). BigDocs-7.5M contains samples from the training split of TabFact, WTQ, and TextVQA. However, any evaluation dataset may *a priori* overlap with training datasets through less direct dependencies. We favor a transparency strategy: search for overlaps and report what was found. Figure 3 gives an overview of the main observations on this front; see Appendix A.3 for additional details.











3.2.1 THE RESULTING BIGDOCS-7.5M

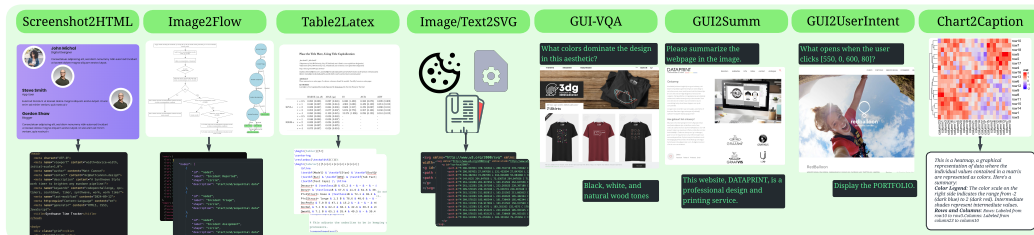
BigDocs-7.5M consists of 7.5M image-text pairs for training (4M unique images), 500k for validation (234k unique images), and 470k for testing (261k unique images). These data points aggregate four document-related tasks – OCR, structured parsing, captioning, and question-answering – enabling models to handle diverse document use cases (see Figure 1 and Appendix A and A.1 for more details). Low-quality data is filtered out, and metadata details our best-effort licensing compliance, making the dataset suitable for training foundational models, even in commercial applications.

4 BUILDING BIGDOCS-BENCH


In the previous section, we introduced BigDocs-7.5M, a unified and permissive dataset for training models on document understanding tasks. Building on this, we present BigDocs-Bench, a benchmark suite for evaluating downstream tasks that transform visual inputs into structured outputs, such as GUI2UserIntent (fine-grained reasoning), Image2Flow (structured output), Chart2Caption (understanding), and Screenshot2HTML (creative generation). BigDocs-Bench includes ten specialized tasks, with 329k training samples, 11k validation samples, 10k testing samples, and an additional hidden test set. Refer to Table 1 for task details and Figure 4 for examples.


Table 1: Statistics of the ten downstream tasks in BigDocs-Bench. GPT2 tokenizer is used to produce token numbers of both queries and annotations (if any), where the format is (avg \pm std).


Downstream Task	# Training	# Validation	# Public Test	# Hidden Test	# Text Tokens
 Screenshot2HTML	9,338	1,000	500	500	32,700 \pm 53,105
 Table2LaTeX	77,669	1,000	500	500	438 \pm 540
 Image2SVG	198,000	2,000	748	748	2,871 \pm 1,728
 Image2Flow _(GraphViz)	8,000	1,000	500	500	418 \pm 124
 Image2Flow _(JSON)	8,000	1,000	500	500	1,771 \pm 601
 Chart2Markdown	4,516	1,000	500	500	1,559 \pm 4,442
 Chart2Caption	5,412	1,300	650	650	94 \pm 49
 GUI2UserIntent	79,000	1,000	500	500	28 \pm 4
 GUI2Summary	79,000	1,000	500	500	132 \pm 25
 GUI-VQA	78,991	1,000	500	500	35 \pm 24


**Figure 4: 8 of the new tasks introduced in BigDocs-Bench.** These tasks share a focus on understanding the underlying structure of visually rich documents, with many also requiring generating lengthy outputs, such as SVG and HTML code. More tasks are shown in Figure 9 and 10.

4.1 BIGDOCS-BENCH TASKS SUITE

 **Screenshot2HTML:** We introduce a benchmark for Screenshot2HTML conversion, with 10,838 real-world website screenshots paired with HTML code (Appendix A.4.2). Curated from diverse, text-heavy websites in the FineWeb corpus (Penedo et al., 2024), it contrasts with synthetic GPT-generated sites from prior work (Laurençon et al., 2024b). Using Playwright, we retrieved, rendered, and filtered sites for accessibility, content, and licensing. External assets (e.g., CSS, fonts) were inlined, JavaScript removed, and images replaced to focus on structure. Screenshot2HTML evaluates the accuracy of HTML generated from webpage screenshots, emphasizing layout fidelity and semantic correctness.

 **Table2LaTeX:** We propose a benchmark for Table2LaTeX conversion, consisting of 79,669 table images paired with original LaTeX code and captions (details in Appendix A.4.3). The dataset was curated by crawling arXiv papers with permissible licenses and extracting tables from PDFs and TeX source files.^c Instead of relying on imperfect PDF detection, tables were rendered from the LaTeX .tex code to ensure accurate visuals. For instance, an image of a table is paired with its corresponding LaTeX snippet code and caption. This benchmark supports precise table extraction and LaTeX generation evaluation from academic documents.

 **Image2SVG:** We present a benchmark for Image2SVG conversion, curated from the existing SVG-Stack collection by StarVector (Rodriguez et al., 2023a) (details in Appendix A.4.4). The dataset includes 200k raster images paired with SVG code (e.g., flowchart image paired with SVG code replicating it) or descriptive text. We filtered for complex designs, using image entropy to exclude simple graphics, and ranked image-text pairs by CLIP Score (Hessel et al., 2022; Radford et al., 2019). This benchmark evaluates models on precise vector image reconstruction and scalability.

 **Image2Flow:** We introduce two benchmarks, Image2Flow_(GraphViz) and Image2Flow_(JSON), mapping flowchart images to JSON or GraphViz code (Appendix A.4.1). The dataset includes 10,000 flowchart samples with GraphViz files generated using LLaMA 3.1 (Dubey et al., 2024) and JSON files detailing nodes and connections. Random colors and styles were applied for diversity. Unlike FlowchartQA (Tannert et al., 2023), which focuses on QA over preprocessed flowcharts, this benchmark tests models' ability to extract structure from raw images.

^c<https://arxiv.org/>

📊 Chart2Markdown: This dataset assesses the models’ capabilities in extracting data values from chart images. Formally, the model is given a chart image and asked to produce a data table of the underlying data table in markdown format. To create this dataset, we crawled recent chart images from the Statista website^d, focusing on charts from 2023 and 2024 that were not used in prior datasets like UniChart (Masry et al., 2023) and ChartQA (Masry et al., 2022). This ensures that the dataset reflects the most up-to-date facts and trends and overlaps less with existing datasets and benchmarks. We collected 6,516 chart images with their data tables and human-written summaries.

📄 Chart2Caption: We introduce a benchmark for Chart2Caption conversion, aiming to generate textual summaries from chart images. The dataset includes 6,516 samples, with charts sourced from Kaggle by running public analytics notebooks and extracting charts and code. Summaries were generated using multimodal InterVL2-26B model (Chen et al., 2023; 2024) based on a custom prompt (see Appendix A.4.5) and augmented with human-written summaries from the Chart2Markdown task. This benchmark evaluates models’ abilities to interpret and summarize visual data representations.

🖱️ GUI2UserIntent: This benchmark interprets user intent from GUI interactions, identifying elements linked to clicked bounding boxes (details in Appendix A.4.7). The dataset, repurposed from SeeClick (Cheng et al., 2024), includes 80,000 website screenshots with bounding box coordinates and corresponding user intents sourced from Common Crawl to capture user interactions effectively.

📄 GUI2Summary: The GUI2Summary task generates descriptions of website screenshots, focusing on web layouts. We synthesized 80,000 summaries (under 100 words each) using InternVL2-8B (Chen et al., 2023) in a zero-shot setting (details in Appendix A.4.8). Each summary provides an overview of the main content, referencing key visual elements, layout, and color schemes.

🗨️ GUI-VQA: The GUI-VQA task answers questions about website screenshots, focusing on content and elements. We generated 80k QA pairs using sentences from GUI-to-Summary and prompting LLaMA 3.1-8b (Dubey et al., 2024) in a zero-shot setting (details in Appendix A.4.9).

4.2 FILTERING AND QUALITY

🗑️ Filtering and Verification with BigDocs Toolkit. To ensure a high-quality, open-access dataset, we employed an NSFW detector (e.g., Llama-Guard-3) and filtering tools to eliminate harmful content, corrupted images, misaligned annotations, and personally identifiable information (PII). The BigDocs Toolkit, adhering to ART principles, streamlined web crawling and filtering processes. This multi-layered approach, iteratively refined using typical errors identified during human verification, ensured a clean and reliable dataset. The test set underwent manual human verification, with at least two annotators per sample to ensure quality and accuracy. Sampling-based checks on the training split further validated the robustness of the filtering process, achieving a 99% pass rate (details in A.13).

5 TRAINING MULTIMODAL MODELS ON BIGDOCS

We trained several state-of-the-art multimodal models of varying sizes and architectures on BigDocs to assess its effectiveness for document-based continual pretraining and downstream finetuning. For comparison, we also trained the models on DocStruct4M, the closest alternative in terms of scale and document-oriented tasks. Additionally, we experiment on the training set from BigDocs-Bench that requires generating long structure outputs, e.g., valid code outputs.

We follow two stages of training: continual pretraining (CPT) and downstream finetuning (FT). The CPT stage involves training on large domain-specific datasets, such as BigDocs and DocStruct4M, learning general tasks like OCR, layout understanding, and captioning. For FT smaller datasets, such as DocDownStream and BigDocs-Bench, to focus on specific tasks like question answering or generating HTML from images. A previous stage of pretraining (PT) is typically performed for general multimodal alignment. In our framework, we do not perform this stage and rely on publicly available checkpoints. While pretraining (PT) is typically performed for general multimodal alignment, we rely on public checkpoints instead. In CPT, we train the image encoder and connector to align image features with the LLM. For FT, both the connector and LLM remain unfrozen. See Figure 11 in Appendix A.5 for more details.

^d<https://www.statista.com/>

5.1 EXPERIMENTAL SETUP

Baseline Models. We selected DocOwl1.5-8B (Hu et al., 2024), Qwen2VL-2B (Bai et al., 2023a), Phi-3.5-Vision-4B (Abdin et al., 2024), and LLaVa-NeXT-7B (Li et al., 2024) for our training experiments. These models were chosen due to their focus on document-related tasks (DocOwl1.5), their openness regarding checkpoints (Qwen2VL, DocOwl1.5), and their state-of-the-art performance and task generalization capabilities (LLaVa-NeXT, Phi-3.5).

Training Details. We conduct all experiments using 8 nodes of 8 H100 GPUs, using Fully Sharded Data Parallel (FSDP) for distributed training. All experiments use a batch size of 256 and a learning rate of $2e-5$, with AdamW as the optimizer. More training details are provided in Appendix A.5.

Evaluation Benchmarks & Metrics. In addition to the newly introduced BigDocs-Bench, we assess performance on well-known document-oriented benchmarks, termed as **General Document Benchmarks**. We select these benchmarks for their relevance and diverse range of document tasks. DocVQA (Mathew et al., 2021b), InfoVQA (Mathew et al., 2021a), DeepForm (Svetlichnaya, 2020), KLC (Stanisławek et al., 2021) (Kleister Benchmark for Key information extraction), WTQ (Pasupat & Liang, 2015) (Wikipedia Tables), TabFact (Chen et al., 2020), ChartQA (Masry et al., 2022), TextVQA (Singh et al., 2019), MMMU (Yue et al., 2024), DUDE (Landeghem et al., 2023), SlideVQA (Tanaka et al., 2023), and TableVQA (Kim et al., 2024). We utilize (and extended) VLM Eval Kit (Duan et al., 2024).

In **BigDocs-Bench**, we employ the following evaluation methods based on each task’s characteristics. For Screenshot2HTML, inspired by related works in this domain (Reis et al., 2004), we compute Tree Edit Distance (TE Dist.) between the Document Object Model (DOM) of ground truth and generation. For Table2LaTeX, we report TeXBLEU (Jung et al., 2024). For Image2SVG, we compare the cosine similarity between the DINOv2 (Oquab et al., 2023) representations of the ground-truth and generated SVG images (DINOScore). For the Image2Flow tasks, we propose the Length-Shape Triplet F1 (**LST F1**) score between ground-truth and generated flowcharts’ edge sets. More specifically, each edge is represented as a (s, e, d) triplet, where e is the edge label, and s and t are the source and destination nodes’ labels concatenated with their shapes, respectively. For Chart2Markdown, we adopt the RMSF1 metric for markdown tables (Liu et al., 2022; Masry et al., 2023; 2024). For summarization and VQA tasks, we report Rouge-L F1 score (Lin, 2004). For more details about the evaluation process, please refer to Appendix A.6.

Setup. For our CPT on DocOwl1.5-8B and Qwen2VL-2B, we used base weights, while on Phi-3.5-Vision-4B and Llava-NeXT-7B, we initialized from their instruction-tuned versions, since their base weights are not publicly available. We first trained each model on a CPT corpus, either DocStruct4M (Hu et al., 2024) or BigDocs-7.5M, for one epoch. Following this, we performed further alignment (finetuning) using DocDownStream to enhance the model’s ability to follow instructions. For each selected model, we also evaluated the author-provided base model and the instruction-tuned version (separate from the base checkpoint, if available) as baselines and reported the performance on general document benchmarks.

We also provide a comprehensive evaluation on the proposed BigDocs-Bench. We conducted an off-the-shelf performance analysis on BigDocs-7.5M using models such as GPT4 (Achiam et al., 2023), Claude (Anthropic, 2024), Gemini Pro (Team et al., 2024a) and Qwen2VL-72B (Wang et al., 2024a) and Idefics2 (Laurençon et al., 2024a). In addition, we also evaluated the previously selected models on their instruction versions, including DocOwl1.5-8B, Qwen2VL-2B, Phi-3.5-Vision-4B, and Llava-NeXT-7B. To incorporate the new capabilities introduced in BigDocs-Bench, we further finetuned these models after BigDocs CPT using the training set from BigDocs-Bench (see Table 3). For each model, we only evaluate the instruction-tuned version (where available) as baselines, reporting their respective performance.

5.2 QUANTITATIVE RESULTS

Results on Existing Document Downstream Tasks. Table 2 presents the models performance across general document benchmarks. Base models perform poorly, mainly due to their inability to follow user instructions, like answering questions. Phi3.5 Vision, originally optimized for reasoning tasks, achieves an average score of 60.80% when finetuned on BigDocs, enhancing its ability to handle complex document-based tasks. For Qwen2-VL, an interesting pattern emerges: while the

Table 2: General Document Benchmarks. Models trained on {BigDocs-7.5M+DocDownstream} perform competitively across multimodal document benchmarks. We compare them to base checkpoints, instruction-tuned models, and those trained on {DocStruct4M+DocDownstream}. BigDocs models show consistent performance.

Model	DocVQA VAL	InfoVQA VAL	DeepForm TEST	KLC TEST	WTQ TEST	TabFact TEST	ChartQA TEST	TextVQA VAL	MMMU VAL	DataMini TEST	SlideVQA-M TEST	TableVQA TEST	Avg. Score
DocOwl1.5-8B (instruct)	80.73	49.94	68.84	37.99	38.87	79.67	68.56	68.91	33.67	34.64	31.62	52.60	53.84
DocOwl1.5-8B (base)	2.07	1.84	0.00	0.00	0.00	0.00	0.00	0.00	24.44	19.07	3.30	13.63	5.36
DocOwl1.5-8B (base) + DocStruct4M	75.99	46.88	62.77	35.21	32.86	71.56	68.36	65.08	33.67	29.00	27.03	46.27	49.56
DocOwl1.5-8B (base) + BigDocs (Ours)	78.70	47.62	64.39	36.93	35.69	72.65	65.80	67.30	32.33	32.55	29.60	49.03	51.05
Qwen2-VL-2B (instruct)	89.16	64.11	32.38	25.18	38.20	57.21	73.40	79.90	42.00	45.23	46.50	43.07	53.03
Qwen2-VL-2B (base)	7.26	0.78	0.00	0.00	0.00	0.00	0.00	1.14	34.89	28.43	14.55	0.00	7.25
Qwen2-VL-2B (base) + DocStruct4M	59.53	32.00	53.98	36.38	28.48	64.24	54.44	55.89	34.89	28.78	22.68	46.53	43.15
Qwen2-VL-2B (base) + BigDocs (Ours)	57.23	31.88	49.31	34.39	31.61	64.75	68.60	61.01	35.67	27.19	17.46	47.53	43.89
Phi3.5-Vision-4B (instruct)	86.00	56.20	10.47	7.49	17.18	30.43	82.16	73.12	46.00	37.20	30.93	70.70	45.66
Phi3.5-Vision-4B + DocStruct4M	86.76	68.90	70.12	37.83	51.30	82.12	79.76	68.60	44.11	35.52	31.90	69.17	60.51
Phi3.5-Vision-4B + BigDocs (Ours)	87.05	70.05	70.97	37.45	51.21	81.24	81.56	68.72	45.00	36.15	32.47	67.77	60.80
LLaVA-NeXT-7B (instruct)	63.51	30.90	1.30	5.35	20.06	52.83	52.12	65.10	38.89	17.94	7.46	32.87	32.36
LLaVA-NeXT-7B + DocStruct4M	60.95	26.14	39.78	28.34	25.90	67.72	61.20	52.25	25.78	21.70	15.33	27.03	37.68
LLaVA-NeXT-7B + BigDocs (Ours)	57.13	24.47	46.38	31.09	27.06	72.58	54.72	49.06	17.78	22.88	16.07	33.13	37.70

instruction-tuned version excels on tasks reported in its technical report (e.g., DocVQA, InfoVQA, ChartQA, MMMU), the BigDocs-trained model surpasses it on new tasks like TabFact, DeepForm, KLC, and TableVQA, suggesting that Qwen2-VL’s instruction-tuning may rely on complex prompt engineering and task-specific optimizations. We find that performing additional continual pretraining and finetuning on instruction-tuned models does not significantly degrade performance. Moreover, we observe substantial improvements on previously underperforming tasks. As shown in Table 2, Phi3.5 and LLaVA-Next show marked gains on DeepForm, KLC, WTQ, and SlideVQA. However, LLaVA’s performance declined on MMMU, indicating the need for more multiple-choice question data. This reinforces our argument that transparency in training datasets is essential for proper evaluation. Finally, across all models, BigDocs training yields higher average scores compared to training on DocStruct4M, even with lower contamination rates on most benchmarks, as we highlighted in Section 3. These findings indicate that **BigDocs supports better generalization and robustness without complex task-specific optimizations while also being license-permissive.**

Table 3: Comparison of model performance in BigDocs-Bench. BigDocs models trained on {BigDocs-7.5M+DocDownstream+BigDocs-Bench train-split}, which combine CPT and FT, outperform all baselines in tasks requiring long-format code generation, particularly in flow generation, GUI reasoning, and image-to-LaTeX generation, surpassing even state-of-the-art closed models. The symbol † denotes that the model required 1-shot prompts as opposed to the default 0-shot prompts.

Model	Chart2MD REASONING	Chart2Cap. REASONING	Image2Flow (Graph Viz) L3M FT	Image2Flow (JS/JSX) L3M FT	GUI2Sum. REASONING	GUI2Intent REASONING	Image2SVG DINO Baseline	Screenshot2HTML DINO Baseline	Table2Latex REASONING	GUI-VQA REASONING	Avg. Score
Open Models											
DocOwl-1.5-8B	0.08	18.69	0.00†	0.00†	11.22	13.88	3.58	3.50	75.07	27.22	15.32
Qwen2-VL-2B	41.17	22.88	0.00†	0.00†	23.98	17.70	23.18	6.46	74.83	26.40	23.66
Phi3.5-V-4B	60.64	21.88	1.61†	0.65†	27.80	10.81	34.57	4.25	74.14	34.96	27.13
LLaVA-NeXT-7B	22.00	20.67	1.58†	0.46†	21.99	12.38	20.53	5.00	73.81	27.54	20.60
Idefics2-8B	25.34	20.95	1.17†	0.00†	8.75	5.06	37.73	3.56	74.50	27.76	20.48
Llama-3.2-90B	45.21	20.60	0.73†	0.52†	22.16	12.04	45.97	7.32	74.79	27.28	25.66
Qwen2-VL-72B	70.47	19.42	1.07†	0.23†	18.80	33.94	54.43	10.03	74.51	30.67	31.36
Closed Models											
GPT-4o 20240806	66.70	25.23	22.66†	27.28†	27.12	17.57	60.34	10.33	74.65	36.58	36.84
Claude-3.5 Sonnet	54.81	23.59	13.92†	37.46†	26.45	13.12	25.46	9.70	74.44	26.58	30.55
GeminiPro-1.5	76.63	25.90	11.51†	33.59†	25.54	16.79	15.21	7.43	75.22	35.35	32.32
BigDocs Models (ours)											
DocOwl-1.5-8B + BigDocs	74.43	33.38	42.16	48.54	45.55	89.15	33.66	3.64	81.28	43.46	49.52
Qwen2-VL-2B + BigDocs	72.25	33.74	41.61	52.11	42.59	71.65	33.51	9.20	78.54	33.97	46.92
LLaVA-NeXT-7B+ BigDocs	72.78	32.88	59.66	71.49	46.14	79.55	60.63	10.40	80.79	40.67	55.50
Phi3.5-v-4B + BigDocs	84.01	36.78	63.07	71.86	47.32	86.91	34.65	12.05	81.94	44.81	56.34

Results on BigDocs-Bench Tasks. Table 3 shows results for our proposed downstream tasks, evaluating models’ ability to generate lengthy structured and valid code outputs, and reasoning from GUIs. Overall, BigDocs models consistently outperform both open and closed models on most tasks, particularly in Flow and GUI tasks such as GUI2UserIntent, GUI2summary, GUI-VQA, and Image2Flow, revealing areas where existing models fall short. The performance gap is narrower on tasks like Screenshot2HTML, Image2SVG and Chart2Caption, suggesting these tasks have been explored in the literature but not extensively enough. Phi3.5-V4B + BigDocs stands out as the top performer in 8 tasks out of 10, with an average score of 50.46. However, its performance on

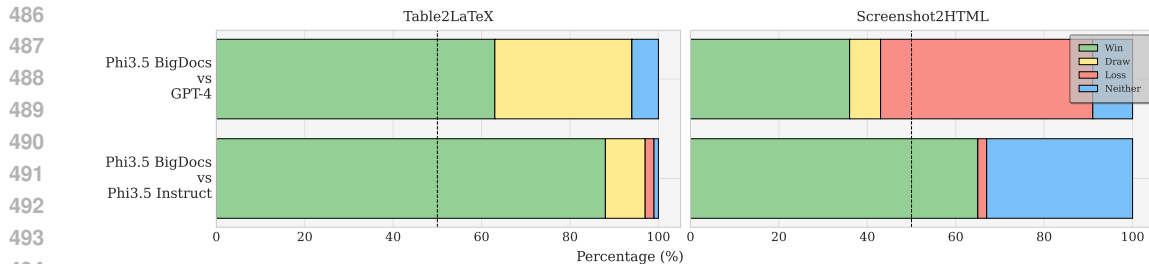


Figure 5: Human evaluation results comparing *Phi3.5 BigDocs-Bench* against *Phi3.5 Instruct* and *GPT-4o* on two tasks: *Table2LaTeX* (Left) and *Screenshot2HTML* (Right).

Image2SVG (25.98 points behind LLaVA-NeXT-7B + BigDocs) indicates less exposure to SVG data in its instruction tuning. We find that the model can generate valid code outputs in different formats, including SVG, HTML, JSON, or Latex, when conditioned on images.

5.3 HUMAN EVALUATIONS AND QUALITATIVE RESULTS

We conducted a human evaluation comparing the performance of Phi-BigDocs, Phi-Instruct, and GPT-4o on Screenshot2HTML and Table2LaTeX tasks. Twenty-eight evaluators participated, providing 1,900 annotations. For Table2LaTeX, evaluators assessed if the LaTeX table matched the input table. For Screenshot2HTML, they evaluated the visual similarity between the rendered HTML and the screenshot. Evaluators chose between “Win” (one output was superior), “Neither” (both were poor), or “Both” (outputs were equally good). See Appendix A.8 for more details on the evaluation platform.

From human evaluation results in Figure 5, for the Table2LaTeX task, Phi3.5 BigDocs wins 88% of the time against Phi3.5 Instruct and achieves a 63% win rate, with a 31% draw rate, against GPT-4o. These results highlight our model’s ability to accurately preserve the table’s structure, including lines, borders, and margins, whereas GPT-4o often struggles to maintain consistent formatting despite capturing content accurately. In the Screenshot2HTML task, Phi3.5 BigDocs achieves a 65% win rate against Phi3.5 Instruct and performs competitively against GPT-4o, with a 36% win rate and 7% draw rate, demonstrating its strong capability to reproduce visual elements faithfully.

Qualitative Results. We provide qualitative results in Appendix A.10. Figure 8 presents outputs from experiments with the Phi-3.5-Vision-4B model on BigDocs-Bench for tasks like Chart2Markdown, Table2LaTeX, and Image2SVG. The model delivers visually consistent outputs and generates valid code across formats, adhering to task instructions. Table 6 compares sample outputs between Phi-3.5-Vision models and GPT-4o, highlighting the strong performance of our BigDocs trained version in captioning and VQA tasks.

6 CONCLUSION

We introduce BigDocs-7.5M, a large-scale, license-permissive dataset for training multimodal models on document and code-related tasks. Along with a comprehensive suite of tools and data analysis, we present BigDocs-Bench, featuring 10 downstream tasks that assess a model’s ability to generate long-format code outputs from images. These tasks serve as practical benchmarks for real-world applications. Our experiments show that models trained on BigDocs outperform those trained on existing datasets. Furthermore, training on the BigDocs-Bench train split endows the resulting models with new capabilities and significantly enhances their ability to generate long, structured outputs. All BigDocs artifacts will be freely available under permissive licenses.

Limitations Our work presents a pioneering license-permissive dataset for multimodal document understanding, achieving strong performance across tasks. However, there are limitations: (1) Suboptimal performance on some public benchmarks, indicating a need to refine the data mixture and explore additional sources. (2) Limited context length, as models are trained with a maximum of 8192 tokens, restricting performance on tasks with long, structured outputs like HTML and SVG. (3) Uncertainty in the commercial viability of base models, as their pretraining data lacks transparency.

540 ETHICS AND REPRODUCIBILITY STATEMENT

541
542 **Ethics Statement** Our work is centered around responsible and transparent curation of datasets for
543 multimodal document understanding models. While we have made extensive efforts to filter harmful
544 content from our dataset, we cannot fully guarantee that the models will not generate offensive
545 language. Additionally, we have taken significant steps to remove personally identifiable information
546 (PII) from the compiled datasets to protect user privacy. However, we cannot ensure that the generated
547 code will be free of malicious snippets, and developers are encouraged to implement protection
548 protocols to safeguard against potential risks. Finally, all human evaluation studies were conducted
549 by collaborator researchers, and no PII was collected during this process.

550
551 **Reproducibility Statement** We are committed to ensuring the reproducibility of our work by
552 providing all necessary details and resources. All artifacts, including code, datasets, model weights,
553 data sheets, and metadata, will be publicly released. Furthermore, we have fully documented all
554 hyperparameters, experimental setups, and evaluation metrics to allow for accurate replication of our
555 results. For human evaluation, we provide clear instructions and describe the environment used for
556 comparison to ensure transparency and consistency.

557
558 REFERENCES

- 559 Marah Abdin, Sam Ade Jacobs, Ammar Ahmad Awan, Jyoti Aneja, Ahmed Awadallah, Hany
560 Awadalla, Nguyen Bach, Amit Bahree, Arash Bakhtiari, Harkirat Behl, et al. Phi-3 technical report:
561 A highly capable language model locally on your phone. *arXiv preprint arXiv:2404.14219*, 2024.
562
- 563 Josh Achiam, Steven Adler, Sandhini Agarwal, Lama Ahmad, Ilge Akkaya, Florencia Leoni Aleman,
564 Diogo Almeida, Janko Altenschmidt, Sam Altman, Shyamal Anadkat, et al. Gpt-4 technical report.
565 *arXiv preprint arXiv:2303.08774*, 2023.
566
- 567 Anthropic. The claude 3 model family: Opus, sonnet, haiku, 2024.
- 568 Credit Mutuel Arkea. Aftdb dataset, 2024. URL <https://huggingface.co/datasets/cmarkea/aftdb>. Hugging Face Dataset.
569
570
- 571 Jinze Bai, Shuai Bai, Yunfei Chu, Zeyu Cui, Kai Dang, Xiaodong Deng, Yang Fan, Wenbin Ge,
572 Yu Han, Fei Huang, Binyuan Hui, Luo Ji, Mei Li, Junyang Lin, Runji Lin, Dayiheng Liu, Gao Liu,
573 Chengqiang Lu, Keming Lu, Jianxin Ma, Rui Men, Xingzhang Ren, Xuancheng Ren, Chuanqi Tan,
574 Sinan Tan, Jianhong Tu, Peng Wang, Shijie Wang, Wei Wang, Shengguang Wu, Benfeng Xu, Jin
575 Xu, An Yang, Hao Yang, Jian Yang, Shusheng Yang, Yang Yao, Bowen Yu, Hongyi Yuan, Zheng
576 Yuan, Jianwei Zhang, Xingxuan Zhang, Yichang Zhang, Zhenru Zhang, Chang Zhou, Jingren Zhou,
577 Xiaohuan Zhou, and Tianhang Zhu. Qwen technical report. *arXiv preprint arXiv: 2309.16609*,
578 2023a.
- 579 Jinze Bai, Shuai Bai, Shusheng Yang, Shijie Wang, Sinan Tan, Peng Wang, Junyang Lin, Chang Zhou,
580 and Jingren Zhou. Qwen-vl: A versatile vision-language model for understanding, localization,
581 text reading, and beyond. *arXiv preprint arXiv:2308.12966*, 2023b.
582
- 583 Jonas Belouadi, Anne Lauscher, and Steffen Eger. Automatizk: Text-guided synthesis of scientific
584 vector graphics with tikz. In *IEEE Conference Computer Vision Pattern Recognition*, 2023.
585
- 586 Jonas Belouadi, Simone Paolo Ponzetto, and Steffen Eger. Detikzify: Synthesizing graphics programs
587 for scientific figures and sketches with tikz, 2024.
- 588 Emily M. Bender and Batya Friedman. Data statements for natural language processing: Toward mit-
589 igating system bias and enabling better science. *Transactions of the Association for Computational*
590 *Linguistics*, 6:587–604, 2018.
591
- 592 Rishi Bommasani, Kevin Klyman, Shayne Longpre, Sayash Kapoor, Nestor Maslej, Betty Xiong,
593 Daniel Zhang, and Percy Liang. The foundation model transparency index. *arXiv preprint*
arXiv:2310.12941, 2023.

- 594 Rishi Bommasani, Kevin Klyman, Sayash Kapoor, Shayne Longpre, Betty Xiong, Nestor Maslej, and
595 Percy Liang. The foundation model transparency index v1.1. *arXiv preprint arXiv:2310.12941*,
596 2024.
- 597 Łukasz Borchmann. Notes on applicability of gpt-4 to document understanding. *arXiv preprint*
598 *arXiv:2405.18433*, 2024.
- 600 Soravit Changpinyo, Piyush Sharma, Nan Ding, and Radu Soricut. Conceptual 12M: Pushing web-
601 scale image-text pre-training to recognize long-tail visual concepts. In *IEEE Conference Computer*
602 *Vision Pattern Recognition*, 2021.
- 604 Ritwick Chaudhry, Sumit Shekhar, Utkarsh Gupta, Pranav Maneriker, Prann Bansal, and Ajay
605 Joshi. Leaf-qa: Locate, encode & attend for figure question answering. In *Winter Conference on*
606 *Applications of Computer Vision*, 2019.
- 607 Wenhui Chen, Hongmin Wang, Jianshu Chen, Yunkai Zhang, Hong Wang, Shiyang Li, Xiyou Zhou,
608 and William Yang Wang. Tabfact: A large-scale dataset for table-based fact verification. In
609 *International Conference Learning Representations*, 2020.
- 611 Xinlei Chen, Hao Fang, Tsung-Yi Lin, Ramakrishna Vedantam, Saurabh Gupta, Piotr Dollár, and
612 C. Lawrence Zitnick. Microsoft coco captions: Data collection and evaluation server. *arXiv*
613 *preprint arXiv:1504.00325*, 2015.
- 614 Zhe Chen, Jiannan Wu, Wenhui Wang, Weijie Su, Guo Chen, Sen Xing, Muyan Zhong, Qinglong
615 Zhang, Xizhou Zhu, Lewei Lu, Bin Li, Ping Luo, Tong Lu, Yu Qiao, and Jifeng Dai. Internvl:
616 Scaling up vision foundation models and aligning for generic visual-linguistic tasks. *arXiv preprint*
617 *arXiv:2312.14238*, 2023.
- 619 Zhe Chen, Weiyun Wang, Hao Tian, Shenglong Ye, Zhangwei Gao, Erfei Cui, Wenwen Tong, Kongzhi
620 Hu, Jiapeng Luo, Zheng Ma, et al. How far are we to gpt-4v? closing the gap to commercial
621 multimodal models with open-source suites. *arXiv preprint arXiv:2404.16821*, 2024.
- 622 Kanzhi Cheng, Qiushi Sun, Yougang Chu, Fangzhi Xu, Li YanTao, Jianbing Zhang, and Zhiyong Wu.
623 SeeClick: Harnessing GUI grounding for advanced visual GUI agents. In *Annual Meeting of the*
624 *Association for Computational Linguistics*, 2024.
- 626 Tri Dao. FlashAttention-2: Faster attention with better parallelism and work partitioning. In
627 *International Conference Learning Representations*, 2024.
- 628 Haodong Duan, Junming Yang, Yuxuan Qiao, Xinyu Fang, Lin Chen, Yuan Liu, Xiaoyi Dong, Yuhang
629 Zang, Pan Zhang, Jiaqi Wang, Dahua Lin, and Kai Chen. Vlmevalkit: An open-source toolkit for
630 evaluating large multi-modality models, 2024.
- 632 Abhimanyu Dubey, Abhinav Jauhri, Abhinav Pandey, Abhishek Kadian, Ahmad Al-Dahle, Aiesha
633 Letman, Akhil Mathur, Alan Schelten, Amy Yang, Angela Fan, Anirudh Goyal, Anthony Hartshorn,
634 Aobo Yang, Archi Mitra, Archie Sravankumar, Artem Korenev, Arthur Hinsvark, Arun Rao, Aston
635 Zhang, Aurelien Rodriguez, Austen Gregerson, Ava Spataru, Baptiste Roziere, Bethany Biron,
636 Binh Tang, Bobbie Chern, Charlotte Caucheteux, Chaya Nayak, Chloe Bi, Chris Marra, Chris
637 McConnell, Christian Keller, Christophe Touret, Chunyang Wu, Corinne Wong, et al. The llama 3
638 herd of models. *arXiv preprint arXiv:2407.21783*, 2024.
- 639 Wikimedia Foundation. Wikimedia downloads, 2024. URL <https://dumps.wikimedia.org>.
- 640 Samir Yitzhak Gadre, Gabriel Ilharco, Alex Fang, Jonathan Hayase, Georgios Smyrnis, Thao Nguyen,
641 Ryan Marten, Mitchell Wortsman, Dhruva Ghosh, Jieyu Zhang, Eyal Orgad, Rahim Entezari, Gi-
642 annis Daras, Sarah Pratt, Vivek Ramanujan, Yonatan Bitton, Kalyani Marathe, Stephen Mussmann,
643 Richard Vencu, Mehdi Cherti, Ranjay Krishna, Pang Wei Koh, Olga Saukh, Alexander J. Ratner,
644 Shuran Song, Hannaneh Hajishirzi, Ali Farhadi, Romain Beaumont, Sewoong Oh, Alexandros G.
645 Dimakis, Jenia Jitsev, Yair Carmon, Vaishaal Shankar, and Ludwig Schmidt. Datacomp: In search
646 of the next generation of multimodal datasets. In *Adv. Neural Information Processing Systems*,
647 2023.

- 648 Timnit Gebru, Jamie Morgenstern, Briana Vecchione, Jennifer Wortman Vaughan, Hanna Wallach,
649 Hal Daumé Iii, and Kate Crawford. Datasheets for datasets. *Communications of the ACM*, 64(12):
650 86–92, 2021.
- 651
- 652 Sylvain Gugger, Lysandre Debut, Thomas Wolf, Philipp Schmid, Zachary Mueller, Sourab Man-
653 grulkar, Marc Sun, and Benjamin Bossan. Accelerate: Training and inference at scale made simple,
654 efficient and adaptable. <https://github.com/huggingface/accelerate>, 2022.
- 655
- 656 Jack Hessel, Ari Holtzman, Maxwell Forbes, Ronan Le Bras, and Yejin Choi. Clipscore: A reference-
657 free evaluation metric for image captioning, 2022.
- 658 Anwen Hu, Haiyang Xu, Jiabo Ye, Ming Yan, Liang Zhang, Bo Zhang, Chen Li, Ji Zhang, Qin Jin,
659 Fei Huang, and Jingren Zhou. mplug-docowl 1.5: Unified structure learning for ocr-free document
660 understanding. *arXiv preprint arXiv:2403.12895*, 2024.
- 661
- 662 Guillaume Jaume, Hazim Kemal Ekenel, and Jean-Philippe Thiran. Funsd: A dataset for form
663 understanding in noisy scanned documents. In *International Conference on Document Analysis
664 and Recognition Workshop*, 2019.
- 665
- 666 Kyudan Jung, Nam-Joon Kim, Hyongon Ryu, Sieun Hyeon, Seung jun Lee, and Hyeok jae Lee.
667 Texbleu: Automatic metric for evaluate latex format. *arXiv preprint arXiv: 2409.06639*, 2024.
- 668
- 669 Kushal Kafle, Brian Price, Scott Cohen, and Christopher Kanan. Dvqa: Understanding data visu-
670 alizations via question answering. In *IEEE Conference Computer Vision Pattern Recognition*,
2018.
- 671
- 672 Samira Ebrahimi Kahou, Vincent Michalski, Adam Atkinson, Ákos Kádár, Adam Trischler, and
673 Yoshua Bengio. Figureqa: An annotated figure dataset for visual reasoning. In *International
674 Conference Learning Representations*, 2017.
- 675
- 676 Yoonsik Kim, Moonbin Yim, and Ka Yeon Song. Tablevqa-bench: A visual question answering
benchmark on multiple table domains. *arXiv preprint arXiv:2404.19205*, 2024.
- 677
- 678 kleister Charity. kleister charity dataset, 2021. URL [https://github.com/applicaai/
679 kleister-charity](https://github.com/applicaai/kleister-charity).
- 680
- 681 Denis Kocetkov, Raymond Li, Loubna Ben Allal, Jia Li, Chenghao Mou, Carlos Muñoz Ferrandis,
682 Yacine Jernite, Margaret Mitchell, Sean Hughes, Thomas Wolf, et al. The stack: 3 tb of permissively
licensed source code. *Transactions Machine Learn Research*, 2022.
- 683
- 684 Jordy Van Landeghem, Rubén Tito, Łukasz Borchmann, Michał Pietruszka, Paweł Józziak, Rafał
685 Powalski, Dawid Jurkiewicz, Mickaël Coustaty, Bertrand Ackaert, Ernest Valveny, Matthew
686 Blaschko, Sien Moens, and Tomasz Stanisławek. Document understanding dataset and evaluation
(dude). In *International Conference Computer Vision*, 2023.
- 687
- 688 Hugo Laurençon, Léo Tronchon, Matthieu Cord, and Victor Sanh. What matters when building
689 vision-language models? *arXiv preprint arXiv:2405.02246*, 2024a.
- 690
- 691 Hugo Laurençon, Léo Tronchon, and Victor Sanh. Unlocking the conversion of web screenshots into
692 html code with the websight dataset. *arXiv preprint arXiv:2403.09029*, 2024b.
- 693
- 694 Hugo Laurençon, Lucile Saulnier, Léo Tronchon, Stas Bekman, Amanpreet Singh, Anton Lozhkov,
695 Thomas Wang, Siddharth Karamcheti, Alexander M. Rush, Douwe Kiela, Matthieu Cord, and
696 Victor Sanh. Obelics: An open web-scale filtered dataset of interleaved image-text documents,
2023.
- 697
- 698 Hugo Laurençon, Léo Tronchon, Matthieu Cord, and Victor Sanh. What matters when building
699 vision-language models? *arXiv preprint arXiv: 2405.02246*, 2024.
- 700
- 701 Bo Li, Yuanhan Zhang, Dong Guo, Renrui Zhang, Feng Li, Hao Zhang, Kaichen Zhang, Yanwei Li,
Ziwei Liu, and Chunyuan Li. Llava-onevision: Easy visual task transfer. *arXiv preprint arXiv:
2408.03326*, 2024.

- 702 Minghao Li, Lei Cui, Shaohan Huang, Furu Wei, Ming Zhou, and Zhoujun Li. Tablebank: A
703 benchmark dataset for table detection and recognition. *arXiv preprint arXiv:1903.01949*, 2020a.
704
- 705 Minghao Li, Yiheng Xu, Lei Cui, Shaohan Huang, Furu Wei, Zhoujun Li, and Ming Zhou. Docbank:
706 A benchmark dataset for document layout analysis. In *International Conference on Computational*
707 *Linguistics*, 2020b.
- 708 Raymond Li, Loubna Ben Allal, Yangtian Zi, Niklas Muennighoff, Denis Kocetkov, Chenghao Mou,
709 Marc Marone, Christopher Akiki, Jia Li, Jenny Chim, et al. Starcoder: may the source be with
710 you! *Transactions Machine Learn Research*, 2023.
711
- 712 Chin-Yew Lin. ROUGE: A package for automatic evaluation of summaries. In *Text Summarization*
713 *Branches Out*. Association for Computational Linguistics, 2004.
714
- 715 Fangyu Liu, Julian Martin Eisenschlos, Francesco Piccinno, Syrine Krichene, Chenxi Pang, Kenton
716 Lee, Mandar Joshi, Wenhui Chen, Nigel Collier, and Yasemin Altun. Deplot: One-shot visual
717 language reasoning by plot-to-table translation. *arXiv preprint arXiv:2212.10505*, 2022.
- 718 Haotian Liu, Chunyuan Li, Yuheng Li, and Yong Jae Lee. Improved baselines with visual instruction
719 tuning. *arXiv preprint arXiv:2310.03744*, 2023a.
720
- 721 Haotian Liu, Chunyuan Li, Qingyang Wu, and Yong Jae Lee. Visual instruction tuning. In *Adv.*
722 *Neural Information Processing Systems*, 2023b.
- 723 Haotian Liu, Chunyuan Li, Yuheng Li, Bo Li, Yuanhan Zhang, Sheng Shen, and Yong Jae Lee.
724 Llava-next: Improved reasoning, ocr, and world knowledge, January 2024. URL [https://](https://llava-vl.github.io/blog/2024-01-30-llava-next/)
725 llava-vl.github.io/blog/2024-01-30-llava-next/.
726
- 727 Tengchao Lv, Yupan Huang, Jingye Chen, Lei Cui, Shuming Ma, Yaoyao Chang, Shaohan Huang,
728 Wenhui Wang, Li Dong, Weiyao Luo, et al. Kosmos-2.5: A multimodal literate model. *arXiv*
729 *preprint arXiv:2309.11419*, 2023.
730
- 731 Inbal Magar and Roy Schwartz. Data contamination: From memorization to exploitation. In
732 *Proceedings of the 60th Annual Meeting of the Association for Computational Linguistics (Volume*
733 *2: Short Papers)*, Dublin, Ireland, May 2022. Association for Computational Linguistics. URL
734 <https://aclanthology.org/2022.acl-short.18>.
- 735 Ahmed Masry, Do Xuan Long, Jia Qing Tan, Shafiq Joty, and Enamul Hoque. Chartqa: A bench-
736 mark for question answering about charts with visual and logical reasoning. *arXiv preprint*
737 *arXiv:2203.10244*, 2022.
738
- 739 Ahmed Masry, Parsa Kavehzadeh, Xuan Long Do, Enamul Hoque, and Shafiq Joty. UniChart: A
740 universal vision-language pretrained model for chart comprehension and reasoning. In *Empirical*
741 *Methods in Natural Language Processing*, 2023.
- 742 Ahmed Masry, Mehrad Shahmohammadi, Md Rizwan Parvez, Enamul Hoque, and Shafiq Joty.
743 ChartInstruct: Instruction tuning for chart comprehension and reasoning. In *Annual Meeting of the*
744 *Association for Computational Linguistics*, 2024.
745
- 746 Minesh Mathew, Viraj Bagal, Rubèn Pérez Tito, Dimosthenis Karatzas, Ernest Valveny, and C. V
747 Jawahar. Infographicvqa. In *Winter Conference on Applications of Computer Vision*, 2021a.
748
- 749 Minesh Mathew, Dimosthenis Karatzas, and C. V. Jawahar. Docvqa: A dataset for vqa on document
750 images. In *Winter Conference on Applications of Computer Vision*, 2021b.
- 751 Anand Mishra, Shashank Shekhar, Ajeet Kumar Singh, and Anirban Chakraborty. Ocr-vqa: Visual
752 question answering by reading text in images. In *International Conference on Document Analysis*
753 *and Recognition*, 2019.
754
- 755 OpenAI. GPT-4V(ision) System Card. [https://cdn.openai.com/papers/GPTV_](https://cdn.openai.com/papers/GPTV_System_Card.pdf)
[System_Card.pdf](https://cdn.openai.com/papers/GPTV_System_Card.pdf), September 2023. Accessed: 2023-11-05.

- 756 Maxime Oquab, Timothée Darcet, Théo Moutakanni, Huy Vo, Marc Szafraniec, Vasil Khalidov,
757 Pierre Fernandez, Daniel Haziza, Francisco Massa, Alaaeldin El-Nouby, Mahmoud Assran, Nicolas
758 Ballas, Wojciech Galuba, Russell Howes, Po-Yao Huang, Shang-Wen Li, Ishan Misra, Michael
759 Rabbat, Vasu Sharma, Gabriel Synnaeve, Hu Xu, Hervé Jegou, Julien Mairal, Patrick Labatut,
760 Armand Joulin, and Piotr Bojanowski. Dinov2: Learning robust visual features without supervision.
761 *arXiv preprint arXiv:2304.07193*, 2023.
- 762 Vicente Ordonez, Girish Kulkarni, and Tamara Berg. Im2text: Describing images using 1 million
763 captioned photographs. In *Adv. Neural Information Processing Systems*, 2011.
- 764 Seunghyun Park, Seung Shin, Bado Lee, Junyeop Lee, Jaeheung Surh, Minjoon Seo, and Hwalsuk
765 Lee. Cord: A consolidated receipt dataset for post-ocr parsing. In *Adv. Neural Information
766 Processing Systems Workshop*, 2019.
- 767 Panupong Pasupat and Percy Liang. Compositional semantic parsing on semi-structured tables. In
768 *Annual Meeting of the Association for Computational Linguistics*, 2015.
- 769 Guilherme Penedo, Hynek Kydlíček, Loubna Ben allal, Anton Lozhkov, Margaret Mitchell, Colin
770 Raffel, Leandro Von Werra, and Thomas Wolf. The fineweb datasets: Decanting the web for the
771 finest text data at scale, 2024.
- 772 Alec Radford, Jeffrey Wu, Rewon Child, David Luan, Dario Amodei, Ilya Sutskever, et al. Language
773 models are unsupervised multitask learners. *OpenAI blog*, 1(8):9, 2019.
- 774 Alec Radford, Jong Wook Kim, Chris Hallacy, Aditya Ramesh, Gabriel Goh, Sandhini Agarwal,
775 Girish Sastry, Amanda Askell, Pamela Mishkin, Jack Clark, Gretchen Krueger, and Ilya Sutskever.
776 Learning transferable visual models from natural language supervision. In *International Conference
777 Machine Learning*, 2021.
- 778 N Reimers. Sentence-bert: Sentence embeddings using siamese bert-networks. *arXiv preprint
779 arXiv:1908.10084*, 2019.
- 780 D. C. Reis, P. B. Golgher, A. S. Silva, and A. F. Laender. Automatic web news extraction using tree
781 edit distance. In *International Conference on World Wide Web*, 2004.
- 782 Juan A Rodriguez, Shubham Agarwal, Issam H Laradji, Pau Rodriguez, David Vazquez, Christopher
783 Pal, and Marco Pedersoli. Starvector: Generating scalable vector graphics code from images.
784 *arXiv preprint arXiv:2312.11556*, 2023a.
- 785 Juan A Rodriguez, David Vazquez, Issam Laradji, Marco Pedersoli, and Pau Rodriguez. Figgen: Text
786 to scientific figure generation. In *International Conference Learning Representations*, 2023b.
- 787 Juan A Rodriguez, David Vazquez, Issam Laradji, Marco Pedersoli, and Pau Rodriguez. Ocr-vqgan:
788 Taming text-within-image generation. In *Winter Conference on Applications of Computer Vision*,
789 2023c.
- 790 Piyush Sharma, Nan Ding, Sebastian Goodman, and Radu Soricut. Conceptual captions: A cleaned,
791 hypernymed, image alt-text dataset for automatic image captioning. In *Annual Meeting of the
792 Association for Computational Linguistics*, 2018.
- 793 Oleksii Sidorov, Ronghang Hu, Marcus Rohrbach, and Amanpreet Singh. Textcaps: a dataset for
794 image captioning with reading comprehension. In *European Conference Computer Vision*, 2020.
- 795 Amanpreet Singh, Vivek Natarajan, Meet Shah, Yu Jiang, Xinlei Chen, Dhruv Batra, Devi Parikh,
796 and Marcus Rohrbach. Towards vqa models that can read. In *IEEE Conference Computer Vision
797 Pattern Recognition*, 2019.
- 798 Amanpreet Singh, Niranjan Balasubramanian, and A B. Open4business(o4b): An open access dataset
799 for summarizing business documents. *arXiv preprint arXiv:2011.07636*, 2020.
- 800 Amanpreet Singh, Guan Pang, Mandy Toh, Jing Huang, Wojciech Galuba, and Tal Hassner. Textocr:
801 Towards large-scale end-to-end reasoning for arbitrary-shaped scene text. In *IEEE Conference
802 Computer Vision Pattern Recognition*, 2021.

- 810 Brandon Smock, Rohith Pesala, and Robin Abraham. Pubtables-1m: Towards comprehensive table
811 extraction from unstructured documents. In *IEEE Conference Computer Vision Pattern Recognition*,
812 2022.
- 813 Ian Soboro. Complex document information processing (cdip) dataset. [https://doi.org/10.](https://doi.org/10.18434/mds2-2531)
814 [18434/mds2-2531](https://doi.org/10.18434/mds2-2531), 2022. Accessed: 2024-06-20.
- 816 Tomasz Stanisławek, Filip Graliński, Anna Wróblewska, Dawid Lipiński, Agnieszka Kaliska, Paulina
817 Rosalska, Bartosz Topolski, and Przemysław Biecek. Kleister: key information extraction datasets
818 involving long documents with complex layouts. In *International Conference on Document*
819 *Analysis and Recognition*, 2021.
- 820 S Svetlichnaya. Deepform: Understand structured documents at scale, 2020.
- 821 Ryota Tanaka, Kyosuke Nishida, Kosuke Nishida, Taku Hasegawa, Itsumi Saito, and Kuniko Saito.
822 Slidevqa: A dataset for document visual question answering on multiple images. In *Association*
823 *for the Advancement of Artificial Intelligence*, 2023.
- 825 Simon Tannert, Marcelo G. Feighelstein, Jasmina Bogojeska, Joseph Shtok, Assaf Arbelle, Peter
826 W. J. Staar, Anika Schumann, Jonas Kuhn, and Leonid Karlinsky. FlowchartQA: The first
827 large-scale benchmark for reasoning over flowcharts. In Pioush Aggarwal, V'ozge Alaccam,
828 Carina Silberer, Sina Zarrie\ss, and Torsten Zesch (eds.), *Proceedings of the 1st Workshop on*
829 *Linguistic Insights from and for Multimodal Language Processing*, pp. 34–46, Ingolstadt, Germany,
830 September 2023. Association for Computational Linguistics. URL [https://aclanthology.](https://aclanthology.org/2023.limo-1.5)
831 [org/2023.limo-1.5](https://aclanthology.org/2023.limo-1.5).
- 832 Gemini Team, Rohan Anil, Sebastian Borgeaud, Jean-Baptiste Alayrac, Jiahui Yu, Radu Soricut,
833 Johan Schalkwyk, Andrew M. Dai, Anja Hauth, Katie Millican, David Silver, Melvin Johnson,
834 Ioannis Antonoglou, Julian Schrittwieser, Amelia Glaese, Jilin Chen, Emily Pitler, Timothy
835 Lillicrap, Angeliki Lazaridou, Orhan Firat, James Molloy, Michael Isard, Paul R. Barham, Tom
836 Hennigan, Benjamin Lee, Fabio Viola, Malcolm Reynolds, Yuanzhong Xu, Ryan Doherty, Eli
837 Collins, Clemens Meyer, and Others. Gemini: A family of highly capable multimodal models.
838 *arXiv preprint arXiv:2312.11805*, 2024a.
- 839 Gemini Team, Petko Georgiev, Ving Ian Lei, Ryan Burnell, Libin Bai, Anmol Gulati, Garrett Tanzer,
840 Damien Vincent, Zhufeng Pan, Shibo Wang, Soroosh Mariooryad, Yifan Ding, Xinyang Geng,
841 Fred Alcober, Roy Frostig, Mark Omernick, Lexi Walker, Cosmin Paduraru, Christina Sorokin,
842 Andrea Tacchetti, Colin Gaffney, Samira Daruki, Olcan Sercinoglu, Zach Gleicher, and Others.
843 Gemini 1.5: Unlocking multimodal understanding across millions of tokens of context. *arXiv*
844 *preprint arXiv:2403.05530*, 2024b.
- 845 Shengbang Tong, Ellis Brown, Penghao Wu, Sanghyun Woo, Manoj Middepogu, Sai Charitha
846 Akula, Jihan Yang, Shusheng Yang, Adithya Iyer, Xichen Pan, et al. Cambrian-1: A fully open,
847 vision-centric exploration of multimodal llms. *arXiv preprint arXiv:2406.16860*, 2024.
- 848 Andreas Veit, Tomas Matera, Lukas Neumann, Jiri Matas, and Serge Belongie. Coco-text: Dataset and
849 benchmark for text detection and recognition in natural images. *arXiv preprint arXiv:1601.07140*,
850 2016.
- 851 Caitlin Vogus and Emma Llansóe. Making transparency meaningful: A framework for policymakers.
852 *Center for Democracy and Technology*, 2021.
- 853 Štěpán Šimsa, Milan Šulc, Michal Uříčář, Yash Patel, Ahmed Hamdi, Matěj Kocián, Matyáš Skalický,
854 Jiří Matas, Antoine Doucet, Mickaël Coustaty, and Dimosthenis Karatzas. Docile benchmark
855 for document information localization and extraction. In *International Conference on Document*
856 *Analysis and Recognition*, 2023.
- 857 Bryan Wang, Gang Li, Xin Zhou, Zhourong Chen, Tovi Grossman, and Yang Li. Screen2words:
858 Automatic mobile ui summarization with multimodal learning. In *ACM Symposium on User*
859 *Interface Software and Technology*, 2021.
- 860 Dongsheng Wang, Natraj Raman, Mathieu Sibue, Zhiqiang Ma, Petr Babkin, Simerjot Kaur, Yulong
861 Pei, Armineh Nourbakhsh, and Xiaomo Liu. Docllm: A layout-aware generative language model
862 for multimodal document understanding. *arXiv preprint arXiv: 2401.00908*, 2023a.

- 864 Peng Wang, Shuai Bai, Sinan Tan, Shijie Wang, Zhihao Fan, Jinze Bai, Keqin Chen, Xuejing Liu,
865 Jialin Wang, Wenbin Ge, et al. Qwen2-vl: Enhancing vision-language model’s perception of the
866 world at any resolution. *arXiv preprint arXiv:2409.12191*, 2024a.
- 867
868 Weihan Wang, Zehai He, Wenyi Hong, Yean Cheng, Xiaohan Zhang, Ji Qi, Shiyu Huang, Bin
869 Xu, Yuxiao Dong, Ming Ding, and Jie Tang. Lvbench: An extreme long video understanding
870 benchmark, 2024b.
- 871 Zilong Wang, Yichao Zhou, Wei Wei, Chen-Yu Lee, and Sandeep Tata. Vrdu: A benchmark for
872 visually-rich document understanding. In *International Conference on Knowledge Discovery &*
873 *Data Mining*, 2023b.
- 874
875 Thomas Wolf, Lysandre Debut, Victor Sanh, Julien Chaumond, Clement Delangue, Anthony Moi,
876 Pierric Cistac, Tim Rault, Rémi Louf, Morgan Funtowicz, et al. Huggingface’s transformers:
877 State-of-the-art natural language processing. *arXiv preprint arXiv:1910.03771*, 2019.
- 878 Zhengyuan Yang, Linjie Li, Kevin Lin, Jianfeng Wang, Chung-Ching Lin, Zicheng Liu, and Li-
879 juan Wang. The dawn of Imms: Preliminary explorations with gpt-4v (ision). *arXiv preprint*
880 *arXiv:2309.17421*, 2023.
- 881
882 Xiang Yue, Yuansheng Ni, Kai Zhang, Tianyu Zheng, Ruoqi Liu, Ge Zhang, Samuel Stevens, Dongfu
883 Jiang, Weiming Ren, Yuxuan Sun, Cong Wei, Botao Yu, Ruibin Yuan, Renliang Sun, Ming Yin,
884 Boyuan Zheng, Zhenzhu Yang, Yibo Liu, Wenhao Huang, Huan Sun, Yu Su, and Wenhua Chen.
885 Mmmu: A massive multi-discipline multimodal understanding and reasoning benchmark for expert
886 agi. In *IEEE Conference Computer Vision Pattern Recognition*, 2024.
- 887
888 Tianyu Zhang, Suyuchen Wang, Lu Li, Ge Zhang, Perouz Taslakian, Sai Rajeswar, Jie Fu, Bang Liu,
and Yoshua Bengio. Vcr: Visual caption restoration. *arXiv preprint arXiv: 2406.06462*, 2024.
- 889
890 Yanli Zhao, Andrew Gu, Rohan Varma, Liang Luo, Chien-Chin Huang, Min Xu, Less Wright, Hamid
891 Shojanazeri, Myle Ott, Sam Shleifer, et al. Pytorch fsdp: experiences on scaling fully sharded data
892 parallel. *arXiv preprint arXiv:2304.11277*, 2023.
- 893
894 Boyuan Zheng, Boyu Gou, Jihyung Kil, Huan Sun, and Yu Su. Gpt-4v (ision) is a generalist web
agent, if grounded. *arXiv preprint arXiv:2401.01614*, 2024.
- 895
896 Fengbin Zhu, Wenqiang Lei, Fuli Feng, Chao Wang, Haozhou Zhang, and Tat-Seng Chua. Towards
897 complex document understanding by discrete reasoning. In *ACM International Conference on*
898 *Multimedia*, 2022.
- 899
900
901
902
903
904
905
906
907
908
909
910
911
912
913
914
915
916
917

A APPENDIX

A.1 BIGDOCS-7.5M TASKS

1. **OCR-Related Tasks:** These tasks involve converting images of text (e.g., scanned documents) into machine-readable formats, including transformations such as bounding-box-to-text and text-to-bounding-box (text localization as described in [Hu et al. \(2024\)](#)). Models learn to recognize and map textual information within images.
2. **Structured Parsing and Extraction:** This task focuses on extracting and transforming structured data from documents, like parsing tables, forms, and charts into formats such as JSON or Markdown. It includes handling documents with complex visual layouts and sometimes incorporates bounding box information for individual elements.
3. **Captioning and Summarization:** This task requires models to generate captions or summaries for visual or textual content, such as figures, charts, or document sections. The models provide concise descriptions or overviews, enhancing document comprehension.
4. **Question-Answering (QA):** QA tasks involve responding to questions posed over structured or visual data (e.g., tables, figures). This includes multi-turn QA, where models address a series of related questions to improve their reasoning and comprehension.

A.2 DATASETS INCLUDED IN BIGDOCS-7.5M

The following datasets are utilized in our work, supporting the four core tasks mentioned in Section 3.2.1. We reference the task supported by each dataset via the index in Section A.1. Note that datasets with * are those fully or partially curated by us (details explained in the description of each of them).

1. **TabFact** ([Chen et al., 2020](#)): [Task included: (2), (4)] TabFact is used for question-answering tasks, where models check whether a given statement is supported or refuted by a table. It also involves structured parsing, helping models extract and process structured table data into formats like Markdown.
2. **Open4Business (O4B)** ([Singh et al., 2020](#)): [Task included: (2), (3)] O4B is a dataset focused on business-related documents and is processed for structured parsing and extraction, as well as captioning and summarization, allowing models to retrieve key insights from documents and generate summaries or descriptions.
3. **WikiTQ** ([Pasupat & Liang, 2015](#)): [Task included: (2), (4)] WikiTableQuestions is used for question-answering tasks over tables, where models answer questions based on table data, and structured parsing for converting table data into Markdown.
4. **CORD** ([Park et al., 2019](#)): [Task included: (1), (2)] CORD is a dataset for parsing receipts, used for both OCR-related tasks and structured parsing and extraction, helping models interpret structured financial data from document layouts. This latter task requires extracting entities and providing their text, category, and location as a JSON output.
5. **UniChart** ([Masry et al., 2023](#)): [Task included: (2), (4)] UniChart is used for structured parsing and extraction to extract structured information from chart-like tables, converting complex visual layouts into formats like JSON or Markdown. And also for question-answering tasks, where models answer questions related to the chart content.
6. **TextOCR** ([Sidorov et al., 2020](#)): [Task included: (1)] TextOCR is processed for OCR-related tasks, enabling models to perform bounding-box-to-text transformations on scene text from images.
7. **COCO-Text** ([Veit et al., 2016](#)): [Task included: (1)] COCO-Text is used for OCR-related tasks, helping models extract and recognize text from real-world images with natural scene text.
8. **CDIP-1M***: [Task included: (1), (2)] **To create this dataset, we sourced from the original IIT-CDIP (Soboro, 2022) dataset and curated it into CDIP-1M.** CDIP-1M is processed for OCR-related tasks and structured parsing, focusing on extracting text and structure from large-scale scanned document collections. We used an in-house OCR engine to get the text

(i.e. annotations) from its 11M documents from the source. Like the text localization task in DocStruct4M [Hu et al. \(2024\)](#), we generate word-, line- and block-level bounding-box-to-text and text-to-bounding-box QA pairs. We subsample zones randomly, and based on OCR confidence, a large fraction of the images are pretty noisy. In addition, for the block level, we generate structured parsing QA pairs where text lines and their location need to be given as JSON by the model.

9. **PubTables-1M** ([Smock et al., 2022](#)): [Task included: (1), (2)] PubTables-1M is a large dataset of tables from scientific papers. It is used for **OCR-related tasks** to extract information in tables. It is also processed for **structured parsing and extraction**, allowing models to handle scientific tables and convert them into markdown.
10. **FigureQA** ([Kahou et al., 2017](#)): [Task included: (4)] FigureQA is focused on question-answering tasks, where models answer questions based on charts and figures, improving reasoning over visual and tabular data.
11. **DocBank** ([Li et al., 2020b](#)): [Task included: (2), (4)] DocBank is utilized for structured parsing and extraction and question-answering tasks, enabling models to interact with scholarly documents and extract structured data from layouts.
12. **TableBank** ([Li et al., 2020a](#)): [Task included: (2)] TableBank is a large dataset used for structured parsing and extraction, helping models parse table structures from both Word and LaTeX documents into structured formats.
13. **OCRVQA** ([Mishra et al., 2019](#)): [Task included: (1),(4)] OCRVQA focuses on OCR-related tasks and question-answering tasks over OCR-extracted text, where models answer questions based on text and visual data from real-world scenes.
14. **Datikz** ([Belouadi et al., 2023](#)): [Task included: (2), (3)] Datikz is processed for captioning and summarization as well as structured parsing, enabling models to describe and interpret complex diagrams and generate structured data from them.
15. **ArxivOCR***: [Task included: (1)] The ArxivOCR dataset contains OCR-scanned academic papers and is used for OCR-related tasks, where models perform bounding-box-to-text transformations, improving accessibility and structure for scholarly articles. This dataset is curated by us. We filter out the papers from Arxiv that have permissive licenses, i.e. CC-BY 4.0 and CC0 in this case. Then we use in-house OCR engines to produce OCR results on the pages from the papers collected.
16. **ArxivTableCap***: [Task included: (3)] The ArxivTable dataset focuses on generating captions for the tables and figures extracted from Arxiv papers, helping models describe the content and context of tables in academic papers. Among the 156.2k samples, 70k of them are from AFTdb [Arkea \(2024\)](#). We perform the filtering to make sure all the selected ones are in papers with permissive licenses, i.e. CC-BY 4.0 and CC0 in this case.
17. **SVGCap Dataset** ([Rodriguez et al., 2023a](#)): [Task included: (3)] The SVG Dataset supports captioning and summarization tasks, where models generate descriptive captions for SVG content, summarizing the structure and elements of vector graphics.

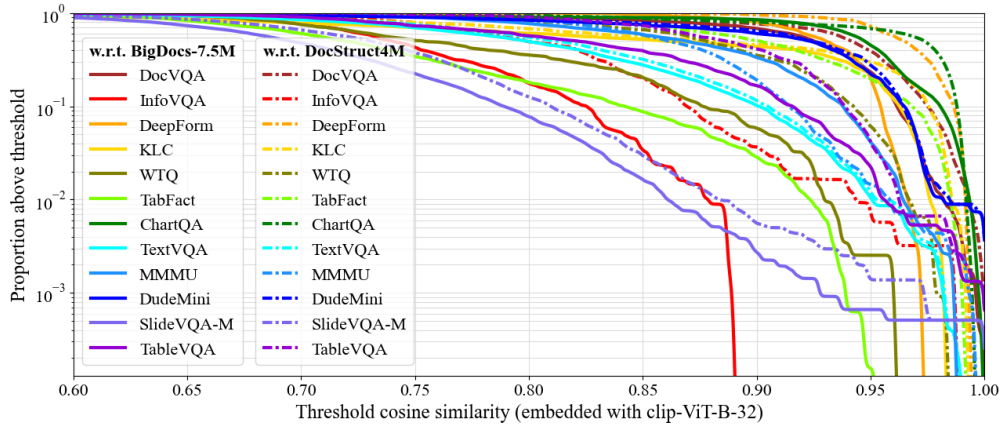
A.3 ASSESSING CONTAMINATION

BigDocs-7.5M’s direct dependency on TabFact, WTQ, and TextVQA is restricted to their training splits, and DocStruct4M reports a similar dependency on DocVQA, InfoVQA, DeepForm, KLC, ChartQA, TabFact, WTQ, and TextVQA. However, overlaps between either of these training sets and evaluation datasets may emerge through indirect means (e.g., the same source material was involved).

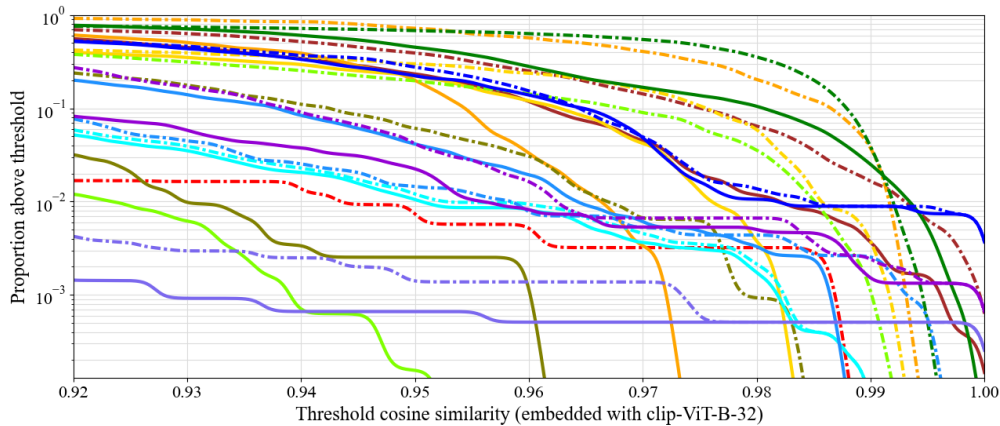
Our primary “automatic” approach to assess contamination consists of embedding all images from the reference dataset (i.e., BigDocs-7.5M or DocStruct4M) using a pretrained CLIP ([Radford et al., 2021](#)), namely `clip-viT-B-32` from `sentence-transformers` ([Reimers, 2019](#)). We similarly embed each image from an evaluation dataset and retrieve the reference image with the highest cosine similarity: the closer this measure is to 1.0, the more likely it is that the evaluation image is part of the reference dataset. Figures 3 and 6, as well as table 4 all report these values.

Except when the cosine similarity is exactly 1.0 – indicating an exact match – interpretations of these scores must be grounded in human evaluations. However, assessing whether two images are “the same” can be a non-trivial task, even for human eyes.

1026
1027
1028
1029
1030
1031
1032
1033
1034
1035
1036
1037
1038
1039
1040
1041
1042
1043
1044
1045
1046
1047
1048
1049
1050
1051
1052
1053
1054
1055
1056
1057
1058
1059
1060
1061
1062
1063
1064
1065
1066
1067
1068
1069
1070
1071
1072
1073
1074
1075
1076
1077
1078
1079



(a) *InfoVQA, SlideVQA-M, and TabFact overlap very little with BigDocs-7.5M (train).*

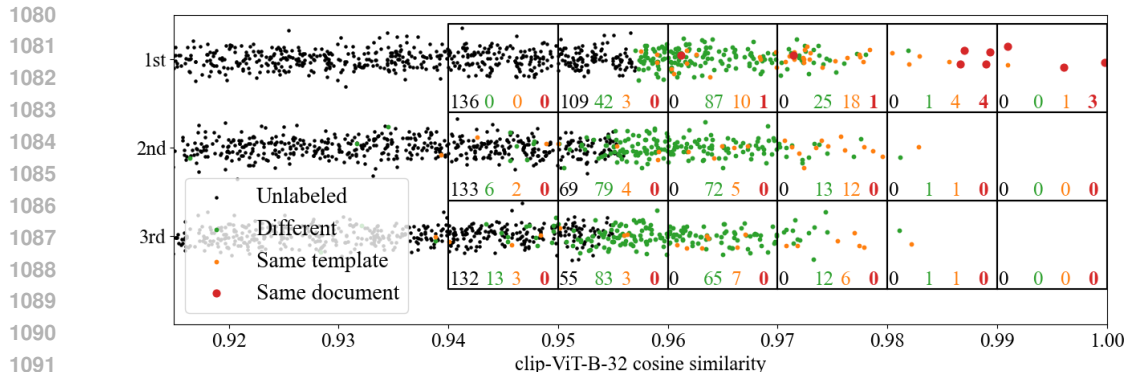


(b) *Zoom on the above (same legend).*

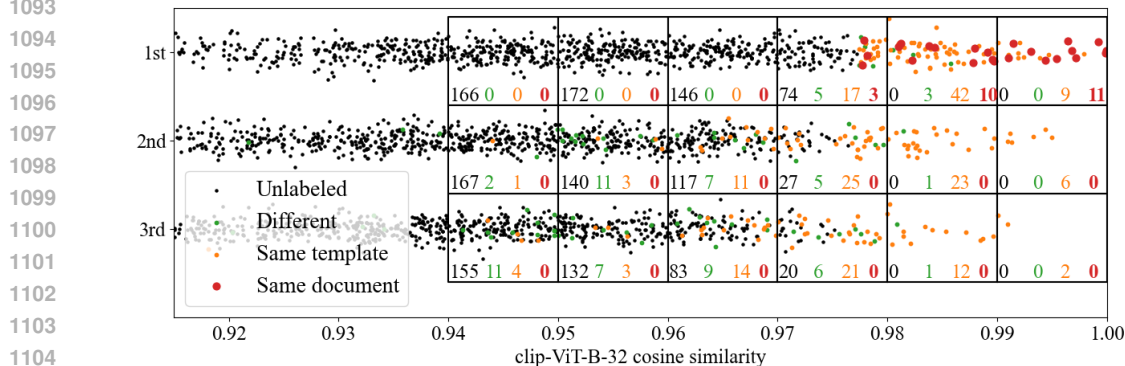
Figure 6: Cumulative distribution by cosine similarity. Each curve shows the proportion of samples in an evaluation dataset for which there exists at least one sample in the reference dataset with cosine similarity higher than the specified threshold. Lower values are better; higher cosine similarity thresholds are more pertinent. Based on human evaluations, samples with cosine similarity < 0.96 are unlikely to be problematic, whereas those > 0.98 are most likely problematic. Except for MMMU, and DudeMini, BigDocs-7.5M appears less contaminated than DocStruct4M.

Table 4: Detailed Results on Contamination Experiments, related to Figure 6. Lower values are better; higher cosine similarity thresholds are more pertinent. Except for MMMU and DudeMini, BigDocs-7.5M appears to be less contaminated by these metrics than DocStruct4M. Figure 3’s data comes from this table.

Cosine Similarity Threshold	Reference Dataset	DocVQA	InfoVQA	DeepForm	KLC	WTQ	TabFact	ChartQA	TextVQA	MMMU	DudeMini	SlideVQA-M	TableVQA
0.99	DocStruct4M	0.016	0.0	0.037	0.0033	0.0	0.00039	0.034	0.0	0.0026	0.0089	0.0	0.0027
	BigDocs-7.5M	0.0036	0.0	0.0	0.0	0.0	0.0	0.025	0.0	0.0	0.0089	0.0	0.0
0.98	DocStruct4M	0.065	0.0032	0.20	0.061	0.0	0.036	0.36	0.0020	0.0044	0.013	0.0	0.0067
	BigDocs-7.5M	0.012	0.0	0.0	0.0033	0.0	0.0	0.10	0.0	0.0035	0.011	0.0	0.0053
0.97	DocStruct4M	0.14	0.0032	0.41	0.16	0.0064	0.089	0.55	0.0044	0.0053	0.048	0.0014	0.0067
	BigDocs-7.5M	0.049	0.0	0.0	0.043	0.0	0.0	0.17	0.0	0.0061	0.053	0.0	0.0053
0.96	DocStruct4M	0.26	0.0057	0.57	0.24	0.031	0.14	0.63	0.0096	0.0070	0.15	0.0014	0.017
	BigDocs-7.5M	0.12	0.0	0.033	0.12	0.0	0.0	0.28	0.0	0.021	0.14	0.0	0.0087
0.95	DocStruct4M	0.39	0.0057	0.72	0.30	0.062	0.20	0.68	0.012	0.015	0.28	0.0014	0.04
	BigDocs-7.5M	0.24	0.0	0.21	0.22	0.0	0.0	0.45	0.0	0.045	0.22	0.0012	0.023
Number of samples		5349	2801	1500	4872	4343	12722	2500	5000	1140	5275	19600	1500
Number of unique images		1284	500	300	608	421	1693	1509	3166	1100	609	3596	751



(a) With respect to BigDocs-7.5M; top 200 samples human-labeled.



(b) With respect to DocStruct4M; top 100 samples human-labeled

Figure 7: Human evaluation of DocVQA’s overlap. Among the 1284 unique images in DocVQA’s samples, we use the same cosine similarity method as in figure 6 to identify the samples that are the most similar to samples in the corresponding training set. Although we prioritize using only the closest match, we also retrieve the second and third closest matches after deduplication (i.e., if the next closest match is identical to the previous match, skip it). A human is then tasked to label the top matches as either “different”, “same template” or “same document” (see text for definitions). Counts are provided for the most relevant 0.01-wide cosine similarity intervals. Most samples below 0.96 are “different”, and most samples above 0.98 are not. From these numbers, we expect less than 10% of the samples with cosine similarity below 0.97 to be “same template”, and less than 1% of the samples with cosine similarity below the same threshold to be “same document”. All identified “same document” are found at the first rank. There is only one instance where the first rank is “different” but a “same template” is identified at higher rank.

Consider the following edge cases:

- receipts for recurring orders emitted on different days;
- the same form filed by different people;
- different versions of the same form at the same company; and
- different full-page table from the same appendix of the same report.

Technically, all these cases involve pairs of different documents. However, one could argue that training on one such samples confers an unfair advantage to a model evaluated on the other sample. For this reason, we annotate such instances as *same template* whenever we encounter them.

Conversely, the “actual” same document can appear as quite diversified images. Indeed, stamps, watermarks, censorship, and/or annotations may be apposed *a posteriori* to a document, in addition to scaling, crops, rotations, and fax-induced artifacts. In all these cases, the original intent to communicate the same information matters: different copies of the same memorandum, scanned separately, are here treated as the *same document*.

With these definitions in hand, a human is tasked with labeling the samples that are most likely to be problematic in the DocVQA evaluation dataset. Figure 7 reports the results, calibrating how we interpret the cosine similarities for other evaluation datasets.

Note that this labeling procedure does not alter the composition of BigDocs-7.5M: we leave all samples, problematic or not, in the dataset. Instead, we release the annotations, which may help the community develop an intuition of the overlaps that may not have been identified yet, or even enable better detection strategies in the future.

A.4 DESCRIPTION OF DOWNSTREAM TASKS PROPOSED IN BIGDOCS-BENCH

The following is a formal description of the downstream tasks we aim to solve using the proposed BigDocs-Bench dataset.

A.4.1 IMAGE2FLOW

The task at hand is an image-to-flow conversion, where the input is an image of a flowchart, and the output is the corresponding information in JSON format. This JSON includes the nodes and edges that represent the flowchart’s structure.

Formally, given an image I representing a flowchart, the goal is to extract a graph $G = (V, E)$ where V is the set of nodes, and E is the set of directed edges between these nodes. The output $\text{JSON}(G)$ contains two main components: (1) a list of nodes V with their corresponding attributes such as node ID, label, shape, and description, and (2) a list of edges E with their source node ID, destination node ID, and label (if any).

The dataset for this task consists of 10,000 samples. Each sample includes an image of a flowchart, its corresponding Graphviz file, and a JSON representation.

The dataset was generated using the following pipeline: First, a random number between 5 and 15 was generated to determine the number of nodes in each flowchart. Based on the total number of nodes, a distribution was assigned to different types of nodes, such as conditions (diamond shape), statements (rectangular nodes), and others (parallelogram, circle). A random flow direction was then selected from the options: BT (bottom to top), TB (top to bottom), LR (left to right), and RL (right to left). Using the LLaMA 3.1 model, we used the prompt in Table A.4.1 to generate a Graphviz file.

Prompt used with Llama 3.1 to generate Graphviz data

```
Create a directed flowchart graph in DOT format with the
following specifications:
- The direction of the graph should be {direction}.
- Total number of nodes: {total_nodes}.
- Nodes distribution: {nodes}.
- The edges should connect the nodes in a way that makes sense:
* Each node should have at least one outgoing edge.
* For 'diamond' nodes, there should be at least two outgoing
edges. The graph can include any colors or additional styling.
Generate a valid and coherent graph. The graph should
represent an enterprise-level workflow like the steps of an
incident resolution workflow. The enterprise-level workflow
labels are so important. Just give me the graph in Graphviz
format no need for any python code or any description about the
graph.
```

Random colors and styles were applied to remove model biases toward specific stylings. The generated Graphviz files (.gv) were then converted to PNG images and JSON files. The JSON files contain two main components: Each node has an ID, label, shape, and a description of the shape (e.g., diamonds represent conditions). Each edge contains the source and destination node IDs and a label if present (the label represents the text on the edge).

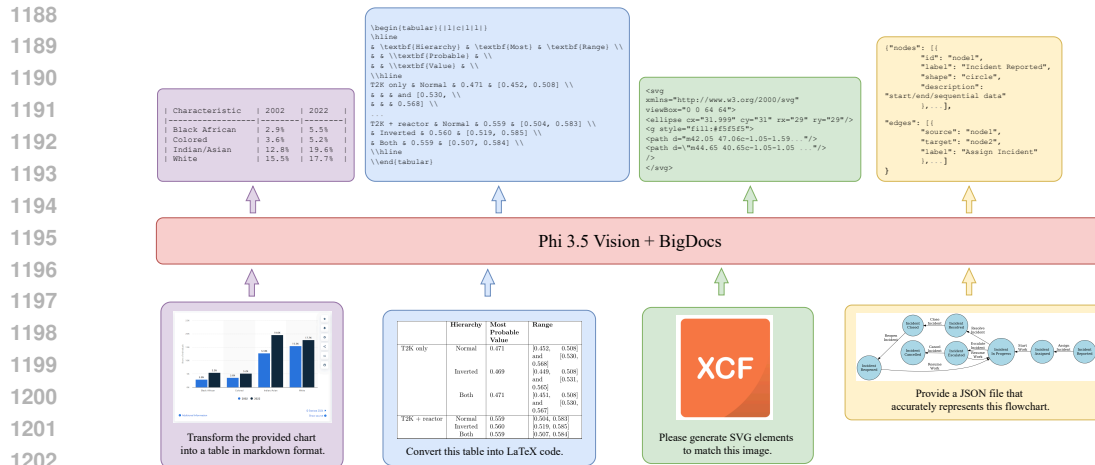


Figure 8: Qualitative Results. Generations of our Phi3.5-Vision model on the presented document downstream tasks, as part of the test set of BigDocs-Bench. We show samples of Chart2Markdown, Table2LaTeX, Image2SVG, and Image2Flow (JSON). A single model trained on BigDocs datasets can generate image-conditioned code in different coding languages while providing valid outputs.

A.4.2 SCREENSHOT2HTML

The Screenshot-to-HTML conversion task involves transforming an image of a website’s layout, such as a screenshot, into the corresponding HTML code that accurately reconstructs the structure and content of the original website. This process enables the generation of a functional website solely from its visual representation, facilitating applications in web design automation, accessibility enhancements, and rapid prototyping.

Formally, given an input image I depicting the visual layout of a website, the objective is to generate the HTML structure H that includes essential web elements such as headers, paragraphs, images, links, forms, and navigation bars. The resulting HTML code $\text{HTML}(H)$ should not only replicate the visual appearance of the original website but also ensure semantic correctness and structural integrity, enabling the recreated website to be interactive and accessible.

Data Collection and Filtering Process. The Image-to-HTML dataset was curated through an automated pipeline designed to ensure the quality and diversity of website layouts. Utilizing the Playwright library, the system asynchronously retrieves and renders websites from a comprehensive list of URLs (Penedo et al., 2024). Each website undergoes a series of checks to verify its accessibility, compliance with robots.txt directives, and predominance of English content. Additionally, content appropriateness is assessed by filtering out websites containing NSFW language.

External CSS and JavaScript resources are inlined to maintain consistency and reduce dependencies, and unnecessary or oversized scripts are removed. Images are replaced with placeholders, and background images are eliminated to focus on structural elements. The viewport is adjusted to capture only the visible portion of each page, enhancing the clarity of the layout representations.

Websites are further evaluated based on performance and structural metrics, including load time, page size, number of JavaScript and CSS files, DOM depth, and total number of HTML elements. Technologies and frameworks used by each website are identified to exclude those utilizing disallowed technologies, e.g., allowing a website to render without JavaScript. We also removed comments and prettified the HTML for standardization. Only websites that meet all predefined criteria are included in the final dataset.

Dataset Statistics. The resulting dataset comprises 11,000 website samples, each with a high-resolution screenshot and its corresponding HTML representation. On average, each layout contains 20.3 HTML elements, reflecting a diverse range of website designs. This diversity provides a robust foundation for training and evaluating image-to-HTML conversion models, ensuring the dataset is both comprehensive and representative of various web structures.

1242 A.4.3 TABLE2LATEX

1243
1244 The task involves identifying and associating tables in academic PDFs with their corresponding
1245 LaTeX code and captions. The aim is to precisely match each table image with the LaTeX source
1246 used to generate it and the relevant caption, ensuring accurate alignment between the visual content
1247 and its textual description.

1248 More specifically, given a table image I , the LaTeX code C used to render the table, and the caption
1249 T_{caption} , the goal is to create a dataset $\text{Dataset}(I, C, T_{\text{caption}})$ that establishes a reliable association
1250 between the tables, their LaTeX source, and their descriptive captions.

1251 We crawled publicly available, license-compliant arXiv papers to create this dataset, collecting both
1252 their PDFs and associated TeX source files. We began by parsing the TeX files to extract the LaTeX
1253 code for tables and their captions. Next, we used the PDF parsing library `PYMuPDF` to locate tables
1254 within the PDFs. However, this table detection process proved to be imperfect, as the algorithm
1255 frequently misidentified content with parallel lines as tables, leading to false positives.

1256 To address this challenge, we adopted an alternative approach. Instead of cropping tables directly
1257 from the PDFs—where false positives were common—we chose to render the parsed LaTeX table
1258 code to generate accurate table images. This method ensured that the images faithfully represented
1259 the original table formatting, reducing detection errors and improving the reliability of the dataset.
1260 As a result, we created a high-quality dataset comprising over 95,000 table images, each paired with
1261 its corresponding LaTeX code and caption, providing a valuable resource for further research into
1262 table structures in academic papers.

1264 A.4.4 IMAGE2SVG & TEXT2SVG

1265 Scalable Vector Graphics (SVG) provide a precise alternative to pixel-based images, capable of
1266 representing diagrams, icons, plots, and graphic designs with superior detail and scalability. Unlike
1267 raster images, SVGs can be scaled to any resolution without losing quality. In this work, we introduce
1268 the task of image-to-SVG generation, where the goal is to process an input image and generate
1269 SVG code that closely resembles the image upon rendering. This task requires advanced parsing
1270 capabilities for textual and numerical data and an understanding of various shapes, such as squares
1271 and arrows, commonly found in diagrams. Given an input image I , the model outputs SVG code
1272 C that visually replicates the image. Additionally, the task can extend to scenarios where a textual
1273 description T serves as input, yielding SVG code that aligns with the described content.

1274 We curate a dataset of images, SVG codes, and texts sourced from the SVG-Stack dataset introduced
1275 by StarVector (Rodriguez et al., 2023a). The curation process involves filtering to ensure high-quality
1276 samples. First, we filter based on image entropy to select images with complex designs and intricate
1277 details, excluding simpler icons or shapes. Second, we compute the CLIP Score (Hessel et al., 2022;
1278 Radford et al., 2019) for image-text pairs and retain the top 100k examples to build our curated
1279 SVG dataset. The SVG-Stack dataset adheres to permissive licensing standards, originating from
1280 TheStack (Kocetkov et al., 2022), carefully designed for open and permissive use.

1283 A.4.5 CHART2MARKDOWN

1284 This dataset is a novel contribution of our work, designed to assess the models’ capabilities in
1285 extracting data values from chart images. In this task, the model is given a chart image I and asked to
1286 produce a data table T of the underlying data table in markdown format.

1287 To create this dataset, we crawled recent chart images from the Statista website^e, focusing on charts
1288 from 2023 and 2024 that were not used in prior datasets like UniChart Masry et al. (2023) and
1289 ChartQA Masry et al. (2022). This ensures that the dataset reflects the most up-to-date facts and
1290 trends and overlaps less with existing datasets and benchmarks. We collected 6,516 chart images,
1291 their corresponding data tables, and human-written summaries.

1292
1293
1294
1295
^e<https://www.statista.com/>

1296 A.4.6 CHART2CAPTION

1297

1298 The task at hand is a chart-to-caption conversion. The input consists of an image of a chart along with
 1299 the code used to generate it and the dataset’s name and description. The output is a textual caption of
 1300 the important insights and information conveyed by the chart.

1301

1302 Formally, given a chart image I , the code C used to generate the chart, and the dataset information
 1303 D , the goal is to produce a caption $\text{Caption}(I, C, D)$ that highlights key insights and information
 1304 represented in the chart.

1305

1306 The dataset for this task consists of 1,496 pairs of chart images and the corresponding code that
 1307 generated these charts. The data was collected by selecting various Kaggle public datasets and their
 1308 associated data analytics notebooks. We executed these notebooks locally and parsed their outputs to
 1309 generate the chart-image and code pairs.

1309

1310 To generate the captions, we used the prompt below with the provided chart image, code, dataset
 1311 name, and description. The caption was generated by using InternVL2-26B (Chen et al., 2023; 2024).
 1312 This process allows us to leverage the model’s capabilities to generate meaningful captions based on
 1313 the provided context of the chart, code, and dataset description.

1313

1314  Prompt used with InternVL2-26B to generate chart summaries

1315

```
1316 You are a powerful data analyst. This is a notebook with name
1317 "{dataset_name}". In the description of this dataset, it's
1318 told that: "{dataset_description}". You are seeing a plot
1319 from this notebook. Here is the code that was used to generate
1320 this plot:
1321 {code}
```

1320

```
1321 Now as a data analyst, summarize the important insights and
1322 information about the chart.
```

1322

1323

1324

1325

1326

1327

1328

1329

1330

1331

1332

1333

1334

1335

1336

1337

1338

1339

1340

1341

1342

1343

1344

1345

1346

1347

1348

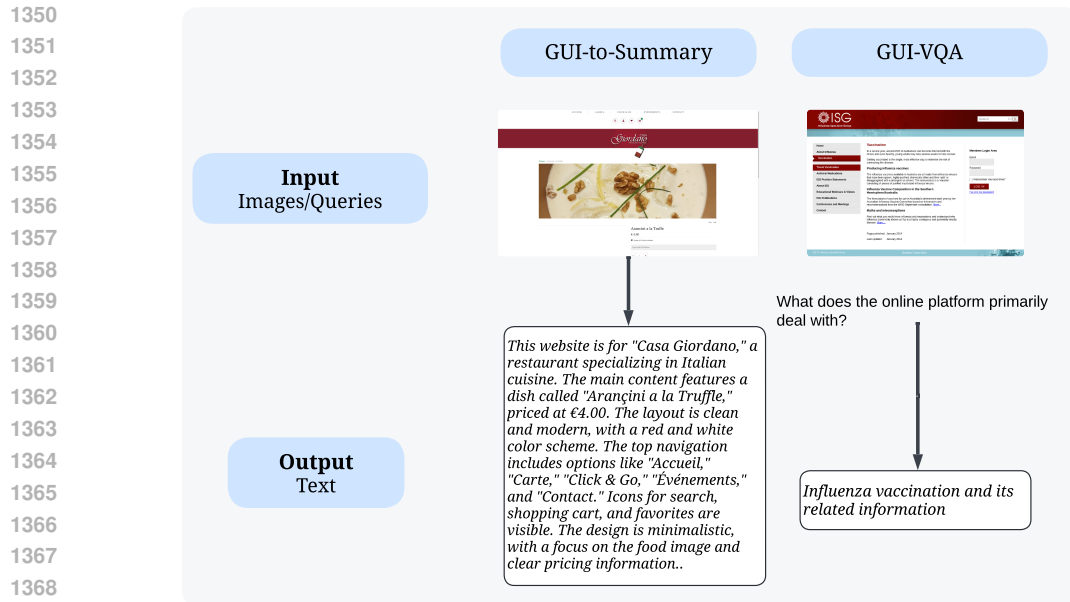
1349

1348

1349

1346  Prompt used with InternVL2-8B to generate website screenshot summaries

```
1348 Summarize this website in less than 100 words. Cover the main
1349 content, layout, color, and other style elements.
```



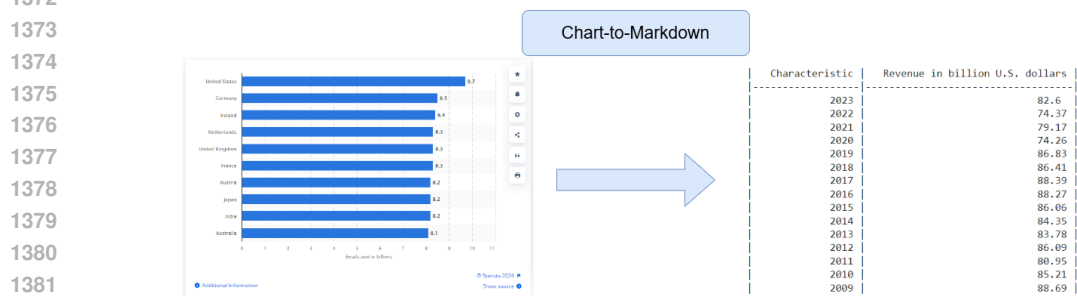
1369 **Figure 9: GUI-to-Summary and GUI-VQA introduced in BigDocs-Bench.**

1370

1371

1372

1373



1389 **Figure 10: Chart-to-Markdown task introduced in BigDocs-Bench.**

1387 A.4.9 GUI-VQA

1388

1389 In the GUI-VQA task, the model answers questions about website screenshots, covering the overall
 1390 content and specific elements like buttons, text boxes, and menu items. This task requires recognizing
 1391 key components within the GUI and understanding their functionalities and interdependencies. We
 1392 synthesized data for GUI-VQA using the GUI-to-Summary dataset. Specifically, we sampled a
 1393 sentence from each summary and prompted LLaMA 3.1-8b (Dubey et al., 2024) to convert it into a
 1394 QA pair. The prompt is shown in Appendix A.4.9.

1395  **Prompt used with InternVL2-8B to convert a summary to a QA pair.**

1397 You will be provided with a sentence. Your task is to convert
 1398 it into a question-answer pair. The question should focus
 1399 on factual information and avoid subjective inquiries. Do
 1400 not generate Yes/No questions. Structure the response in the
 1401 format:

1402 Q: {question}
 1403 A: {answer}

1404
1405
1406
1407
1408
1409
1410
1411
1412
1413
1414
1415
1416
1417
1418
1419
1420
1421
1422
1423
1424
1425
1426
1427
1428
1429
1430
1431
1432
1433
1434
1435
1436
1437
1438
1439
1440
1441
1442
1443
1444
1445
1446
1447
1448
1449
1450
1451
1452
1453
1454
1455
1456
1457

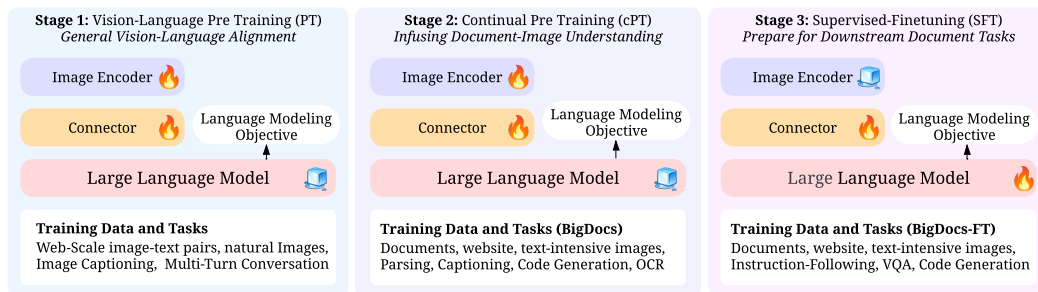


Figure 11: Training Stages for BigDocs. Three-Stage Training Pipeline for multimodal Document Understanding with BigDocs. Our approach consists of: (1) General Vision-Language Pretraining, (2) Document-Specific Continual Pretraining, and (3) Supervised Finetuning for Document Tasks. We evaluate the impact of BigDocs by using checkpoints of models after Stage 1, as provided by their original authors, and comparing them with models that undergo all three stages. Performance is assessed based on standard document tasks and novel tasks, including HTML/SVG code generation, flowchart generation/parsing, and LaTeX interpretation.

A.5 DETAILS ON TRAINING VISION-LANGUAGE MODELS ON BIGDOCS

Figure 11 illustrates our training pipeline for evaluating the quality of BigDocs and its impact compared to other datasets. The process has three stages: (1) Pretraining, which focuses on general modality alignment; (2) Continual pretraining, where models are further aligned to a specific domain, such as documents, using general tasks like OCR and captioning; and (3) Finetuning, which uses smaller datasets to prepare models for specific downstream tasks, like document processing.

We did not perform stage 1 in this paper, instead relying on checkpoints after pretraining. Additionally, we conducted some experiments using instruction-tuned checkpoints. Throughout all three stages, we employ a generative loss objective, specifically a categorical cross-entropy loss, to predict the next token given the context. The goal of BigDocs-7.5M is to enhance the model’s understanding and alignment with document-specific structures. At the same time, BigDocs-Bench focuses on training models to handle tasks that require processing images and converting them into structured code representations. These outputs often follow strict validity constraints to ensure they are syntactically correct. Additionally, the BigDocs-Bench test sets introduce novel benchmarks comprising five company-related downstream tasks, further validating the model’s ability to generalize to real-world document-based applications.

Training Details. We conduct all our experiments on a cluster of 64 H100 80GB GPUs leveraging the Transformers library (Wolf et al., 2019) for model development. Using Accelerate (Gugger et al., 2022) and Fully Sharded Data Parallel (FSDP) (Zhao et al., 2023), we distribute training over all GPUs in our cluster. We wrap the transformer blocks in both the encoder and the decoder into separate FSDP units with activation checkpointing to achieve a data parallel of 64 without running out of memory. FlashAttention-2 (Dao, 2024) gives a significant speedup on our training runs. For reproducibility, we provide the hyperparameters and training details of our experiments. All experiments maintain a constant total batch size of 256 and a learning rate of $2e-5$. We utilize the AdamW optimizer with the following parameters: a cosine learning rate scheduler, 60 warm-up steps, a beta1 coefficient of 0.95, a beta2 coefficient of 0.999, a weight decay of $1e-6$, and an epsilon value of $1e-8$. For the CPT experiments, models are trained for 1 epoch, while the finetuning experiments on the DocDownstream dataset and BigDocs-Bench are conducted over 3 epochs.

A.6 DETAILS ON BIGDOCS-BENCH’S EVALUATION

In this section, we dive into more details of the evaluation process for BigDocs-Bench, including the preprocessing procedure before the evaluation and the implementation details of the metrics.

A.6.1 PREPROCESSING

Before conducting the evaluation, we perform the following preprocessing step for both the ground truth and generation texts:

- 1458
1459
1460
1461
1462
1463
1464
1465
1466
1467
1468
1469
1470
1471
1472
1473
1474
1475
1476
1477
1478
1479
1480
1481
1482
1483
1484
1485
1486
1. **Image2Flow (GraphViz)**: If the text contains markdown-style fenced code blocks, we use a regular expression to extract the contents within the first code block; otherwise, we treat the entire text as GraphViz code and remove anything before `digraph` or `graph` if either exists. The flowchart triplets are extracted with the `pydot` library.
 2. **Image2Flow (JSON)**: If the text contains markdown-style fenced code blocks, we use a regular expression to extract the contents within the first code block; otherwise, we remove all contents outside the first “{” and last “}” in the text.
 3. **Screenshot2HTML**: If the text contains markdown-style fenced code blocks, we use a regular expression to extract the contents within the first code block; otherwise, we treat the entire text as the output HTML code. We first normalize the HTML code with `htmlmin.minify()`, which removes the comments in HTML and condenses the attributes to their most miniature possible representations. Then, we create the DOM tree with `BeautifulSoup4`.
 4. **Table2LaTeX**: If the text contains markdown-style fenced code blocks, we use a regular expression to extract the contents within the first code block; otherwise, we treat the entire text as the output LaTeX code. We use a series of regular expressions to normalize the contents. This procedure removes the comments, excessive whitespaces, and commands such as `\label`, `\cite`, `\citep`, `\citet`, `\ref`, `\eqref`, and `\pageref`.
 5. **Image2SVG & Text2SVG**: If the text contains markdown-style fenced code blocks, we use a regular expression to extract the contents within the first code block; otherwise, we treat the entire text as the output SVG code. We parse the SVG code and generate a PNG image with the `cairosvg` library.
 6. **Chart2Markdown**: If the text contains markdown-style fenced code blocks, we use a regular expression to extract the contents within the first code block; otherwise, we treat the entire text as the output Markdown code. We use regular expressions to remove the code’s comments, links, and excessive whitespaces.
 7. **Chart2Caption, GUI2UserIntent, GUI2Summary, & GUI-VQA**: We directly evaluate the generated texts against the ground truth.

1487 A.6.2 METRICS

1488
1489 Here, we provide brief explanations of BigDocs-Bench’s evaluation metrics.

- 1490
1491
1492
1493
1494
1495
1496
1497
1498
1499
1500
1501
1502
1503
1504
1505
1506
1507
1508
1509
1. **Flowchart Triplet F1**: Designed for Image2Flow tasks, this metric evaluates the accuracy of node relationships in flowchart codes, focusing on the correctness of edge triplets (s, e, d) extracted from GraphViz or JSON representations. Here, e denotes the edge label (set to `None` if unlabeled), while s and d represent the source and destination nodes, formatted as “label#shape”. The Triplet F1 score is calculated by comparing the generated triplet list against the ground truth, disregarding the ordering of nodes and edges to emphasize relational accuracy.
 2. **HTML DOM Tree Edit Distance**: Applicable to Screenshot2HTML tasks, this metric measures the similarity between generated and ground-truth DOM trees using the Tree Edit Distance. Leveraging `BeautifulSoup4` with `lxml` parsing and the `zss` library, the distance is normalized by the larger node count of the compared trees. Invalid GraphViz or JSON generations receive a Triplet F1 score of 0.
 3. **TeXBLEU (Jung et al., 2024)^f**: Utilized for the Table2LaTeX task, TeXBLEU employs a LaTeX-trained tokenizer and a finetuned embedding model with positional encoding. Unlike traditional BLEU, TeXBLEU assesses similarity based on n-gram token precision, demonstrating a higher correlation with human evaluations of LaTeX math expressions compared to BLEU, SacreBLEU, and Rouge (Jung et al., 2024).
 4. **RMSF1 (Liu et al., 2022)^g**: Used for the Chart2Markdown task, RMS F1 treats tables as mappings from headers to values, measuring textual and numeric similarity through

1510 ^fAvailable at <https://github.com/KyuDan1/TeXBLEU>.

1511 ^gAvailable at <https://github.com/google-research/google-research/tree/master/deplot>.

normalized Levenshtein distance and relative distance. This approach ensures robustness against row and column permutations and transpositions, making it well-suited for evaluating flexible Markdown table structures.

5. **DINOv2Score**: Employed in the Image2SVG task, this metric calculates the cosine similarity between representations of the ground-truth and generated images using DINOv2 (Oquab et al., 2023), which better captures image similarity than comparable models^h. Invalid SVG generations are assigned a DINOv2Score of 0.
6. **Rouge-L F1** (Lin, 2004): Applied to summarization and VQA tasks, Rouge-L F1 measures the longest common subsequence between the generated and reference texts. We compute this score using the implementation provided by `torchmetrics`.

A.7 MAKING BIGDOCS LICENSE-PERMISSIBLE

We dedicated significant effort to acquiring a license-permissible dataset suitable for training models for commercial purposes in document images. We aim to create a large-scale dataset that supports various tasks relevant to companies while adhering to accountability, responsibility, and transparency principles. To achieve this, we thoroughly investigated all public datasets concerning their licenses, evaluating both the sources of the images and their annotations. Our complete analysis, summarized in Table 5, enabled us to identify and retain only the sources that meet permissive licensing criteria.

Dataset licensing frameworks are crucial in determining how data can be used, shared, and modified, generally falling into two categories: *permissive* and *restrictive* licenses. *Permissive licenses* offer the most freedom, allowing for broad usage and modification of the data. For instance, the **CC0** license places the data in the public domain, enabling unrestricted use, modification, and distribution. The **MIT License** permits both commercial and non-commercial applications, provided the license terms are retained in any distribution. In contrast, the **Apache 2.0** License extends these freedoms with an additional grant of patent rights.

In contrast, *restrictive licenses* imposes certain limitations on data usage. The CC BY license requires users to provide attribution to the original creator. In contrast, the **CC BY-SA** license demands that any derivative works also carry the same licensing terms. More restrictive options, like the **CC BY-NC** and **CC BY-ND** licenses, prohibit commercial use and modifications, respectively. In cases where the licensing terms are *unclear*, it is prudent to exercise caution in using the data, as misinterpretation can lead to legal risks.

Additionally, the concept of **Fair Use** allows for limited use of copyrighted material without explicit permission, particularly for purposes such as research, criticism, or commentary. However, Fair Use does not equate to unrestricted permission, and its applicability can vary, necessitating careful consideration when applied to dataset usage in research contexts.

A.8 HUMAN EVALUATION

To ensure fairness and minimize bias, we invited evaluators from diverse backgrounds, including PhD researchers, ML practitioners, multimodal AI experts, and individuals from both technical and non-technical domains. Key authors were excluded from participating to avoid conflicts of interest. Some non-key authors, such as advisors and authors who performed smaller tasks on the data creation effort, participated. These authors did not know the performance of models on the proposed tasks. For the evaluation, we used our own web interface, to make sure that all participants were anonymous and model outputs were randomized to prevent pattern recognition. We are open to releasing the detailed human evaluation results, as a supplementary document.

We developed a web application using Flask, Javascript, and HTML/CSS where users are presented with pairs of outputs from two models and are asked to judge which model has better output for a given input image. See Figure 12 for a snapshot of the platform.

1566
1567
1568
1569
1570
1571
1572
1573
1574
1575
1576
1577
1578
1579
1580
1581
1582
1583
1584
1585
1586
1587
1588
1589
1590
1591
1592
1593
1594
1595
1596
1597
1598
1599
1600
1601
1602
1603
1604
1605
1606
1607
1608
1609
1610
1611
1612
1613
1614
1615
1616
1617
1618
1619

Table 5: Datasheet of candidate datasets. For transparency purposes, we provide a detailed description of over 100 datasets considered in curating our BigDocs dataset. This table presents a systematic analysis of public datasets, including information on medium types, source documents, text structures, languages, years, annotation types and methods, and licensing for both data and annotations. We also share sample counts across different modalities and splits. Some fields may be blank due to unavailable information. This comprehensive overview enables assessment of each dataset’s characteristics and potential contributions to BigDocs.

Dataset Name	Medium	Source Document Type	Data Sourcing	Text Type	Text Structure	Text Languages	Annotation Type	Annotation Method	Images	Annotations	Permissions	Documents	Annotations	Documents	Annotations	
ArxivBank	Photo	Article	Repository - Governed	Computer Generated	Structures - Chats	English	Q&A (Question and Answer)	Automated	MIT	MIT	Good to use	302997	302997	Image - Figure	Full page annotation	
ArxivBank	Photo	Article	Repository - Governed	Computer Generated	Structures - Chats	English	Q&A (Question and Answer)	Automated	MIT	MIT	Good to use	176039	200000	Image - Figure	Full page annotation	
ArxivBank	Digital - Work-Lines	Article - Scientific paper	Repository - AOVV	Computer Generated	Text with Structures	English	OCR - Layout	Weak Supervision	Apache 2	Apache 2	Good to use	500000	500000	Page	Full page annotation	
ArxivBank	Digital - Work-Lines	Article - Scientific paper	Repository - AOVV	Computer Generated	Text with Structures	English, Chinese, Japanese, Arabic, Other	OCR - Table Detection/Extraction	Weak Supervision	Unknown license	Apache 2	Borderline	424045	502597	Multi-page	Element - Table structure	
ArxivBank	Scanned, Digital	Legal, Business	Repository - Governed	Handwritten, Typewritten, Computer Generated	Structures, Text with Structures	English	OCR, Q&A (Question and Answer)	Annotation - Crowd-sourced	Fair Use	MIT	Borderline	12567	50000	Multi-page	Element - Q&A pair	
ArxivBank	Digital	Infographics	Repository - Governed	Computer Generated	Infographics	English	Q&A (Question and Answer)	Annotation - In-house	Unknown license	CC BY	Borderline	5485	30035	Image	Element - Q&A pair	
ArxivBank	Digital	Book - Textbook, Infographics	Repository - Governed	Computer Generated	Text with Structures	English	Q&A (Question and Answer)	Weak Supervision	CC - BY-NC 4.0	CC - BY-NC 4.0	Not good to use	1096	26260	Multi-page	Element - Q&A pair	
ArxivBank	Photo	Natural Scene	Dataset	Computer Generated	Natural Image	English	OCR - Layout	Weak Supervision	CC BY 2.0	CC - BY 2.0	Good to use	11839	130818	Image	Word	
ArxivBank	Digital - Web	Book - Manual	Repository - Governed	Computer Generated	Text with Images	English	Q&A (Question and Answer)	Weak Supervision	Various Licenses	Various Licenses	Not sure	19797	30786	Multi-page	Element - Q&A pair	
ArxivBank	Photo	Natural Scene	Dataset	Computer Generated	Natural Image	English	Q&A (Question and Answer)	Annotation - Crowd-sourced	Unknown license	Unknown license	Not sure	22026	30791	Image	Element - Q&A pair	
ArxivBank	Digital	Synthetic	Computer Generated	Computer Generated	Structures - Figures	English	Q&A (Question and Answer)	Synthetic	MIT	MIT	Good to use	140000	180000	Image	Element - Q&A pair	
ArxivBank	Scanned	Infographics	Dataset	Computer Generated	Infographics - Covers	English	Q&A (Question and Answer)	Weak Supervision	Fair Use	Apache 2	Borderline	20752	100000	Image	Element - Q&A pair	
ArxivBank	Digital	Synthetic	Computer Generated	Computer Generated	Structures - Chats	English	Q&A (Question and Answer)	Weak Supervision	CC - BY-NC 4.0	CC - BY-NC 4.0	Not good to use	306	348104	Image	Element - Q&A pair	
ArxivBank	Photo	Natural Scene	Dataset	Computer Generated	Natural Image	English, Chinese, French, German, Italian, Spanish, Bulgarian, Croatian, Serbian	Q&A (Question and Answer)	Weak Supervision	CC - BY-SA 4.0	Apache 2	Good to use	20932	20932	Multi-page	Element - Answers	
ArxivBank	Digital	Business	Repository - Governed	Computer Generated	Structures	English	Key-Info Extraction	Annotation - Crowd-sourced	Custom	Custom	Not good to use	106608	106608	Multi-page	Full page annotation	
ArxivBank	Digital	Synthetic	Repository - Governed	Computer Generated	Structures - Chats	English	Q&A (Question and Answer)	Weak Supervision	Unknown license	Unknown license	Not sure	2406	1388	Image - Figure	Element - Q&A pair	
ArxivBank	Digital	Article - Wikipedia	Repository - Governed	Computer Generated	Structures - Tables	English	Q&A (Question and Answer)	Annotation - Crowd-sourced	CC - BY 4.0	CC - BY 4.0	Good to use	2108	22033	Image - Table	Element - Q&A pair	
ArxivBank	Digital - Web	Book - Textbook	Repository - Governed	Computer Generated	Text with Structures	English	Q&A - Referred to a Book	Annotation - Crowd-sourced	Unknown license	Custom	Not good to use	10000	30562	Image	Element - Q&A pair	
ArxivBank	Digital	Report - Financial	Repository - Governed	Computer Generated	Text with Structures	English	Q&A - Referred to a Summary	Weak Supervision	CC - BY 3.0	CC 0	Good to use	17458	17458	Multi-page	Element - Summary	
ArxivBank	Digital	Article - Wikipedia	Repository - Governed	Computer Generated	Structures - Tables	English	Q&A - True/False	Annotation - Crowd-sourced	CC - BY-SA 4.0	CC - BY-SA 4.0	Good to use	16375	117854	Image	Element - Sentence	
ArxivBank	Digital	Report - Financial	Repository - Governed	Computer Generated	Structures - Tables	English	Q&A - True/False	Weak Supervision	CC - BY-SA 4.0	CC - BY-SA 4.0	Good to use	112887	112887	Image - Table	Element - Table structure	
ArxivBank	Photo	Natural Scene	Dataset	Computer Generated	Natural Image	English	Q&A (Question and Answer)	Weak Supervision - Permissible like GPT	Various Licenses	Various Licenses	Not sure	100077	424011	Image	Element - Q&A pair	
ArxivBank	Digital	Report	Repository - Governed	Computer Generated	Text with Structures	English	NIE (Name-Entity Recognition)	Weak Supervision	Unknown license	Unknown license	Not sure	2778	2778	Multi-page	Full page annotation	
ArxivBank	Digital - PDF	Business	Repository - Governed	Computer Generated	Structures	English	Q&A (Question and Answer)	Weak Supervision	Unknown license	Unknown license	Not sure	2000	2000	Image	Full page annotation	
ArxivBank	Scanned	Business - Receipts	Crowdsourced	Computer Generated	Structures - Forms	English	OCR - Layout, Key-Info	Annotation - Crowd-sourced	CC BY 4.0	CC BY 4.0	Good to use	1000	1000	Image	Full page annotation	
ArxivBank	Scanned	Business	Dataset	Computer Generated	Structures - Forms	English	OCR - Layout, Key-Info	Annotation - Crowd-sourced	Unknown license	Unknown license	Not good to use	199	199	Image	Full page annotation	
ArxivBank	Digital - PDF	Administrative	Repository - Governed	Computer Generated	Text with Structures	English	Key-Info Extraction, OCR	Annotation - Volunteers	MIT	MIT	Not sure	20000	20000	Multi-page	Full page annotation	
ArxivBank	Photo	Natural Scene	Dataset	Computer Generated	Natural Image	English	Caption - Bounding box	Annotation - Crowd-sourced	Unknown license	CC - BY 4.0	CC - BY 4.0	Not sure	2000	2000	Image	Word
ArxivBank	Photo	Natural Scene	Dataset	Computer Generated	Natural Image	English	Caption - Bounding box	Annotation - In-house	CC - BY 4.0	CC - BY 4.0	Good to use	20134	90369	Image	Word	
ArxivBank	Digital - PDF	Article - Scientific paper	Repository - Published	Computer Generated	Structures - Tables	English	OCR - Table	Annotation	MIT	MIT	Good to use	940000	-	Multi-page	-	
ArxivBank	Digital - PDF	Article - Scientific paper	Repository - Published	Computer Generated	Structures - Tables	English	OCR - Table	Annotation	MIT	MIT	Good to use	940000	-	Multi-page	-	
ArxivBank	Photo	Natural Scene	Dataset	Computer Generated	Structures - Forms	English	OCR - Layout	Annotation	Unknown license	Unknown license	Not sure	1915	-	Multi-page	Full page annotation	
ArxivBank	Digital - PDF	Administrative	Repository - Governed	Computer Generated	Structures - Forms	English	OCR - Layout	Annotation - In-house	Unknown license	Unknown license	Not sure	641	-	Multi-page	-	
ArxivBank	Digital - Web	Synthetic	Repository - Governed	Computer Generated	Text with Images	English	OCR - Layout	Annotation - In-house	Unknown license	Unknown license	Not sure	82000	-	Image - Screenshot	Code	
ArxivBank	Digital - Web	Synthetic	Repository - Governed	Computer Generated	Text with Images	English	OCR - Layout	Annotation - In-house	Unknown license	Unknown license	Not sure	641	-	Multi-page	-	
ArxivBank	Photo	Natural Scene	Dataset	Computer Generated	Natural Image	English	OCR - Q&A (Question and Answer)	Annotation	CC BY 4.0	CC - BY 4.0	Good to use	200000	-	Image - Screenshot	Code	
ArxivBank	Photo	Natural Scene	Dataset	Computer Generated	Natural Image	English	OCR - Q&A (Question and Answer)	Annotation	CC BY 4.0	CC - BY 4.0	Good to use	28408	43336	Image	Element - Q&A pair	
ArxivBank	Digital	Article - Scientific paper	Repository - AOVV	Computer Generated	Structures - Figures	English	Q&A	Annotation	Various Licenses	Various Licenses	Borderline	10435	10245	Image	Element - Caption	
ArxivBank	Photo	Natural Scene	Repository - No Text	No Text	Caption	English	LLM generated - Permissible like GPT	Annotation	Various Licenses	Various Licenses	Good to use	2523247	34330	Image	Element - Caption	
ArxivBank	Scanned	Article, Report, Legal documents	Repository - Governed	Handwritten, Typewritten, Computer Generated	Text with Structures	English	OCR - Class	Annotation	CC - BY 4.0	CC - BY 4.0	Good to use	399999	399999	Image	Full page annotation	
ArxivBank	Scanned	Article, Report, Legal documents	Repository - Governed	Handwritten, Typewritten, Computer Generated	Text with Structures	English	OCR - Class	Annotation	CC - BY 4.0	CC - BY 4.0	Good to use	11000000	11000000	Image	Full page annotation	
ArxivBank	Scanned	Article, Report, Legal documents	Repository - Governed	Handwritten, Typewritten, Computer Generated	Text with Structures	English	OCR - Class	Annotation	WTFPL	WTFPL	Good to use	2621635	2621635	Page	Full page annotation	
ArxivBank	Digital - PDF	Various	Dataset	Computer Generated	Text with Structures	English	Caption	LLM generated - Permissible like GPT	Various Licenses	Various Licenses	Not good to use	100000	100000	Image	Element - Caption	
ArxivBank	Photo	Natural Scene	Dataset	No Text	Caption	English	LLM generated - Permissible like GPT	Various Licenses	CC - BY 4.0	CC - BY 4.0	Not good to use	120000	120000	Image	Element - Caption	
ArxivBank	Photo	Natural Scene	Dataset	No Text	Caption	English	LLM generated - Permissible like GPT	Various Licenses	CC - BY 4.0	CC - BY 4.0	Not good to use	150000	150000	Image	Element - Q&A pair	
ArxivBank	Photo	Natural Scene	Dataset	No Text	Caption	English	LLM generated - Permissible like GPT	Various Licenses	CC - BY 4.0	CC - BY 4.0	Not good to use	395000	395000	Image	Element - Q&A pair	
ArxivBank	Photo	Natural Scene	Dataset	No Text	Caption	English	LLM generated - Permissible like GPT	Various Licenses	CC - BY 4.0	CC - BY 4.0	Not good to use	41500000	41500000	Image	Element - Caption	
ArxivBank	Photo	Natural Scene	Dataset	No Text	Caption	English	LLM generated - Permissible like GPT	Various Licenses	CC - BY 4.0	CC - BY 4.0	Not good to use	385000000	385000000	Image	Element - Caption	
ArxivBank	Photo	Natural Scene	Dataset	No Text	Caption	English	LLM generated - Permissible like GPT	Various Licenses	CC - BY 4.0	CC - BY 4.0	Not good to use	600000000	600000000	Image	Element - Caption	
ArxivBank	Photo	Natural Scene	Dataset	No Text	Caption	English	LLM generated - Permissible like GPT	Various Licenses	CC - BY 4.0	CC - BY 4.0	Not good to use	130000000	130000000	Image	Element - Caption	
ArxivBank	Photo	Natural Scene	Dataset	No Text	Caption	English	LLM generated - Permissible like GPT	Various Licenses	CC - BY 4.0	CC - BY 4.0	Not good to use	10000	20000	Image	Element - Q&A pair	
ArxivBank	Photo	Natural Scene	Dataset	No Text	Caption	English	LLM generated - Permissible like GPT	Various Licenses	CC - BY 4.0	CC - BY 4.0	Not good to use	100077	117158	Image	Element - Q&A pair	
ArxivBank	Photo	Natural Scene	Dataset	No Text	Caption	English	LLM generated - Permissible like GPT	Various Licenses	CC - BY 4.0	CC - BY 4.0	Not sure	14011	14025	Image	Element - Q&A pair	
ArxivBank	Photo	Natural Scene	Dataset	No Text	Caption	English	LLM generated - Permissible like GPT	Various Licenses	CC - BY 4.0	CC - BY 4.0	Not sure	23500	24000	Image	Element - Q&A pair	
ArxivBank	Photo	Natural Scene	Dataset	No Text	Caption	English	LLM generated - Permissible like GPT	Various Licenses	CC - BY 4.0	CC - BY 4.0	Not sure	133000	133000	Image	Element - Q&A pair	
ArxivBank	Digital	Infographics	Crowdsourced	Computer Generated	Text with Images	English	Class	Annotation - Crowd-sourced	Custom	Custom	Not sure	10000	10000	Image	Element - Class	
ArxivBank	Digital	Article	Dataset	Computer Generated	Structures - Tables	English	Q&A (Question and Answer)	LLM generated - Permissible like GPT	Various Licenses	Various Licenses	Not good to use	97000	15000	Image - Table	Element - Q&A pair	

A.9 DETAILS OF UNIFIED METADATA FRAMEWORK

We propose a unified metadata framework for the BigDocs dataset to ensure transparency and traceability. This framework is organized into three primary keys: license, origin, and an optional features section. By adopting this structure, we provide a standardized and flexible system that enhances the dataset’s usability, ensuring clarity for research and commercial applications.

Along with the dataset, we include two separate files named `tracking_instructions.json` and `tracking_transformations.json`, which are dictionaries that store information standards across large subsets of samples, reducing redundancy and promoting consistency in metadata.

License Metadata The `license` key is mandatory and provides detailed information regarding the licensing terms of both the images and annotations. It is structured as a dictionary with three sub-keys:

^h<https://medium.com/aimonks/clip-vs-dinov2-in-image-similarity-6fa5aa7ed8c6>

1620
1621
1622
1623
1624
1625
1626
1627
1628
1629
1630
1631
1632
1633
1634
1635
1636
1637
1638
1639
1640
1641
1642
1643
1644
1645
1646
1647
1648
1649
1650
1651
1652
1653
1654
1655
1656
1657
1658
1659
1660
1661
1662
1663
1664
1665
1666
1667
1668
1669
1670
1671
1672
1673

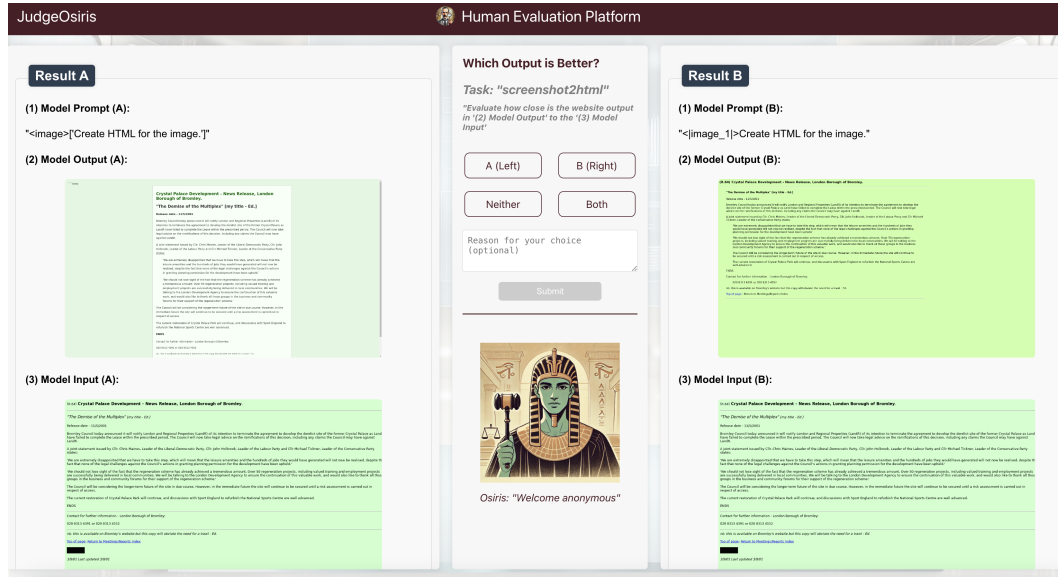


Figure 12: Human Evaluation Platform. A user is presented with two model outputs and asked to select the one that is more accurate in relation to the original model input.

Proposed metadata of a data sample from TabFact dataset (Chen et al., 2020)

```

metadata: features: {image_height: 1584, image_width: 1224}, license: {annotation_license: CC BY 4.0, image_license: CC BY-SA 4.0}, origin: {table_path: data/all_csv/2-15401676-3.html.csv, data_id: 2-15401676-3.html.csv, dataset_url: https://github.com/wenhuchen/Table-Fact-Checking.git, tracking_instruction_id: tabfact, tracking_transformation_id: tabfact_1}
tracking_instructions.json: tabfact: "Clone repo from dataset_url, locate CSV via table_path, render image."
tracking_transformations.json:

```

ID	Description
tabfact_1	Use table title as image caption.
tabfact_2	Concatenate annotation facts as summary.
tabfact_3	Load table using csv, convert to markdown.

Figure 13: Metadata framework from our BigDocs Toolkit for a sample in the BigDocs 7.5M dataset. It includes details about image properties, licenses, data sources, and transformation steps, such as using the table title as an image caption.

- `image_license` (mandatory): Specifies the license under which the image is provided.
- `annotation_license` (mandatory): Indicates the license for the annotations or labels associated with the image (e.g., text, bounding boxes, tables).
- `license_note` (optional): Includes additional licensing information or clarifications, such as specific usage conditions or exceptions. This allows for clear communication of any nuances in licensing terms.

Origin Metadata The `origin` key is mandatory and serves as a traceability mechanism, allowing users to track each data sample back to its source. This key is also structured as a dictionary and includes the following sub-keys:

- `data_id` (mandatory): A unique identifier for each data sample (e.g., file name, index, or ID in the source dataset).
- `tracking_instruction_id` (mandatory): A reference to an entry in the `tracking_instructions.json` file, specifying how to use the metadata fields to trace the data sample back to its source.

- 1674 • `tracking_transformation_id` (optional): A reference to an entry in the
1675 `tracking_transformations.json` file, providing a high-level description of any
1676 transformations or modifications applied to the original sample.
- 1677 • `dataset_url` (optional): The URL of the original dataset from which the sample was
1678 obtained, if applicable.
- 1679 • `image_path` (optional): The local path to the image within the raw dataset files, if
1680 available. This key is helpful when the dataset is stored in raw form.
- 1681 • `image_url` (optional): The URL from which the image was initially downloaded.
- 1682 • `Misc.` (optional): Other information related to the origin of the data entry.

1685 **Features Metadata** The `features` key provides detailed characteristics of the data sample. This
1686 can be useful for downstream tasks that require specific information about the sample, like the image
1687 size and type of annotations.

- 1688 • `image_height`: The height of the image, in pixels.
- 1689 • `image_width`: The width of the image, in pixels.

1692 **Common Metadata Files.** The `tracking_instructions.json` and
1693 `tracking_transformations.json` files are designed to store information common
1694 to many samples, minimizing redundancy and ensuring consistency. Each file is structured as a
1695 dictionary:

- 1696 • `tracking_instructions.json`: Contains instructions on how to use the metadata
1697 fields (such as `data_id`, `dataset_url`, etc.) to trace the data sample back to its source.
1698 Each entry is uniquely identified and can be referenced in the individual sample metadata by
1699 `tracking_instruction_id`.
- 1700 • `tracking_transformations.json`: Contains descriptions of any transformations,
1701 processing steps, or additions to the original samples. This includes synthetic gen-
1702 eration processes, data augmentation steps, or other modifications. Each transforma-
1703 tion is uniquely identified and can be referenced in the individual sample metadata by
1704 `tracking_transformation_id`.

1706 A.10 QUALITATIVE RESULTS

1708 **We provide a detailed qualitative analysis to highlight the performance of different models**
1709 **on tasks within BigDocs-Bench. Table 6 showcases the outputs of our best-performing model,**
1710 **Phi-3.5-Vision trained on BigDocs, alongside a publicly available instruction-tuned model**
1711 **and GPT4o. The analysis covers tasks such as GUI-VQA, Chart2Caption, Image2Latex,**
1712 **and Screenshot2HTML. Notably, the BigDocs-trained model demonstrates more concise and**
1713 **accurate free-form outputs for VQA tasks, generates perfect LaTeX tables from table images,**
1714 **and produces precise HTML code from web screenshots.**

1715 **Additionally, we present a series of qualitative examples across BigDocs-Bench tasks, detailed**
1716 **in Tables 9-28. These examples provide direct comparisons of outputs from all models discussed**
1717 **in the paper. The examples are accompanied by a thorough error analysis that highlights each**
1718 **model’s strengths, limitations, and both success and failure cases.**


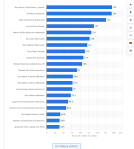






1720 A.11 GLOSSARY & TASK DEFINITIONS

1721 We facilitate a list of concepts introduced and utilized throughout our research. Below is a list of
1722 these concepts and tasks, along with their definitions, including descriptions, inputs, and outputs.

1724 1. Text with Structures

- 1725 • **Description:** Analyzing documents combining text with elements like headers, lists, and
1726 paragraphs to understand the overall structure and organization.
- 1727 • **Input:** Documents containing structured text elements such as headers, lists, and paragraphs.

Table 6: Task Structure and Samples with Model Outputs for Phi Models and GPT-4o

Task	Query	Phi-3.5-Vision Instruct	Phi-3.5-Vision Instruct-BigDocs	GPT-4o
GUI-VQA	 [What opens when the user clicks [550, 0, 600, 80]?]	[The image does not provide information on what opens when the user clicks the specified coordinates.]	[View the news]	[By clicking on the coordinates [620, 50, 650, 70], the user will navigate to the "news" section of the website.]
Chart2Caption	 [I need a caption for the chart in the image, please]	[The image displays a pie chart with various segments, each representing a different range of values and their corresponding percentages. The segments are color-coded and labeled with both the value range and the percentage they represent. The chart is sourced from Statista 2024]	[In 2022, the most common salary range for employees in the United Kingdom was between 100,000 and 149,999 British pounds, with 19.3 percent of employees falling into this bracket. Employees earning between 200,000 and 249,999 British pounds made up the second most common salary range, at 15.8 percent.]	[Distribution of Income Levels: A Pie Chart Showing the Percentage of Households by Income Bracket in 2024]
Image2Latex	 [Create LaTeX code to produce this table.]			
Screenshot2HTML	 [Could you create Hypertext Markup Language code from the screenshot?]			

- **Output:** A structured representation of the document’s content.

2. Structures - Figures

- **Description:** Identifying and interpreting figures, diagrams, and other visual elements in documents to extract the information they represent.
- **Input:** Documents with embedded figures, diagrams, and visual elements.
- **Output:** A detailed understanding or extraction of the visual content.

3. Infographics - Covers

- **Description:** Examining infographics and cover pages that use a mix of text and graphics to communicate information visually.
- **Input:** Infographics and cover pages containing text and visual elements.
- **Output:** A comprehensive analysis of the combined visual and textual information.

4. Structures - Tables

- **Description:** Finding and understanding tables in documents, focusing on accurately capturing the data and relationships they present.
- **Input:** Documents containing tabular data.
- **Output:** A structured dataset or representation of the tabular information.

5. Structures - Forms

- **Description:** Recognizing and processing forms within documents, extracting data from fields and labels typically found in structured forms.

- **Input:** Documents with structured forms, including fields and labels.
- **Output:** An organized collection of the extracted form data.

6. Natural Image

- **Description:** Analyzing photographs or natural images in documents, interpreting their content in the context of the surrounding text.
- **Input:** Documents containing photographs or natural images.
- **Output:** An interpreted or categorized representation of the image content.

A.12 ABLATION EXPERIMENTS

A.12.1 ABLATIONS ON DATA CURATION

We ablated the main data curation procedures on BigDocs, namely the use of 1) VQA format during CPT, i.e. using (question, image, answer) tuples with *assistant* and *user* conversation formats, 2) the use of heavy OCR tasks during CPT (converting most of our document images into OCR tasks) and our 3) text-image alignment tasks, mainly captioning of many datasets.

Experiment Setup. Using the Phi3.5-Vision-Instruct model, we created three modified versions

Table 7: Ablation Experiment on the effect of VQA formatting, presence of OCR data, and presence of captioning data in BigDocs-7.5M. Results show the importance of including these curation steps and tasks. See discussion in Section A.12.

Model	DocVQA VAL	InfoVQA VAL	DeepForm TEST	KLC TEST	WTQ TEST	TabFact TEST	ChartQA TEST	TextVQA VAL	MMMU VAL	DuDeMini TEST	SlideVQA-M TEST	TableVQA TEST	Avg. Score
Original	87.05	70.05	70.97	37.45	51.21	81.24	81.56	68.72	45.00	36.15	32.47	67.77	60.80
No VQA	82.65 (-4.4)	54.92 (-15.13)	40.64 (-30.33)	28.8 (-8.65)	36.93 (-14.28)	65.3 (-15.94)	78.4 (-3.16)	65.24 (-3.48)	42.33 (-2.67)	34.71 (-1.44)	8.37 2(-4.1)	61.13 (-6.64)	51.62 (-9.19)
30% OCR	85.79 (-1.26)	60.03 (-10.02)	54.19 (-16.78)	34.9 (-2.55)	52.68 (1.47)	73.76 (-7.48)	81.56 (0)	72.07 (3.35)	42.56 (-2.44)	36.72 (0.57)	32.07 (-0.4)	70.83 (3.06)	58.1 (-2.71)
30% caption	85.36 (-1.69)	57.98 (-12.07)	53.36 (-17.61)	35.09 (-2.36)	50.91 (-0.3)	72.5 (-8.74)	82.4 (0.84)	71.92 (3.2)	40.89 (-4.11)	36.76 (0.61)	31.97 (-0.5)	69.37 (1.6)	57.38 (-3.43)

of BigDocs-7.5M: one without the VQA format, one with OCR tasks removed, and one with reduced captioning tasks (text-image alignment). Each dataset variant was used to train the model, followed by fine-tuning the model on our instruction-tuning datasets. We evaluated these models on the benchmarks listed in Table 2 (General Document Benchmarks). The results are presented below. In parentheses, we show the delta with respect to the original result.

Main Findings.

1. **VQA Format:** VQA formatting proved crucial, as its removal led to a 9.19% average performance decrease. This was especially apparent in InfoVQA (-15.13), DeepForm (-30.33), WTQ (-14.28), and TabFact (-15.94). A common pattern observed here is a lack of adherence to the requested output format as demonstrated in the example in Table X. We hypothesize that the VQA format used in the continual pre-training stage (CPT) enables better instruction tuning and supports multitask generalization.
2. **OCR Impact:** Removing OCR tasks led to an average performance drop of 2.71%, with varying impacts across benchmarks. Notably, we observed significant declines on InfoVQA (-10.02), DeepForm (-16.78), and TabFact (-7.48), while results on DUDE, SlideVQA, and ChartQA remained largely unaffected. The reduction in OCR data increased hallucination in tasks requiring precise information extraction. For instance, in DeepForm, the true negative rate dropped from 62% to 0%, as models began hallucinating unrelated values from other parts of the document. Examples illustrating this behavior are provided in Tables X and Y. Interestingly, in some cases such as TableVQA (+3.06) and TextVQA (+3.35), performance improved, likely due to the nature of the question-answering tasks, which often favor free-form text generation over exact OCR matches. Table 21 shows an example of this phenomenon.

- 1836 3. **Text-Image Alignment:** Reducing text-image alignment tasks, particularly captioning,
 1837 resulted in a 3.4% performance drop, with notable declines on InfoVQA (-12.07),
 1838 DeepForm (-17.61), and TabFact (-8.74). This drop primarily stemmed from errors in
 1839 parsing values for arithmetic operations, especially when data formats varied, such as
 1840 converting text or unique visual elements into percentages illustrated by examples in
 1841 Table X, Table Y and Table Z. Tasks without significant drops, like WTQ and ChartQA,
 1842 involve simpler text-visual correspondences that don't require complex conversions.
 1843 See Table 22 for a qualitative example

1844 1845 1846 A.12.2 ABLATION ON CONTEXT LENGTH

1847
1848 The results presented thus far have been limited to a context length of 8192 tokens. Given that
 1849 the Screenshot2HTML task averages around 32k tokens per example (as shown in Table 1), it
 1850 encounters significant challenges under this 8k-token constraint. This task ranks among those
 1851 with the lowest scores (see Table 3), which contributes to a decline in the overall aggregated
 1852 average score.

1853 Despite this limitation, we found that the generated HTML code remains compilable, and the
 1854 resulting DOM can still be evaluated using the DOM Tree Edit Distance metric, even though the
 1855 HTML output is truncated due to the context limit. However, this inability to handle complete
 1856 HTML outputs highlights the necessity for models capable of processing extended context
 1857 lengths.

1858 To better understand this issue, we analyzed the model outputs (HTML code) in terms of
 1859 a histogram of token lengths, comparing them with the ground truth lengths in the test set
 1860 (see Figure 18). It is important to note that the test set is designed so that the images can be
 1861 represented in fewer than 8192 tokens (as shown in the left figure). This figure highlights that
 1862 token length constraints can adversely affect the task, as most samples approach the maximum
 1863 token length of 6k (after accounting for image tokens), as seen in the right figure. Although the
 1864 test set is designed to be generated within a reasonable token length, the model's training on
 1865 larger contexts leads it to attempt to generate longer HTML outputs.

1866 We fixed the context length at 8192 tokens for several key reasons. First, not all models
 1867 evaluated in our benchmark natively support larger context lengths, and extending this limit
 1868 could disadvantage some models. Second, increasing context lengths significantly boosts GPU
 1869 memory usage, complicating both training and inference at scale. Finally, to ensure fair
 1870 comparisons across all models, we standardized the context length at 8k tokens.

1871 We conducted an ablation study on context length by training the Phi3.5-Vision model with a
 1872 context length of 32k tokens. Subsequently, we re-evaluated the Screenshot2HTML task using
 1873 context lengths ranging from 512 to 16k tokens. However, generating 32k tokens resulted in
 1874 out-of-memory errors. The results are presented in Table 29, where we applied greedy decoding
 1875 (second column) and beam search with a width of 2 and a length penalty of -1.0 (third column).

1876 The results are revealing. We do not observe any performance boost when training and
 1877 evaluating with longer context lengths. The greedy decoding algorithm performs worse with
 1878 longer contexts, not exceeding a score of 10.99. In contrast, beam search with a length penalty
 1879 approach yields better results, reaching 15.80, but still does not benefit from larger context
 1880 lengths.

1881 Additionally, we conducted a qualitative error analysis (see Figures 19 - 22) and found that the
 1882 model often struggles with stopping generation, frequently hallucinating repetitive patterns such
 1883 as nested `<div>` elements or excessively long URLs and references. However, well-formatted
 1884 HTML code is generated in approximately 40% of cases (Figure 18, top figure). Applying
 1885 a length penalty helps mitigate this hallucination, leading to improved performance. This
 1886 indicates further potential for enhancing results with alternative generation techniques.

1887 This indicates that the performance issue may not stem from context length but rather from the
 1888 inherent difficulty of the Screenshot2HTML task. This aligns with the observation that the test
 1889 set's average context length is approximately 3k tokens (Figure 18, left) and does not require
 more than 8k tokens. We suspect that the primary limitation lies in the insufficient amount of

training data (currently around 10k samples) which may hinder the model’s ability to learn HTML generation effectively.

A.13 DETAILS IN DATA VERIFICATION ON BIGDOCS-BENCH

This section provides a detailed description of the verification methodology, evaluation criteria, and measures taken to ensure the quality and reliability of BigDocs-Bench. We outline the qualifications of the human annotators, the multi-step verification process combining automated filtering and human review, and the strategies used to address the challenges posed by the dataset’s large size and synthetic nature. The section also discusses our sampling-based quality assurance for the training split, inter-rater reliability measures, and the conservative approach we adopted to prioritize recall and dataset safety. These steps collectively demonstrate our commitment to maintaining high standards in creating a robust and ethical benchmark.

A.13.1 VERIFICATION METHODOLOGY

We generally follow a 4-step strategy to perform human verification as follows,

1. Automatic Filtering Tools. We implemented multiple automatic filtering tools as the first step in our quality control process. These tools were designed to detect issues such as bad annotations, NSFW content (Llama-Guard-3 from <https://huggingface.co/meta-llama/Llama-Guard-3-11B-Vision>), and Personally Identifiable Information (PII). This automated process reduced the volume of problematic samples before any human verification was performed.

2. Human Verification for Test Split. To ensure a high-quality test split, we only do human verification focused on the test set as our automatic filtering is already quite robust. Annotators identified and removed problematic samples following the guideline, for example, unnecessary comments in LaTeX and HTML code (e.g., in Table2LaTeX and Screenshot2HTML tasks), which could cause rendering issues. Similarly, flowcharts with excessively isolated nodes in tasks like Image2Flow were flagged and removed. For Image2SVG and three GUI-related datasets, we spotted and removed those images with PII or NSFW content. All these typical errors were collected and documented during this process to inform our automatic filtering tools.

3. Refining Automatic Filtering Tools for Training Split. The typical errors identified during human verification of the test set were used to iteratively improve our automatic filtering tools. This enhancement enabled the tools to better detect and handle similar issues in the training split, which was impractical to verify comprehensively through human labor. **4. Sampling-Based Human Verification for Training Split.** To ensure the training split met quality standards, we randomly sampled 100 samples from all tasks, proportional to the size of their respective training splits. These samples were verified by annotators based on the criteria mentioned below, and the overall pass rate was 99% (i.e. 99 good samples), reflecting a high level of quality for the training data after applying the refined filtering tools. Specifically, every task has a pass rate of 100% except GUI-VQA, which has a pass rate of 92% (i.e. 1 bad sample out of 13, which is not relevant to the task since the question is not quite related to the given image).

A.13.2 VERIFICATION CRITERIA FOR VERIFIERS

The verification process for BigDocs-Bench prioritized several critical aspects to ensure the dataset’s quality, reliability, and suitability for real-world applications.

1. First, data integrity was a primary focus, ensuring accurate alignment between inputs and outputs. For example, in tasks like Image2SVG, visual elements in images were verified to match their corresponding SVG annotations, ensuring precise vector representation. Similarly, for Screenshot2HTML, rendered HTML outputs were checked against the screenshots to confirm structural and semantic fidelity.
2. Second, the relevance of synthetic samples was thoroughly assessed to confirm that they were realistic and reflective of the intended task objectives. For instance, in the Image2Flow task, flowchart samples were evaluated to ensure that the generated JSON or GraphViz code meaningfully represented the logical flow of the diagrams without

Table 8: General Document Benchmarks. Models trained on {BigDocs-7.5M+DocDownstream} perform competitively across multimodal document benchmarks. We compare them to base checkpoints, instruction-tuned models, and those trained on {DocStruct4M+DocDownstream}. We also report scores on state-of-the-art models >7B for reference. BigDocs models show consistent performance across tasks. * Refers the use of Chain-of-Thought (CoT)

Model	DocVQA VAL	InfoVQA VAL	DeepForm TEST	KiTC TEST	WTQ TEST	TabFact TEST	ChartQA TEST	TextVQA VAL	MMMU VAL	DocIE TEST	SlideVQA-M TEST	TableVQA TEST	Avg. Score
DocOwl1.5-8B (instruct)	80.73	49.94	68.84	37.99	38.87	79.67	68.56	68.91	33.67	34.64	31.62	52.60	53.84
DocOwl1.5-8B (base)	2.07	1.84	0.00	0.00	0.00	0.00	0.00	0.00	24.44	19.07	3.30	13.63	5.36
DocOwl1.5-8B (base) + DocStruct4M	75.99	46.88	62.77	35.21	32.86	71.56	68.36	65.08	33.67	29.00	27.03	46.27	49.56
DocOwl1.5-8B (base) + BigDocs (Ours)	78.70	47.62	64.39	36.93	35.69	72.65	65.80	67.30	32.33	32.55	29.60	49.03	51.05
Qwen2-VL-2B (instruct)	89.16	64.11	32.38	25.18	38.20	57.21	73.40	79.90	42.00	45.23	46.50	43.07	53.03
Qwen2-VL-2B (base)	7.26	0.78	0.00	0.00	0.00	0.00	0.00	1.14	34.89	28.43	14.55	0.00	7.25
Qwen2-VL-2B (base) + DocStruct4M	59.53	32.00	53.98	36.38	28.48	64.24	54.44	55.89	34.89	28.78	22.68	46.53	43.15
Qwen2-VL-2B (base) + BigDocs (Ours)	57.23	31.88	49.31	34.39	31.61	64.75	68.60	61.01	35.67	27.19	17.46	47.53	43.89
Phi3.5-Vision-4B (instruct)	86.00	56.20	10.47	7.49	17.18	30.43	82.16	73.12	46.00	37.20	30.93	70.70	45.66
Phi3.5-Vision-4B + DocStruct4M	86.76	68.90	70.12	37.83	51.30	82.12	79.76	68.60	44.11	35.52	31.90	69.17	60.51
Phi3.5-Vision-4B + BigDocs (Ours)	87.05	70.05	70.97	37.45	51.21	81.24	81.56	68.72	45.00	36.15	32.47	67.77	60.80
LLaVA-NeXT-7B (instruct)	63.51	30.90	1.30	5.35	20.06	52.83	52.12	65.10	38.89	17.94	7.46	32.87	32.36
LLaVA-NeXT-7B + DocStruct4M	60.95	26.14	39.78	28.34	25.90	67.72	61.20	52.25	25.78	21.70	15.33	27.03	37.68
LLaVA-NeXT-7B + BigDocs (Ours)	57.13	24.47	46.38	31.09	27.06	72.58	54.72	49.06	17.78	22.88	16.07	33.13	37.70
Llama-3.2-90B	74.15*	48.71	4.18	1.81	24.20	63.01	11.36*	71.69	57.78	41.24	26.09	41.57	38.82
GPT-4o 20240806	92.80	66.37	38.39	29.92	46.63	81.10	85.70	70.46	69.10	54.55	67.58	72.87	64.62
Glaude-3.5 Sonnet	88.48	59.05	31.41	24.82	47.13	53.48	51.84	71.42	64.78	35.11	0.00	81.27	50.73
GeminiPro-1.5	91.23	73.94	32.16	24.07	50.29	71.22	34.68	68.16	58.22	48.15	52.05	80.43	57.05
Qwen2-VL-72B	96.50	84.50	30.45	24.78	55.63	0.00	88.30	85.50	64.50	35.87	2.15	74.23	58.40

excessive isolated nodes or disconnected components, which could compromise their utility.

- Finally, to ensure content safety, NSFW content and PII, such as explicit material, or personal data, were removed.

A.13.3 DETAILS ON HUMAN VERIFIERS

We engaged a team of 6 human verifiers, consisting of graduate-level researchers and professionals with expertise in multimodal datasets and document analysis. All human verifiers were thoroughly trained on the verification criteria outlined below before commencing the review process. Each data sample was reviewed by at least two verifiers to ensure thoroughness.

A.13.4 INTER-RATER RELIABILITY

In the test split of our benchmark, we prioritized recall to ensure no potentially problematic samples were missed. For tasks like filtering NSFW content, detecting annotation errors, or identifying corrupted data, any sample flagged as problematic by a single verifier was removed. This conservative recall-focused approach maximized dataset quality and safety while addressing misalignment between raters.

A.14 RESULTS ON LARGER MODELS

We have executed larger models in general document benchmarks. We present them in Table 8.

A.15 CORRELATION ANALYSIS OF BIGDOCS-BENCH WITH OTHER VLM BENCHMARKS

To assess the novelty of BigDocs-Bench in the VLM landscape, we conduct a correlation analysis that highlights how BigDocs-Bench distinguishes itself from existing benchmarks. Specifically, we leverage model results across VLM benchmarks to demonstrate that BigDocs-Bench offers unique dimensions of model evaluation and analysis.

First, we analyze the correlation between Document Benchmarks by comparing the results from Table 2 and Table 1. Following this, we expand the analysis to include results from several widely used VLM benchmarks, providing a comprehensive view of the relationship between BigDocs-Bench and prior benchmarks in the field.

Analysis Setup. We selected all benchmarks listed in Tables 2 and 1, encompassing both General Document Benchmarks and our proposed BigDocs-Bench, respectively. We constructed a

matrix encompassing all models presented in the paper, namely DocOwl-1.5-8B, Qwen2-VL-2B, LLaVA-NeXT-7B, Phi3.5-v-4B, both the off-the-shelf public versions and the ones trained on BigDocs. We also extended Table 2 with scores for GPT4o, Claude 3.5 Sonet, Qwen2-VL-72B, GeminiPro-1.5, and Llama-3.2-90B, to obtain a full matrix. Note that we have now extended our baselines with Llama-3.2-90B. Finally, we aggregated results for all metrics in the two groups of benchmarks. We have edited our manuscript to include Table 8, which is an extension of Table 2 with scores from all models.

In our broader study with general VLM benchmarks, including but not limited to documents, we expanded the analysis to encompass 28 additional VLM benchmarks (see Figure 16 for the full list). Missing scores were imputed using the mean to complete the matrix for models and benchmarks.

Methods.

1. **Cosine similarity matrix and dendrograms:** We normalize metric scores by centering (subtracting the mean) and scaling (dividing by the Euclidean norm). We then apply hierarchical clustering using cosine distance to group benchmarks and visualize their relationships. Cosine similarity matrices and dendrograms illustrate these clusters.
2. **Principal Components Analysis (PCA):** We represent each benchmark as a feature array composed of scores from all models and project these arrays onto the two principal dimensions.

A.15.1 CORRELATION WITH DOCUMENT BENCHMARKS

Our results shown in Figures 14 and 15 show that BigDocs-Bench tasks and benchmarks are different from every other document dataset.

Figure 14 presents the correlation matrix and dendrograms. Circles represent BigDocs-Bench tasks (our benchmarks), while triangles denote other document benchmarks included in the paper. These results demonstrate that BigDocs-Bench tasks are notably distinct from other benchmarks, as indicated by their low correlation with them. A clear grouping emerges for tasks related to VQA, as well as BigDocs-Bench tasks involving code generation in LaTeX, JSON, GraphViz, HTML, and SVG. Notably, HTML and SVG tasks form a cluster, likely due to their characteristically long output sequences. Additionally, DeepForm and KLC stand out as a separate cluster, distinct from all others.

Figure 15 illustrates the PCA results. The clusters distinctly separate BigDocs-Bench tasks from other benchmarks, reaffirming their unique characteristics. Notably, the average aggregated score from BigDocs-Bench (left side) is the furthest from the aggregated score of other benchmarks (right side), highlighting the distinctiveness of our benchmarks. However, certain tasks, such as Image2SVG and Screenshot2HTML, show stronger correlations with KLC, DeepForm, and TabFact. This is likely due to the shared level of difficulty across these benchmarks.

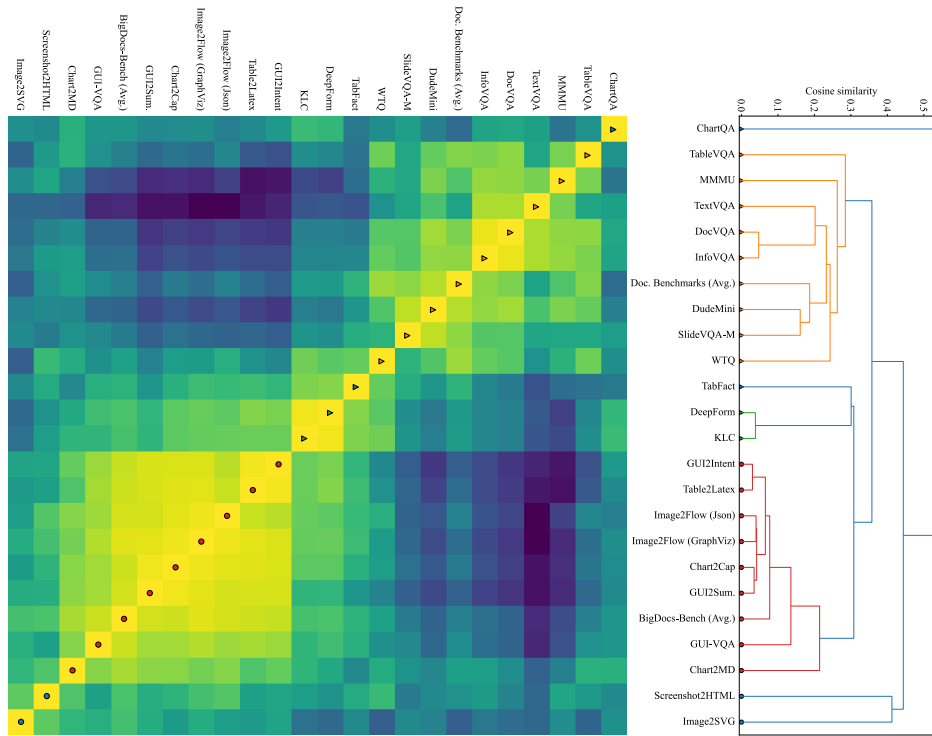
A.15.2 CORRELATION WITH GENERAL VLM BENCHMARKS

Figures 16 and 17 show that BigDocs-Bench tasks and benchmarks are unique in the broad VLM space.

Figure 16 presents the correlation matrix and dendrograms. Circles represent BigDocs-Bench tasks (our benchmarks), upward triangles denote other document benchmarks included in the paper, and downward triangles denote general VLM benchmarks. BigDocs-Bench tasks demonstrate distinctive evaluation characteristics compared to existing benchmarks in the VLM space. This is evidenced by the clear clustering pattern, where BigDocs-Bench tasks form their own correlated group while showing minimal correlation with other benchmark types. Results also reveal three main clusters of tasks: general vision-language tasks (like COCO VAL and VCR), document understanding tasks, and GUI/table-related tasks (such as our tasks GUI2Sum and Table2Latex). This clustering pattern suggests that BigDocs-Bench is addressing unique aspects of document understanding that isn't captured by existing benchmarks.

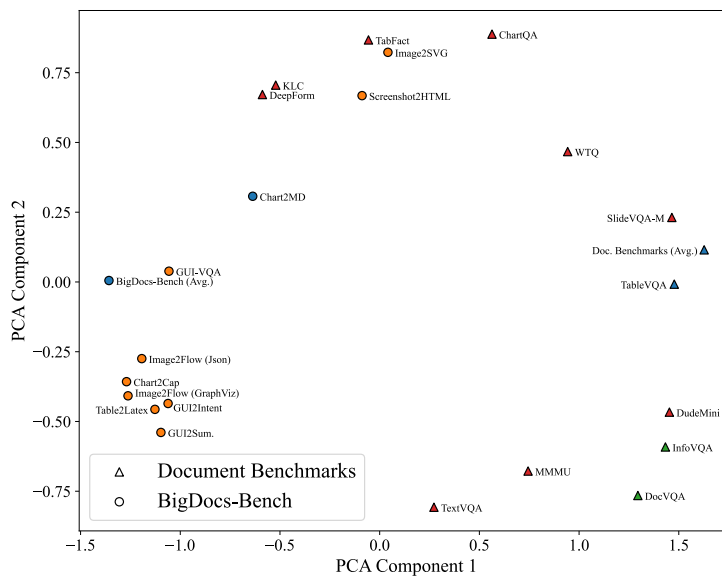
Figure 17 illustrates the PCA results, revealing that most BigDocs-Bench tasks are clustered in the bottom-right corner, distinctly separated from other benchmarks. Notably, tasks within

2052
2053
2054
2055
2056
2057
2058
2059
2060
2061
2062
2063
2064
2065
2066
2067
2068
2069
2070
2071
2072
2073
2074
2075



2076 **Figure 14: Correlation matrix and dendrogram for BigDocs-bench and General Document Benchmarks.** The
2077 matrix (left) shows benchmark relationships, with BigDocs-Bench tasks (circles) clustering separately from other
2078 General Document Benchmarks (triangles). The dendrogram (right) highlights distinct groupings, including
2079 BigDocs-Bench tasks for code and GUI generation clustering together and VQA tasks forming a separate cluster.
2080 Tasks like DeepForm and KLC align closely, reflecting their shared complexity.

2081
2082
2083
2084
2085
2086
2087
2088
2089
2090
2091
2092
2093
2094
2095
2096
2097
2098
2099
2100
2101
2102
2103
2104
2105



2106 **Figure 15: PCA of BigDocs-Bench and General Document Benchmarks.** BigDocs-Bench (circles) form
2107 distinct clusters from other document benchmarks (triangles), emphasizing their unique characteristics. Tasks
2108 related to code generation, such as Image2Flow and Table2Latex, cluster together, while VQA tasks, including
2109 those from other benchmarks, are further apart.

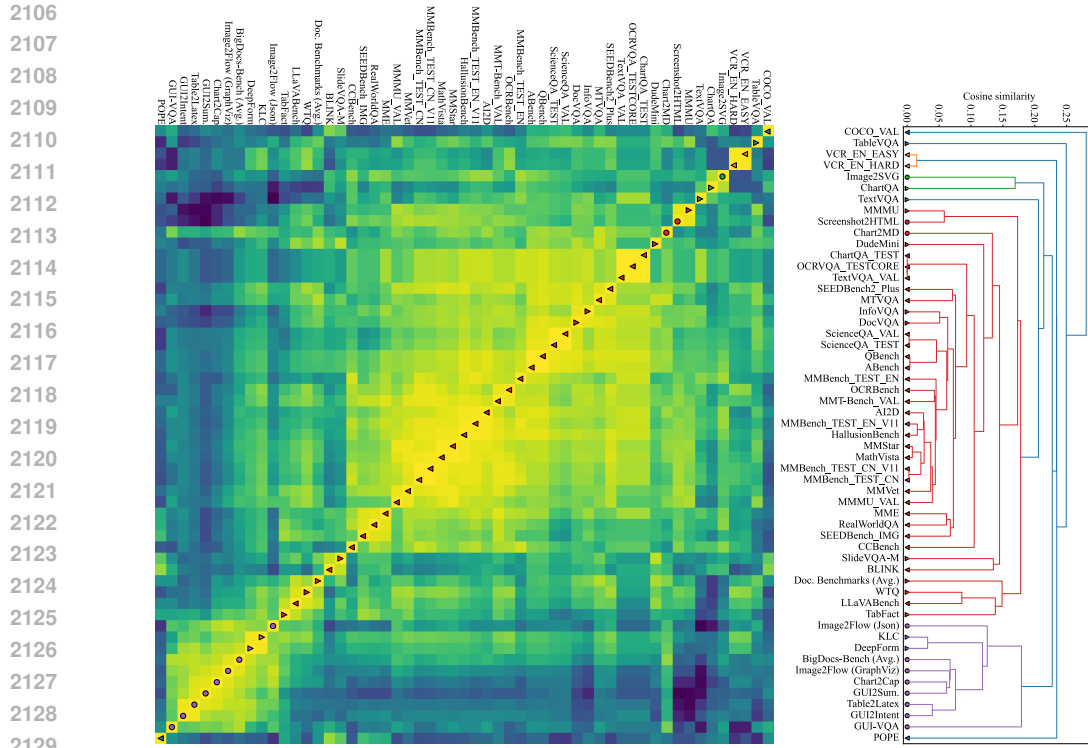


Figure 16: Correlation matrix and dendrogram for BigDocs-Bench and General VLM Benchmarks. The matrix (left) illustrates benchmark relationships, with BigDocs-Bench tasks (circles) clustering separately from other benchmarks. The dendrogram (right) reveals three main clusters: general VLM tasks (e.g., COCO, VCR), document understanding tasks, and GUI/table-related tasks (such as GUI2Sum and Table2Latex).

BigDocs-Bench form clear clusters based on their type, such as VQA, Flows, Charts, or GUIs. General VLM benchmarks create a dense cluster, while document benchmarks are more sparse. Additionally, the aggregated BigDocs-Bench average score is positioned far from other benchmarks, further highlighting its uniqueness.

2160
2161
2162
2163
2164
2165
2166
2167
2168
2169
2170
2171
2172
2173
2174
2175
2176
2177
2178
2179
2180
2181
2182
2183
2184
2185
2186
2187
2188
2189
2190
2191
2192
2193
2194
2195
2196
2197
2198
2199
2200
2201
2202
2203
2204
2205
2206
2207
2208
2209
2210
2211
2212
2213

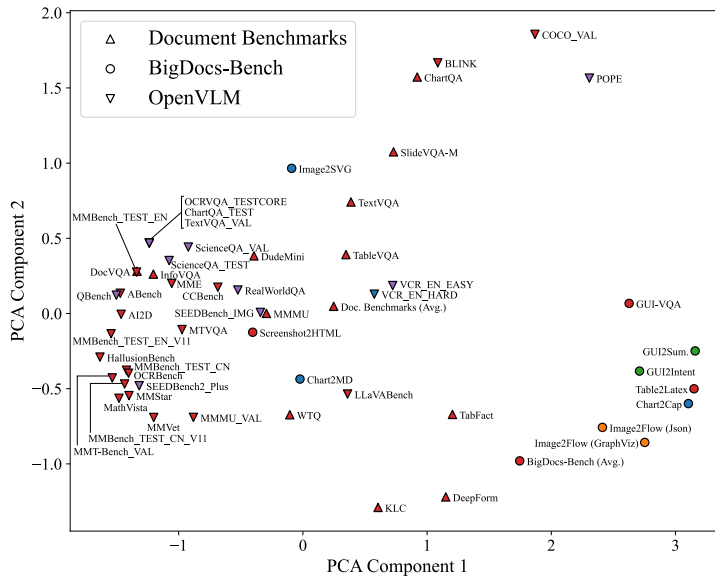
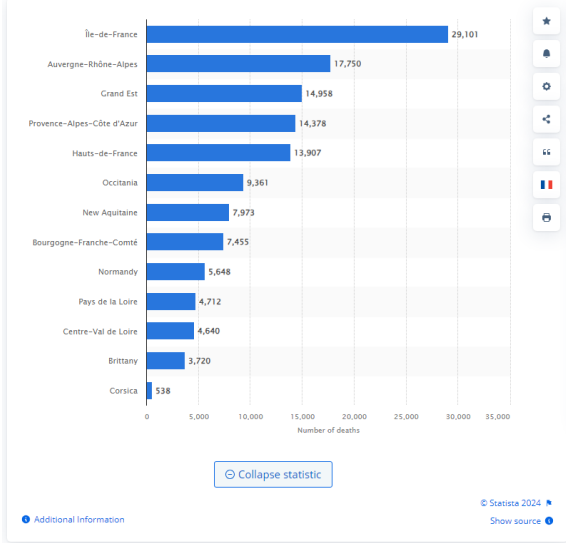


Figure 17: PCA of BigDocs-Bench and General VLM Benchmarks. BigDocs-Bench (circles) form distinct clusters, clearly separated from other benchmarks, highlighting its unique characteristics. A dense cluster is observed for general VLM benchmarks (downward triangles), while document benchmarks (upward triangles) are more dispersed.

2214
2215
2216
2217
2218
2219
2220
2221
2222
2223
2224
2225
2226
2227
2228
2229
2230
2231
2232
2233
2234
2235
2236
2237
2238
2239
2240
2241
2242
2243
2244
2245
2246
2247
2248
2249
2250
2251
2252
2253
2254
2255
2256
2257
2258
2259
2260
2261
2262
2263
2264
2265
2266
2267

Table 9: Test Example for the task of Chart2Caption. All models other than Phi3.5-V-4B make mistakes in the caption. LLaVA-NeXT-7B does not offer relevant information about the chart, but about its format and LLaVA-NeXT-7B + BigDocs hallucinates. BigDocs models make factual mistakes, while Claude and GPT4o have trouble with the accent marks.

Component	Content
	
Input Image	
User Query	Can you give me a caption for the chart in the image?
Ground Truth	The novel coronavirus (COVID-19) caused a certain number of deaths within the French population. With 29,101 victims, the Paris Region, Île-de-France, recorded the highest number of deaths in France as of June 30, 2023. On the other hand, the regions of metropolitan France least affected were those of Brittany and Corsica. For further information about the coronavirus (COVID-19) pandemic, please visit our dedicated Facts and Figures page.
Phi3.5-V-4B	The chart is a horizontal bar graph displaying the number of deaths in various regions of France. The x-axis represents the number of deaths, ranging from 0 to 35,000, and the y-axis lists the regions. Île-de-France has the highest number of deaths at 29,101 , followed by Auvergne-Rhône-Alpes with 17,750, and Grand Est with 14,958. The graph continues to list other regions with descending numbers of deaths, ending with Corsica at 538. The source of the data is indicated as Statista 2024.
Phi3.5-V-4B + BigDocs	In 2022, the department of Île-de-France recorded the highest number of deaths in France, with 29,101 deaths. The department of Hauts-de-France recorded the second highest number of deaths , with 13,907 deaths.
LLaVA-NeXT-7B	The chart in the image is a bar graph titled "Collapse statistic" and it shows the number of deaths for various locations in France. The locations are listed on the left side of the chart, and the number of deaths is represented by the height of each bar. The bars are color-coded, and the chart includes a legend to explain the color coding. The chart also has a button labeled "Collapse statistic" at the bottom, suggesting that the user can interact with the chart to collapse or expand the data.
LLaVA-NeXT-7B + BigDocs	Since the start of the French Revolution in 1793, over 38,000 people have been executed in France. The most common cause of death was by guillotine, a procedure in which a sharp knife is swung to the victim's neck to sever the head from the body. The most recent execution was carried out on October 5, 2023, following the death of a retired police officer.
Qwen2-VL-2B	Number of deaths in France by region in 2020
Qwen2-VL-2B + BigDocs	The French department with the highest number of deaths due to the coronavirus (COVID-19) was Île-de-France, with 29,101 deaths as of January 13, 2023. The French authorities are constantly trying to increase the testing capacity to conduct PCR tests on people who have symptoms in order to try and discover the exact death toll.
DocOwl-1.5-8B	The department with the highest number of deaths in France in 2019 was Île-de-France.
DocOwl-1.5-8B + BigDocs	In 2022, there were 29,101 deaths in France. Of these deaths, 7,455 were in the Bourgogne region, making it the department with the highest number of deaths in France that year.
Claude	A suitable caption for this chart could be: Number of COVID-19 Deaths by Region in France This horizontal bar chart shows the number of deaths, presumably from COVID-19, across different regions of France. The regions are listed on the left, with 00cele-de-France having the highest number of deaths at 29,101, while Corsica has the lowest at 538. The data appears to be presenting cumulative death tolls, likely over the course of the pandemic, for each of France's administrative regions.
GPT4o	Number of Deaths by Region in France: 00cele-de-France Leads with 29,101 Deaths, Followed by Auvergne-Roie-Alpes and Grand Est.

2268
2269
2270
2271
2272
2273
2274
2275
2276
2277
2278
2279
2280
2281
2282
2283
2284
2285
2286
2287
2288
2289
2290
2291
2292
2293
2294
2295
2296
2297
2298
2299
2300
2301
2302
2303
2304
2305
2306
2307
2308
2309
2310
2311
2312
2313
2314
2315
2316
2317
2318
2319
2320
2321

Table 10: Chart2Caption: Comparison of model responses showing that models using the BigDocs dataset produce more concise and relevant captions than baseline models while still making some factual errors.

Component	Content
Input Image	
User Query	I need a caption for the chart in the image, please.
Ground Truth	This graph shows the male civilian labor force participation rate in the United States from 1990 to 2023. In 2023, 68.1 percent of the male civilian population participated in the job market.
Phi3.5-V-4B	The chart is a line graph that represents the labor force participation rate over a span of years from 1990 to 2023. The vertical axis is labeled as "Labor force participation rate" and is measured in percentages, ranging from 66% to 78%. The horizontal axis represents years, marked at two-year intervals from 1990 to 2020, with additional single-year markers for 2021, 2022, and 2023. The line graph shows a general downward trend in the labor force participation rate over the observed period. The rate starts at approximately 76% in 1990, experiences slight fluctuations, and then begins a more consistent decline from around 2000 onwards, reaching its lowest point at about 67% in 2020. After 2020, there is a slight increase, followed by a plateau around 68% in the most recent years displayed.
Phi3.5-V-4B + BigDocs	In 2023, 68.1 percent of the female labor force participated in the job market. This is a slight increase from the previous year, when 67.7 percent of the female labor force participated in the job market.
LLaVA-NeXT-7B	The chart in the image shows a line graph with a downward trend, indicating a decrease in a certain metric over time. The metric is labeled as "Labor Force Participation Rate," which is a measure of the number of people who are either working or actively seeking employment as a percentage of the total population. The graph is set against a white background with a blue line representing the data points, and there are additional information icons at the top right corner, suggesting that the user can click on them for more details or options. The chart is titled "Additional Information" and includes a "Show source" link, indicating that the data is sourced from Statista 2024.
LLaVA-NeXT-7B + BigDocs	In 2022, the labor force participation rate in the United States stood at 67.3 percent. The term labor force participation rate is used by the U.S. Bureau of Labor Statistics (BLS) to describe the percentage of the civilian non-institutional non-military population that is employed or seeking employment.
Qwen2-VL-2B	The chart depicts the labor force participation rate in the United States from 1990 to 2023. The labor force participation rate is the percentage of the population that is either employed or actively seeking employment. The data shows a significant decline in the labor force participation rate over the years, with a notable drop in the late 2000s and early 2010s.
Qwen2-VL-2B + BigDocs	In 2023, about 68.5 percent of the labor force participated in job-related activities in the United States. This is a decrease from the previous year, when about 69.1 percent of the labor force participated in job-related activities. The labor force participation rate peaked in 2021, at 70.4 percent.
DocOwl-1.5-8B	The blue line chart represents the labor force participation rate of the labor force in the United States.
DocOwl-1.5-8B + BigDocs	In 2023, the labor force participation rate in the United States was 68.2 percent. This is a decrease from the previous year, when the labor force participation rate stood at 68.4 percent.
Claude	A suitable caption for this chart could be: "Labor Force Participation Rate in the United States, 1990-2023" This caption accurately describes what the graph is showing: a trend line of the labor force participation rate in the US over a period of approximately 33 years, from 1990 to 2023. The graph demonstrates a general decline in the labor force participation rate over this time period, starting at around 76% in 1990 and ending at about 68% in 2023.
GPT4o	Trends in Labor Force Participation Rate (1990-2022): A Decline with Recent Stabilization.

Table 11: Evaluation Example for GUI-VQA: Models utilizing the BigDocs dataset consistently produce the most accurate and concise outputs, perfectly matching the ground truth without any extraneous or unnecessary information.



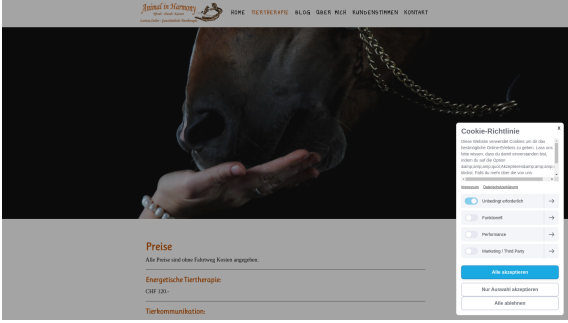
Component	Content
Input Image	
User Query	[What information appears when clicking [330, 530, 390, 590]?)
Ground Truth	Access the Laundrette.
Phi3.5-V-4B	The image does not provide information on what appears when clicking [330, 530, 390, 590].
Phi3.5-V-4B + BigDocs	Access the Laundrette.
LLaVA-NeXT-7B	The image you've provided appears to be a screenshot of a webpage or a document with a list of services offered by a company. The services are listed under different categories, and when you click on the numbers (330, 530, 390, 590), it seems to be a way to navigate to different sections of the website or document.
LLaVA-NeXT-7B + BigDocs	Access the Laundry.
Qwen2-VL-2B	When clicking on the "Motor Repair" button, the information that appears is related to the maintenance and repair of motor systems.
Qwen2-VL-2B + BigDocs	Access the Laundrette.
DocOwl-1.5-8B	The information that appears when clicking [330, 530, 390, 590] is the same as the information that appears when clicking [330, 530, 390, 610].
DocOwl-1.5-8B + BigDocs	Access the Laundrette.
Claude	The image doesn't show interactive elements or clickable areas. However, at the approximate coordinates you mentioned [330, 530, 390, 590], there is a green button labeled "Exhaust" in the left sidebar menu of the webpage. This button is part of a list of services offered by FilterXchange, which includes other options like Filters, Canopies, Fans, Motor Repair, and several others.
Gpt4o	Clicking on the coordinates [330, 530, 390, 590] would likely correspond to the Fans button. The information related to Fans would appear, detailing services such as fan maintenance and repairs.

Table 12: Qualitative test example for the task of GUI-VQA. GPT-4o (20240806), LLaVA-NeXT-7B, Phi3.5-V-4B, and Qwen2-VL-2B tend to hallucinate the response, mostly ignoring the input image. LLaVA-NeXT-7B and Claude are more conversational, however, the latter predicts correctly that the answer is 'Home Security'

Component	Content
Input Image	
User Query	Clicking [680, 50, 750, 110] gives the user access to what?
Ground Truth	Display the Home Security.
Phi3.5-V-4B	The 'READ MORE' button
Phi3.5-V-4B + BigDocs	Display the Home Security.
LLaVA-NeXT-7B	The image you've provided appears to be a screenshot of a website for a company that provides CCTV, Alarms, and Security Services. The text "Clicking [680, 50, 750, 110] gives the user access to what?" is not visible in the image. If you're asking about what clicking on the "Read More" button would do, it would likely take the user to a page with more detailed information about the services offered by the company. If you're asking about the content of the image, the visible part of the image shows a security camera mounted on a wall, which is a common piece of equipment used for surveillance in security systems.
LLaVA-NeXT-7B + BigDocs	Display the Home Security.
Qwen2-VL-2B	Clicking [680, 50, 750, 110] gives the user access to Home Automation.
Qwen2-VL-2B + BigDocs	Display the Home Security.
DocOwl-1.5-8B	The user gets access to home automation.
DocOwl-1.5-8B + BigDocs	Display the Home Security.
Claude-3.5 Sonnet	Clicking in the area [680, 50, 750, 110] would likely give the user access to the 'Home Security' section of the website. This can be inferred from the navigation menu at the top of the page, where 'Home Security' is listed as one of the main service categories offered by CRH Communications, along with Smart Wiring, Home Automation, and Home Theater/AV.
GPT-4o (20240806)	Clicking in that area would likely give the user access to the 'Contact' page.

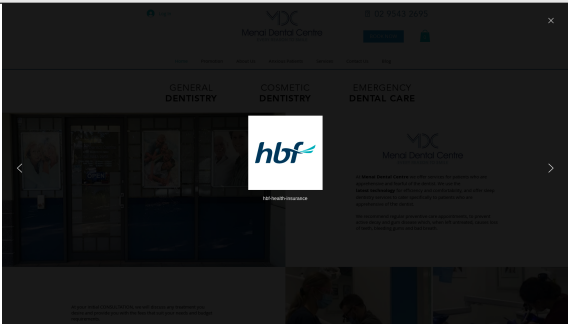
2376
2377

Table 13: Qualitative test example for the task of GUI2Intent. All the models trained with BigDocs along with Qwen2-VL-2B produce the correct intent, while the latter is more conversational. Phi3.5-V-4B, LLaVA-NeXT-7B and DocOwl-1.5-8B infer incorrect sections of the image.

Component	Content
	
Input Image	
User Query	If the user clicks [390, 20, 430, 60], what will they view?
Ground Truth	Display the HOME.
Phi3.5-V-4B	They will view the 'Impressum' section of the website.
Phi3.5-V-4B + BigDocs	Display the HOME.
LLaVA-NeXT-7B	The image you've provided appears to be a screenshot of a webpage with a navigation menu on the left side. If the user clicks on the "Kontakt" menu item, which is the third option from the top, they will likely be taken to a page that provides contact information or a contact form for the website. This is a common feature on websites where users can get in touch with the organization or individuals associated with the site.
LLaVA-NeXT-7B + BigDocs	Display the HOME.
Qwen2-VL-2B	If the user clicks on the "HOME" link, they will be directed to the main page of the website, which typically contains the homepage or a navigation menu with links to different sections of the website.
Qwen2-VL-2B + BigDocs	Display the HOME.
DocOwl-1.5-8B	If the user clicks [390, 20, 430, 60], they will view a Tiertherapie blog.
DocOwl-1.5-8B + BigDocs	Display the HOME.

2391
2392
2393
2394
2395
2396
2397
2398
2399
2400
2401
2402
2403
2404

Table 14: Qualitative test example for the task of GUI2Intent. All the models trained with BigDocs along with Qwen2-VL-2B produce the correct intent, while the latter is more conversational. Phi3.5-V-4B, LLaVA-NeXT-7B and DocOwl-1.5-8B provide confused responses.

Component	Content
	
Input Image	
User Query	What will the user encounter by clicking [400, 160, 450, 190]?
Ground Truth	View the About Us.
Phi3.5-V-4B	The user will encounter a section of the website that is not fully visible in the image.
Phi3.5-V-4B + BigDocs	View the About Us.
LLaVA-NeXT-7B	The image you've provided appears to be a screenshot of a website, specifically a dental clinic's website. By clicking on the coordinates you've mentioned (400, 160, 450, 190), the user would likely be directed to a specific section or page of the website. However, without more context or a clearer view of the website's layout, it's difficult to determine exactly what the user would encounter. It could be a link to a specific service offered by the clinic, a page about a particular dental procedure, a contact form, or any other type of content that is relevant to the clinic's services.
LLaVA-NeXT-7B + BigDocs	View the About Us.
Qwen2-VL-2B	The user will be directed to the "About Us" section of the Menai Dental Centre website.
Qwen2-VL-2B + BigDocs	View the About Us.
DocOwl-1.5-8B	The user will encounter a phone number by clicking on the respective number.
DocOwl-1.5-8B + BigDocs	View the About Us.

2418
2419
2420
2421
2422
2423
2424
2425
2426
2427
2428
2429

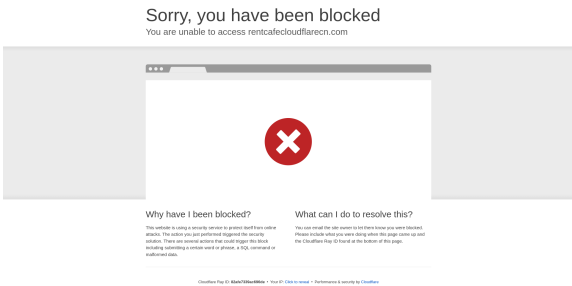
2430
2431
2432
2433
2434
2435
2436
2437
2438
2439
2440
2441
2442
2443
2444
2445
2446
2447
2448
2449
2450
2451
2452
2453
2454
2455
2456
2457
2458
2459
2460
2461
2462
2463
2464
2465
2466
2467
2468
2469
2470
2471
2472
2473
2474
2475
2476
2477
2478
2479
2480
2481
2482
2483

Table 15: Qualitative test example for the task GUI2Sum. BigDocs models accurately capture the spatial orientation and stylistic aspects of of the webpage while making errors parsing the restaurant name. LLaVA-NeXT-7B expresses spatial disorientation, while Qwen2-VL-2B and DocOwl-1.5-8B provide too simplistic and incorrect responses respectively.

Component	Content
Input Image	
User Query	Can you give me a caption for the webpage in the image?
Ground Truth	This website features a modern and colorful food menu for Gunbae, a restaurant offering Korean tapas and small plates. The layout is clean and organized, with a prominent "FOOD MENU" title at the top. The menu is divided into sections for TAPAS, DINNER, and FEED ME, each with a distinct color background and clear pricing. The drinks menu, labeled "DRINK MENU," is displayed below with a vibrant design and includes beer, soju, and cocktails. The website also includes social media icons and a login button, enhancing user engagement.
Phi3.5-V-4B	The image displays a webpage with a food and drink menu for a restaurant named Gunbae. The top of the page has navigation options such as 'Home', 'Gunbae Menu', 'Order Online', 'Location & Hours', 'Book now', and social media icons for Instagram and Facebook. There is also a 'Log In' option. The main content of the page is divided into two sections: 'FOOD MENU' and 'DRINK MENU'. The food menu is colorful and lists various dishes with prices, including 'TAPAS', 'DINNER', 'FEED ME', and 'SMALL PLATES'. It also mentions 'WESTERN', 'GUNBAE FREE', and 'VEGAN' options. The drink menu is partially visible, showing 'BEER' and 'SOJU' categories with specific beer brands and prices. The bottom of the image is cut off, and the full drink menu is not visible.
Phi3.5-V-4B + BigDocs	This website features a food menu for a restaurant named "Gunbae." The main content includes a colorful and organized menu with various dishes categorized under "TAPAS," "FOOD," and "DRINK." The layout is clean and easy to navigate, with a beige background and a mix of vibrant and pastel colors for the menu items. The website also includes social media icons and a login section at the top. The overall style is modern and visually appealing, designed to attract customers with a variety of food and drink options.
LLaVA-NeXT-7B	The image shows a webpage with a food menu on the left and a drink menu on the right. The food menu lists various dishes with their prices, and the drink menu displays a selection of beverages with their respective prices. The design is clean and organized, with a color scheme that includes shades of blue, green, and orange. The layout is user-friendly, with clear headings and easy-to-read text. The overall impression is that of a modern, inviting restaurant or cafe website.
LLaVA-NeXT-7B + BigDocs	This website features a vibrant and modern menu for a restaurant named "Rockin Randy." The layout is clean and organized, with a beige background that contrasts with the colorful menu items. The main content includes a detailed food menu with sections for beer, cider, and drinks, each listing various options with prices and descriptions. Icons and graphics, such as a beer tap and a drink, are used to visually represent the menu items. The website also includes navigation options like "Home," "Gastrobar Menu," "Order Online," "Location & Hours," and "Book now," along with social media icons and a login button. The overall style is contemporary and user-friendly, making it easy for customers to browse and order their drinks.
Qwen2-VL-2B	"Certainly! Here's a caption for the webpage: "Experience the flavors of Gunbae with our delicious food and refreshing drinks!"
Qwen2-VL-2B + BigDocs	This website is a food menu page for Gunbae, featuring a modern and clean layout with a dark background and white text. The main content includes a "FOOD MENU" section with various categories like Tapas, Small Plates, Buffets, and Desserts. The layout is organized with a navigation bar at the top, a large food menu area, and a "DRINK MENU" section below. The color scheme is primarily dark with accents of green and white, creating a sophisticated and inviting atmosphere. The website also includes social media icons and a login button for users.
DocOwl-1.5-8B	"Food Menu" is the caption for the webpage in the image.
DocOwl-1.5-8B + BigDocs	This website features a food menu for a restaurant named "Gunbae." The layout is clean and organized, with a beige background and a mix of black, white, and orange text. The main content includes a detailed menu with various categories such as appetizers, mains, and drinks, each with pricing and descriptions. The menu items are visually appealing with images and icons. The website also has navigation options for Home, Gunbae Menu, Order Online, Location & Hours, and Book now. Social media icons for Facebook and Instagram are present at the top right.

2484
2485
2486
2487
2488
2489
2490
2491
2492
2493
2494
2495
2496
2497
2498
2499
2500
2501
2502
2503
2504
2505
2506
2507
2508
2509
2510
2511
2512
2513
2514
2515
2516
2517
2518
2519
2520
2521
2522
2523
2524
2525
2526
2527
2528
2529
2530
2531
2532
2533
2534
2535
2536
2537

Table 16: *Qualitative test example for GUI2Sum. Phi3.5-V-4B and the BigDocs models are able to extract correct and relevant information from this simple and clean webpage, while the other baseline models make mistakes or are too simplistic in their caption.*

Component	Content
	
Input Image	
User Query	Can you give me a caption for the webpage in the image?
Ground Truth	The website displays a "Sorry, you have been blocked" error message, indicating that the user is unable to access rentcafecloudflare.com. The layout is minimalistic, with a white background and a central red "X" symbolizing the block. The text is divided into two sections: "Why have I been blocked?" and "What can I do to resolve this?" The website explains that the block is due to a security service protecting against online attacks, and suggests contacting the site owner with the provided Cloudflare Ray ID for assistance. The overall style is clean and straightforward, with a focus on delivering the necessary information clearly.
Phi3.5-V-4B	The image shows a webpage with a message indicating that the user has been blocked from accessing the website rentcafecloudflare.com. There is a large red 'X' symbol in the center, which typically represents a block or error. Below the 'X', there are two sections of text providing information on why the user might have been blocked and what actions can be taken to resolve the issue. The text suggests that the block could be due to a security service protecting the website from online attacks and lists potential actions that could have triggered the block. There is also a mention of a Cloudflare Ray ID and an IP address, along with a note that the performance and security are by Cloudflare.
Phi3.5-V-4B -BigDocs	The website displays a blocked access message with a prominent red "X" symbol. The main content explains that the user has been blocked due to triggering a security solution, possibly from submitting certain words, phrases, SQL commands, or malformed data. The layout is minimalistic, with a white background and a simple, clean design. The text is black, except for the red "X" and the Cloudflare logo, which adds a touch of color. The message also provides a Cloudflare Ray ID for the user to include in a support email to the site owner for resolution.
LLaVA-NeXT-7B	"The caption for the webpage in the image could be: "Access Denied: Your Account is Blocked - Unable to Access Rentafire.com""
LLaVA-NeXT-7B + BigDocs	The website displays a "Sorry, you have been blocked" error message, indicating that the user is unable to access rentcafecloudflare.com. The layout is minimalistic, with a white background and a central red "X" symbolizing the block. The text is concise, explaining the block is due to a security service protecting the website from online attacks, and suggests contacting the site owner with the provided Cloudflare Ray ID for resolution. The overall style is clean and straightforward, focusing on delivering the necessary information clearly.
Qwen2-VL-2B	"Sorry, you have been blocked: Unable to access rentcafecloudflare.com"
Qwen2-VL-2B + BigDocs	The website displays a blocked access message with a prominent red "X" symbol. The main content explains that the user has been blocked due to triggering a security solution, possibly through actions like submitting certain words or phrases, SQL commands, or malformed data. The layout is minimalistic, with a white background and a simple, clean design. The text is straightforward and informative, providing reasons for the block and suggesting contacting the site owner for resolution. The Cloudflare Ray ID is also included for further assistance.
DocOwl-1.5-8B	The webpage in the image displays a red cross and the message Sorry, you have been blocked.
DocOwl-1.5-8B + BigDocs	The website displays a blocked access message with a prominent red "X" symbol. The main content explains that the user has been blocked due to triggering a security solution, possibly from submitting inappropriate content or commands. The layout is minimalistic, with a white background and a simple, clean design. The text is black, except for the red "X" and the Cloudflare logo. The message provides a reason for the block and suggests contacting the site owner for resolution, including the Cloudflare Ray ID for reference.

2538
2539
2540
2541
2542
2543
2544
2545
2546
2547
2548
2549
2550
2551
2552
2553
2554
2555
2556
2557
2558
2559
2560
2561
2562
2563
2564
2565
2566
2567
2568
2569
2570
2571
2572
2573
2574
2575
2576
2577
2578
2579
2580
2581
2582
2583
2584
2585
2586
2587
2588
2589
2590
2591

Table 17: Test Example for the task of Table2Latex. BigDocs models preserve the structure of the table, lines from rows and columns, and font styles like bolds or italics.

Component	Content																																																							
	Discrete dynamics(ACC)				Continuous dynamics(σ)																																																			
	SIR	SIS	Threshold	Kirman	Gene	Mutualistic	CML																																																	
<i>T + 1</i>	0.85	0.86	0.89	0.84	0.598	0.958	0.017																																																	
<i>T + 2</i>	0.73	0.80	0.84	0.81	0.602	1.086	0.021																																																	
<i>T + 3</i>	0.81	0.75	0.81	0.82	0.609	1.276	0.024																																																	
<i>T + 4</i>	0.82	0.74	0.74	0.83	0.724	1.512	0.027																																																	
<i>T + 5</i>	0.80	0.74	0.72	0.85	0.822	1.601	0.028																																																	
Input Image																																																								
User Query	[Please generate the necessary LaTeX script to draw this table.]																																																							
	<table border="1"> <thead> <tr> <th>Discrete dynamics (ACC)</th> <th>SIR</th> <th>SIS</th> <th>Threshold</th> <th>Kirman</th> <th>Gene</th> <th>Mutualistic</th> <th>CML</th> </tr> </thead> <tbody> <tr> <td><i>T + 1</i></td> <td>0.85</td> <td>0.86</td> <td>0.89</td> <td>0.84</td> <td>0.598</td> <td>0.958</td> <td>0.017</td> </tr> <tr> <td><i>T + 2</i></td> <td>0.73</td> <td>0.80</td> <td>0.84</td> <td>0.81</td> <td>0.602</td> <td>1.086</td> <td>0.021</td> </tr> <tr> <td><i>T + 3</i></td> <td>0.81</td> <td>0.75</td> <td>0.81</td> <td>0.82</td> <td>0.609</td> <td>1.276</td> <td>0.024</td> </tr> <tr> <td><i>T + 4</i></td> <td>0.82</td> <td>0.74</td> <td>0.74</td> <td>0.83</td> <td>0.724</td> <td>1.512</td> <td>0.027</td> </tr> <tr> <td><i>T + 5</i></td> <td>0.80</td> <td>0.74</td> <td>0.72</td> <td>0.85</td> <td>0.822</td> <td>1.601</td> <td>0.028</td> </tr> </tbody> </table>								Discrete dynamics (ACC)	SIR	SIS	Threshold	Kirman	Gene	Mutualistic	CML	<i>T + 1</i>	0.85	0.86	0.89	0.84	0.598	0.958	0.017	<i>T + 2</i>	0.73	0.80	0.84	0.81	0.602	1.086	0.021	<i>T + 3</i>	0.81	0.75	0.81	0.82	0.609	1.276	0.024	<i>T + 4</i>	0.82	0.74	0.74	0.83	0.724	1.512	0.027	<i>T + 5</i>	0.80	0.74	0.72	0.85	0.822	1.601	0.028
Discrete dynamics (ACC)	SIR	SIS	Threshold	Kirman	Gene	Mutualistic	CML																																																	
<i>T + 1</i>	0.85	0.86	0.89	0.84	0.598	0.958	0.017																																																	
<i>T + 2</i>	0.73	0.80	0.84	0.81	0.602	1.086	0.021																																																	
<i>T + 3</i>	0.81	0.75	0.81	0.82	0.609	1.276	0.024																																																	
<i>T + 4</i>	0.82	0.74	0.74	0.83	0.724	1.512	0.027																																																	
<i>T + 5</i>	0.80	0.74	0.72	0.85	0.822	1.601	0.028																																																	
	Table 1: Comparison of different models for discrete and continuous dynamics.																																																							
Phi3.5-V-4B																																																								
	Discrete dynamics(ACC)				Continuous dynamics(σ)																																																			
	SIR	SIS	Threshold	Kirman	Gene	Mutualistic	CML																																																	
<i>T + 1</i>	0.85	0.86	0.89	0.84	0.598	0.958	0.017																																																	
<i>T + 2</i>	0.73	0.80	0.84	0.81	0.602	1.086	0.021																																																	
<i>T + 3</i>	0.81	0.75	0.81	0.82	0.609	1.276	0.024																																																	
<i>T + 4</i>	0.82	0.74	0.74	0.83	0.724	1.512	0.027																																																	
<i>T + 5</i>	0.80	0.74	0.72	0.85	0.822	1.601	0.028																																																	
Phi3.5-V-4B + BigDocs																																																								
	Discrete dynamics (ACC)				Continuous dynamics (σ)																																																			
	SIR	SIS	Threshold	Kirman	Gene	Mutualistic	CML																																																	
<i>T + 1</i>	0.85	0.86	0.89	0.84	0.598	0.958	0.017																																																	
<i>T + 2</i>	0.73	0.80	0.84	0.81	0.602	1.086	0.021																																																	
<i>T + 3</i>	0.81	0.75	0.81	0.82	0.609	1.276	0.024																																																	
<i>T + 4</i>	0.82	0.74	0.74	0.83	0.724	1.512	0.027																																																	
<i>T + 5</i>	0.80	0.74	0.72	0.85	0.822	1.601	0.028																																																	
Gpt4o																																																								

Table 18: Test Example for the task of Table2Latex. Phi3.5-V-4B was not able to format the table with all the rows, and used incorrect lines, and font style (boldness of first column and row).

Component	Content																			
		Chain 2	Chain 3	Chain 4	Chain 5															
Chain 1		0.81	0.70	0.83	0.78															
Chain 2		1	0.61	0.76	0.67															
Chain 3			1	0.67	0.60															
Chain 4				1	0.76															
Input Image																				
User Query	[Create a LaTeX script to illustrate this table.]																			
	<table border="1"> <thead> <tr> <th>Chain 1</th> <th>Chain 2</th> <th>Chain 3</th> <th>Chain 4</th> <th>Chain 5</th> </tr> </thead> <tbody> <tr> <td>0.81</td> <td>0.70</td> <td>0.83</td> <td>0.78</td> <td>0.67</td> </tr> <tr> <td>1</td> <td>0.61</td> <td>0.67</td> <td>0.60</td> <td>0.76</td> </tr> </tbody> </table>					Chain 1	Chain 2	Chain 3	Chain 4	Chain 5	0.81	0.70	0.83	0.78	0.67	1	0.61	0.67	0.60	0.76
Chain 1	Chain 2	Chain 3	Chain 4	Chain 5																
0.81	0.70	0.83	0.78	0.67																
1	0.61	0.67	0.60	0.76																
	Table 1: Table of Chains																			
Phi3.5-V-4B																				
		Chain 2	Chain 3	Chain 4	Chain 5															
Chain 1		0.81	0.70	0.83	0.78															
Chain 2		1	0.61	0.76	0.67															
Chain 3			1	0.67	0.60															
Chain 4				1	0.76															
Phi3.5-V-4B + BigDocs																				

2592
2593
2594
2595
2596
2597
2598
2599
2600
2601
2602
2603
2604
2605
2606
2607
2608
2609
2610
2611
2612
2613
2614
2615
2616
2617
2618
2619
2620
2621
2622
2623
2624
2625
2626
2627
2628
2629
2630
2631
2632
2633
2634
2635
2636
2637
2638
2639
2640
2641
2642
2643
2644
2645

Table 19: Test Example for the task of Table2Latex: Boldness and details of lines are perfectly aligned with input in the Phi3.5-V-4B + BigDocs example.

Component	Content																												
	<table border="1"> <thead> <tr> <th>Logic Gates</th> <th>(0,0)</th> <th>(0,1)/(1,0)</th> <th>(1,1)</th> </tr> </thead> <tbody> <tr> <td>AND</td> <td>0</td> <td>0</td> <td>1</td> </tr> <tr> <td>NAND</td> <td>1</td> <td>1</td> <td>0</td> </tr> <tr> <td>OR</td> <td>0</td> <td>1</td> <td>1</td> </tr> <tr> <td>NOR</td> <td>1</td> <td>0</td> <td>0</td> </tr> <tr> <td>XOR</td> <td>0</td> <td>1</td> <td>0</td> </tr> <tr> <td>XNOR</td> <td>1</td> <td>0</td> <td>1</td> </tr> </tbody> </table>	Logic Gates	(0,0)	(0,1)/(1,0)	(1,1)	AND	0	0	1	NAND	1	1	0	OR	0	1	1	NOR	1	0	0	XOR	0	1	0	XNOR	1	0	1
Logic Gates	(0,0)	(0,1)/(1,0)	(1,1)																										
AND	0	0	1																										
NAND	1	1	0																										
OR	0	1	1																										
NOR	1	0	0																										
XOR	0	1	0																										
XNOR	1	0	1																										

Input Image

[Please generate the necessary LaTeX script to draw this table.]

Logic Gates	(0,0)	(0,1)/(1,0)	(1,1)
AND	0	0	1
NAND	1	1	0
OR	0	1	1
NOR	1	0	0
XOR	0	1	0
XNOR	1	0	1

Phi3.5-V-4B

Logic Gates	(0,0)	(0,1)/(1,0)	(1,1)
AND	0	0	1
NAND	1	1	0
OR	0	1	1
NOR	1	0	0
XOR	0	1	0
XNOR	1	0	1

Phi3.5-V-4B + BigDocs

Logic Gates	(0,0)	(0,1)/(1,0)	(1,1)
AND	0	0	1
NAND	1	1	0
OR	0	1	1
NOR	1	0	0
XOR	0	1	0
XNOR	1	0	1

Gpt4o

Table 20: Test Example for the task of Table2Latex BigDocs failure. Phi3.5-V-4B+BigDocs was not able to format the question marks in the first row.

Component	Content																		
	<table border="1"> <thead> <tr> <th>Method</th> <th>RGDN [?]</th> <th>PURE-LET [?]</th> <th>DPIR [?]</th> <th>DWDN [?]</th> <th>PhD-Net (Ours)</th> </tr> </thead> <tbody> <tr> <td>PSNR</td> <td>19.80</td> <td>20.88</td> <td>22.09</td> <td>22.85</td> <td>23.48</td> </tr> <tr> <td>SSIM</td> <td>0.476</td> <td>0.501</td> <td>0.548</td> <td>0.561</td> <td>0.566</td> </tr> </tbody> </table>	Method	RGDN [?]	PURE-LET [?]	DPIR [?]	DWDN [?]	PhD-Net (Ours)	PSNR	19.80	20.88	22.09	22.85	23.48	SSIM	0.476	0.501	0.548	0.561	0.566
Method	RGDN [?]	PURE-LET [?]	DPIR [?]	DWDN [?]	PhD-Net (Ours)														
PSNR	19.80	20.88	22.09	22.85	23.48														
SSIM	0.476	0.501	0.548	0.561	0.566														

User Query

[Please create LaTeX code to produce this table.]

Method	RGDN	PURE-LET	DPIR	DWDN	PhD-Net (Ours)
PSNR	19.80	20.88	22.09	22.85	23.48
SSIM	0.476	0.501	0.548	0.561	0.566

Phi3.5-V-4B + BigDocs

2646
2647
2648
2649
2650
2651
2652
2653
2654
2655
2656
2657
2658
2659
2660
2661
2662
2663
2664
2665
2666
2667
2668
2669
2670
2671
2672
2673
2674
2675
2676
2677
2678
2679
2680
2681
2682
2683
2684
2685
2686
2687
2688
2689
2690
2691
2692
2693
2694
2695
2696
2697
2698
2699

Table 21: Qualitative test example 1 for the DeepForm task. When asked a question that cannot be answered from the image, Phi3.5-V-4B + BigDocs(OCR reduction) hallucinates a response while Phi3.5-V-4B + BigDocs correctly answers in the negative, demonstrating the role of OCR data in enhancing precise information extraction.

Component	Content												
	<small>NAB Form PB-17 Issues</small> AGREEMENT FORM FOR NON-CANDIDATE/ISSUE ADVERTISEMENTS												
	<table border="1" style="width: 100%;"> <tr> <td style="width: 70%;">Station and Location: WOTV</td> <td style="width: 30%;">Date: 8/15</td> </tr> </table>	Station and Location: WOTV	Date: 8/15										
Station and Location: WOTV	Date: 8/15												
	<p>I, The Hamburger Company do hereby request station time concerning the following issue:</p> <div style="border: 1px solid black; padding: 5px; width: fit-content; margin: 5px auto;">Michigan Democratic State Central Committee</div>												
	<table border="1" style="width: 100%; text-align: center;"> <thead> <tr> <th>Broadcast Length</th> <th>Time of Day, Rotation or Package</th> <th>Days</th> <th>Class</th> <th>Times per Week</th> <th>Number of Weeks</th> </tr> </thead> <tbody> <tr> <td>See Schedule</td> <td></td> <td>8/21-8/27</td> <td></td> <td></td> <td></td> </tr> </tbody> </table>	Broadcast Length	Time of Day, Rotation or Package	Days	Class	Times per Week	Number of Weeks	See Schedule		8/21-8/27			
Broadcast Length	Time of Day, Rotation or Package	Days	Class	Times per Week	Number of Weeks								
See Schedule		8/21-8/27											
	<p>Total Charges: 4,325</p>												
	<p>This broadcast time will be used by: Michigan Democratic State Central Committee</p>												
	<div style="border: 1px solid black; padding: 5px;"> <p>Does the programming (in whole or in part) communicate "a message relating to any political matter of national importance?"</p> <p style="text-align: center;"> <input type="checkbox"/> Yes <input checked="" type="checkbox"/> No </p> </div>												
	<small>Copyright © 2011 by the National Association of Broadcasters. May Not Be Copied, Reproduced, or Further Distributed. 3</small>												
Input Image													
User Query	What is the value for the contract_num?												
Ground Truth	None												
Phi3.5-V-4B + BigDocs	None												
Phi3.5-V-4B + BigDocs(OCR reduction)	12-15												

2700
2701
2702
2703
2704
2705
2706
2707
2708
2709
2710
2711
2712
2713
2714
2715
2716
2717
2718
2719
2720
2721
2722
2723
2724
2725
2726
2727
2728
2729
2730
2731
2732
2733
2734
2735
2736
2737
2738
2739
2740
2741
2742
2743
2744
2745
2746
2747
2748
2749
2750
2751
2752
2753

Table 22: Qualitative test example 2 for the DeepForm task. When asked a question that cannot be answered from the image, Phi3.5-V-4B + BigDocs(OCR reduction) hallucinates an unrelated response from a different section of the image while Phi3.5-V-4B + BigDocs correctly answers in the negative.

Component	Content		
	FEDERAL STATION ISSUE ADVERTISING REQUEST SHEET (To be filled out and kept on file for public inspection)		
	<table style="width: 100%; border: none;"> <tr> <td style="width: 50%; border: none;"> To: Tara Washburn Station: KGTV San Diego From: National Media Group Date: July 24, 2012 </td> <td style="width: 50%; border: none;"> This request was: <input checked="" type="checkbox"/> Accepted <input type="checkbox"/> Rejected </td> </tr> </table> <hr/> Agency: National Media Group Address: 545 Fifth Avenue, Suite 640 NY, NY 10017 Phone#: 212-424-0100 Fax#: 212-867-1116 Contact: Issue: Candidate Mentioned: Election Mentioned: Congressional Sponsor: National Republican Congressional Committee Address: 320 First St. SE Washington, DC # Phone: 202-479-7000 Executive Officer(s): Guy Harrison Title: Executive Director	To: Tara Washburn Station: KGTV San Diego From: National Media Group Date: July 24, 2012	This request was: <input checked="" type="checkbox"/> Accepted <input type="checkbox"/> Rejected
To: Tara Washburn Station: KGTV San Diego From: National Media Group Date: July 24, 2012	This request was: <input checked="" type="checkbox"/> Accepted <input type="checkbox"/> Rejected		
Input Image			
User Query	What is the value for the flight_from?		
Ground Truth	None		
Phi3.5-V-4B + BigDocs	None		
Phi3.5-V-4B + BigDocs(OCR reduction)	National Media Group		

Table 23: Qualitative test example 1 for the InfoVQA task. Phi3.5-V-4B + BigDocs is able to use the combination of the percentage and the pictorial representation of the relevant data and produce the correct count while Phi3.5-V-4B + BigDocs(caption reduction) gets confused with a different region of the image, demonstrating the robustness to text and image representations that captioning data brings.

Component	Content
	 <p>THIS ISN'T JUSTICE.</p> <p>There are 832% MORE women in prison now than in 1977</p> <p>Black women are incarcerated 3 TIMES MORE than white women</p> <p>1 IN 25 will give birth SHACKLED in prison.</p> <p>75% ARE DOMESTIC VIOLENCE SURVIVORS</p> <p>1 IN 10 will be sexually assaulted in prison</p> <p>82% are survivors of SEVERE CHILD ABUSE</p> <p>colorofchange.org @ultraviolet</p> <p>SHARE IF YOU THINK IT'S TIME TO STOP CRIMINALIZING WOMEN AND SURVIVORS.</p>
Input Image	
User Query	How many women out of every 4 women are domestic violence survivors?
Ground Truth	3
Phi3.5-V-4B + BigDocs	3
Phi3.5-V-4B + BigDocs(caption reduction)	1

2754
2755
2756
2757
2758
2759
2760
2761
2762
2763
2764
2765
2766
2767
2768
2769
2770
2771
2772
2773
2774
2775
2776
2777
2778
2779
2780
2781
2782
2783
2784
2785
2786
2787
2788
2789
2790
2791
2792
2793
2794
2795
2796
2797
2798
2799
2800
2801
2802
2803
2804
2805
2806
2807

Table 24: Qualitative test example 2 for the InfoVQA task. When tasked with extracting a percentage based on a textual and pictographic depiction of data, Phi3.5-V-4B + BigDocs(caption reduction) incorrectly picks a percentage value in the vicinity, while Phi3.5-V-4B + BigDocs correctly infers the answer.

Component	Content
	<p>The infographic is titled "THE AMERICAN IDENTITY ACCORDING TO SOCIAL MEDIA" and features a central dark blue box with the title in white. Surrounding this are various statistics and charts:</p> <ul style="list-style-type: none"> AMERICANS HAVE A LOT TO SAY: 48% of bloggers are US-based. AMERICANS LIKE TO GIVE ADVICE: 28% of U.S. adults say they give advice about purchases on social networking sites. AMERICANS ARE NOSTALGIC: The average Facebook user has 229 friends. AMERICANS ARE OBSESSED WITH ROYALTY: 60% of all social media related to the royal wedding has come from the U.S. in the past month (April). The U.S. has been responsible for just 20% of the U.K. AMERICANS WANT TO BE DISTRACTED FROM REALITY: The more than 63 million active users of Facebook spend an average of 18 minutes a day pretending to chat a fern. Over the course of a year, that's 6.475 minutes—the equivalent of a full-time job for over two weeks! AMERICANS LOVE VIDEO GAMES: Video games are the second most heavily used internet activity, accounting for 10% of all U.S. internet time. AMERICANS ARE CONNECTED: Six out of seven American homes have broadband internet access. AMERICANS ARE CONNECTED: 9 out of 10 Americans are online. AMERICANS ARE SOCIAL: Average friend requests per Facebook member. Especially in North Dakota and New Jersey. AMERICANS ARE INDUSTRIOUS: Just under 50% of LinkedIn's 130 million users are in the United States. AMERICANS LIKE BRANDS: Four out of five Americans on social media platforms (identified as frequent users) are following products, services and brands. AMERICANS ARE OBSESSED WITH CELEBRITIES: The five most followed Twitter accounts are Lady Gaga, Justin Bieber, Barack Obama, Katy Perry and Britney Spears. AMERICANS ARE HYPER-SOCIAL: Social media now reaches the majority of American 12+, with 82% having a profile on one or more social networks.
Input Image	
User Query	What percentage of Americans are online?
Ground Truth	90%
Phi3.5-V-4B + BigDocs	90%
Phi3.5-V-4B + BigDocs(caption reduction)	70%


2808
2809
2810
2811
2812
2813
2814
2815
2816
2817
2818
2819
2820
2821
2822
2823
2824
2825
2826
2827
2828
2829
2830
2831
2832
2833
2834
2835
2836
2837
2838
2839
2840
2841
2842
2843
2844
2845
2846
2847
2848
2849
2850
2851
2852
2853
2854
2855
2856
2857
2858
2859
2860
2861

Table 25: Qualitative test example 3 for the InfoVQA task. Phi3.5-V-4B + BigDocs is able to exploit structure in the image and compute the correct answer, while Phi3.5-V-4B + BigDocs(caption reduction) hallucinates an unrelated answer.

Component	Content
Input Image	
User Query	How long (in years) was the American Civil War?
Ground Truth	4
Phi3.5-V-4B + BigDocs	4
Phi3.5-V-4B + BigDocs(caption reduction)	10

2862
2863
2864
2865
2866
2867
2868
2869
2870
2871
2872
2873
2874
2875
2876
2877
2878
2879
2880
2881
2882
2883
2884
2885
2886
2887
2888
2889
2890
2891
2892
2893
2894
2895
2896
2897
2898
2899
2900
2901
2902
2903
2904
2905
2906
2907
2908
2909
2910
2911
2912
2913
2914
2915

Table 26: Qualitative test example for the InfoVQA task. Phi3.5-V-4B + BigDocs(no VQA format) does not adhere to the requested format and also provides a wrong answer in contrast to Phi3.5-V-4B + BigDocs which gets both the format and the answer correct. These errors highlight the importance of VQA formatting of the BigDocs dataset.

Component	Content
	 <p>LEARN THE FACTS ABOUT SEXUAL VIOLENCE</p> <ul style="list-style-type: none"> 1 IN 2 WOMEN have experienced sexual violence other than rape in their lifetime.* 1 IN 5 WOMEN have experienced completed or attempted rape in their lives.† 41% OF WOMEN reported experiencing physically aggressive street harassment.‡ 1 IN 3 WOMEN experience physical or sexual violence by an intimate partner.‡ Women have a 50% TO 95% chance of developing post-traumatic stress disorder after being raped.‡ 1 IN 6 BOYS are sexually abused before age 16.‡ 18% OF MEN reported experiencing verbal street harassment.‡ Only 26.2% OF MEN who experienced childhood sexual abuse disclosed it to the police.‡ Nearly 1 IN 67 men in the United States have experienced rape or attempted rape.‡ 1 IN 5 MEN have experienced sexual violence other than rape in their lifetime.* 67.5% OF INSTANCES OF RAPE ARE ESTIMATED TO GO UNREPORTED.§ FEWER THAN 5% of completed or attempted rapes against college women were reported to law enforcement.¶ Among college women, 9 OUT OF 10 victims of sexual assault know the person who sexually assaulted them.‡ <p>SEXUAL VIOLENCE THRIVES WHEN IT IS NOT TAKEN SERIOUSLY AND VICTIM BLAMING GOES UNCHECKED.</p> <p>USE YOUR VOICE TO PREVENT IT</p> <p>♥ BELIEVE SURVIVORS ♣ CHALLENGE VICTIM BLAMING Ⓒ RESPECT BOUNDARIES</p> <p>NSVRC WWW.NSVRC.ORG</p> <p><small>*Mills, L. M., C. Beale, K. C. Browning, M. J. Smith, S. G. Walters, M. L. Merrick, M. E. ... & ... (2018). National Intimate Partner and Sexual Violence Survey (NISVS) summary report. Retrieved from the Center for Disease Control and Prevention. https://www.cdc.gov/violenceprevention/nisvs/2018-report-main.html</small></p> <p><small>†Finkelhor, D., Browne, A., & Browne, A. (1985). The traumatic impact of child sexual abuse: A conceptualization. <i>Child Abuse and Neglect</i>, 9(1), 17-30.</small></p> <p><small>‡Finkelhor, D., Browne, A., & Browne, A. (1985). The traumatic impact of child sexual abuse: A conceptualization. <i>Child Abuse and Neglect</i>, 9(1), 17-30.</small></p> <p><small>§Finkelhor, D., Browne, A., & Browne, A. (1985). The traumatic impact of child sexual abuse: A conceptualization. <i>Child Abuse and Neglect</i>, 9(1), 17-30.</small></p> <p><small>¶Finkelhor, D., Browne, A., & Browne, A. (1985). The traumatic impact of child sexual abuse: A conceptualization. <i>Child Abuse and Neglect</i>, 9(1), 17-30.</small></p> <p><small>©2018 National Sexual Violence Research Center. All Rights Reserved.</small></p>
Input Image	
User Query	What percentage of women have experienced completed rape or attempted rape?
Ground Truth	20%
Phi3.5-V-4B + BigDocs	20%
Phi3.5-V-4B + BigDocs(no VQA format)	1 in 2 women have experienced sexual violence other than rape in their lifetime.

2916
2917
2918
2919
2920
2921
2922
2923
2924
2925
2926
2927
2928
2929
2930
2931
2932
2933
2934
2935
2936
2937
2938
2939
2940
2941
2942
2943
2944
2945
2946
2947
2948
2949
2950
2951
2952
2953
2954
2955
2956
2957
2958
2959
2960
2961
2962
2963
2964
2965
2966
2967
2968
2969

Table 27: Evaluation example from the Image2HTML task. The HTML code is rendered for easier comparison and analysis. The original Phi3.5-Vision performs poorly, while the BigDocs fine-tuned version generates highly accurate results. Although GPT-4 produces correct text, its structure differs significantly from the original image. These results demonstrate that fine-tuning on BigDocs leads to a massive improvement in performance on this task.

Component	Content
Original Image	<p>Are There Mountain Lions in PA?</p> <p>Although the PA Game Commission doesn't do, encourage, and rewards and offers an encouraging big cats in their sign in the rugged mountains of northwestern Pennsylvania. Here are some recent examples:</p> <p>Summer 2004 We report you should in July, June and July (and maybe set up a remote webcam monitoring camera along a deer trail on their 200 acre property near the Lehigh River in Lehigh Valley. They also plan to capture an image of a big cat near and far from the deer that they have been observing for some time. They get a continuous image but it will be a single image of a possible camera trap. The photo cannot give a view of the Lehigh County, which means it is not a true image of the county.</p> <p>Summer 2003 We report you should in July, June and July (and maybe set up a remote webcam monitoring camera along a deer trail on their 200 acre property near the Lehigh River in Lehigh Valley. They also plan to capture an image of a big cat near and far from the deer that they have been observing for some time. They get a continuous image but it will be a single image of a possible camera trap. The photo cannot give a view of the Lehigh County, which means it is not a true image of the county.</p> <p>Spring 2003 Back in the month of March for an hour to observe Deer residents outside Fort Allegany. Click here for the full story on this subject</p> <p>June 2000 Recent satellite imagery of the Basin of Conowingo (about 120 miles of Eastern) tracks tracks of the Big Cats in the quarter, the main measurements and makes clear that one can identify an mountain lion tracks, possibly an adult with a juvenile.</p> <p>Summer 1999 Observations within the 175 that near Fort Lehigh in Fort Lehigh County need a mountain lion walking up the trail towards them.</p> <p>1997 deer season In the month of March for an hour to observe Deer residents outside Fort Allegany. Click here for the full story on this subject</p> <p>1996 deer season In the month of March for an hour to observe Deer residents outside Fort Allegany. Click here for the full story on this subject</p>
Phi3.5-V-4B Output (Rendered)	<p>Are There Mountain Lions in PA?</p> <p>Although the PA Game Commission doesn't do, encourage, and rewards and offers an encouraging big cats in their sign in the rugged mountains of northwestern Pennsylvania. Here are some recent examples:</p> <p>Summer 2004 We report you should in July, June and July (and maybe set up a remote webcam monitoring camera along a deer trail on their 200 acre property near the Lehigh River in Lehigh Valley. They also plan to capture an image of a big cat near and far from the deer that they have been observing for some time. They get a continuous image but it will be a single image of a possible camera trap. The photo cannot give a view of the Lehigh County, which means it is not a true image of the county.</p> <p>Summer 2003 We report you should in July, June and July (and maybe set up a remote webcam monitoring camera along a deer trail on their 200 acre property near the Lehigh River in Lehigh Valley. They also plan to capture an image of a big cat near and far from the deer that they have been observing for some time. They get a continuous image but it will be a single image of a possible camera trap. The photo cannot give a view of the Lehigh County, which means it is not a true image of the county.</p> <p>Spring 2003 Back in the month of March for an hour to observe Deer residents outside Fort Allegany. Click here for the full story on this subject</p> <p>June 2000 Recent satellite imagery of the Basin of Conowingo (about 120 miles of Eastern) tracks tracks of the Big Cats in the quarter, the main measurements and makes clear that one can identify an mountain lion tracks, possibly an adult with a juvenile.</p> <p>Summer 1999 Observations within the 175 that near Fort Lehigh in Fort Lehigh County need a mountain lion walking up the trail towards them.</p> <p>1997 deer season In the month of March for an hour to observe Deer residents outside Fort Allegany. Click here for the full story on this subject</p> <p>1996 deer season In the month of March for an hour to observe Deer residents outside Fort Allegany. Click here for the full story on this subject</p>
Phi3.5-V-4B + BigDocs Output (Rendered)	<p>Are There Mountain Lions in PA?</p> <p>Although the PA Game Commission doesn't do, encourage, and rewards and offers an encouraging big cats in their sign in the rugged mountains of northwestern Pennsylvania. Here are some recent examples:</p> <p>Summer 2004 We report you should in July, June and July (and maybe set up a remote webcam monitoring camera along a deer trail on their 200 acre property near the Lehigh River in Lehigh Valley. They also plan to capture an image of a big cat near and far from the deer that they have been observing for some time. They get a continuous image but it will be a single image of a possible camera trap. The photo cannot give a view of the Lehigh County, which means it is not a true image of the county.</p> <p>Summer 2003 We report you should in July, June and July (and maybe set up a remote webcam monitoring camera along a deer trail on their 200 acre property near the Lehigh River in Lehigh Valley. They also plan to capture an image of a big cat near and far from the deer that they have been observing for some time. They get a continuous image but it will be a single image of a possible camera trap. The photo cannot give a view of the Lehigh County, which means it is not a true image of the county.</p> <p>Spring 2003 Back in the month of March for an hour to observe Deer residents outside Fort Allegany. Click here for the full story on this subject</p> <p>June 2000 Recent satellite imagery of the Basin of Conowingo (about 120 miles of Eastern) tracks tracks of the Big Cats in the quarter, the main measurements and makes clear that one can identify an mountain lion tracks, possibly an adult with a juvenile.</p> <p>Summer 1999 Observations within the 175 that near Fort Lehigh in Fort Lehigh County need a mountain lion walking up the trail towards them.</p> <p>1997 deer season In the month of March for an hour to observe Deer residents outside Fort Allegany. Click here for the full story on this subject</p> <p>1996 deer season In the month of March for an hour to observe Deer residents outside Fort Allegany. Click here for the full story on this subject</p>
GPT-4o Output (Rendered)	<p>Are There Mountain Lions in PA?</p> <p>Although the PA Game Commission doesn't do, encourage, and rewards and offers an encouraging big cats in their sign in the rugged mountains of northwestern Pennsylvania. Here are some recent examples:</p> <p>Summer 2004 We report you should in July, June and July (and maybe set up a remote webcam monitoring camera along a deer trail on their 200 acre property near the Lehigh River in Lehigh Valley. They also plan to capture an image of a big cat near and far from the deer that they have been observing for some time. They get a continuous image but it will be a single image of a possible camera trap. The photo cannot give a view of the Lehigh County, which means it is not a true image of the county.</p> <p>Summer 2003 We report you should in July, June and July (and maybe set up a remote webcam monitoring camera along a deer trail on their 200 acre property near the Lehigh River in Lehigh Valley. They also plan to capture an image of a big cat near and far from the deer that they have been observing for some time. They get a continuous image but it will be a single image of a possible camera trap. The photo cannot give a view of the Lehigh County, which means it is not a true image of the county.</p> <p>Spring 2003 Back in the month of March for an hour to observe Deer residents outside Fort Allegany. Click here for the full story on this subject</p> <p>June 2000 Recent satellite imagery of the Basin of Conowingo (about 120 miles of Eastern) tracks tracks of the Big Cats in the quarter, the main measurements and makes clear that one can identify an mountain lion tracks, possibly an adult with a juvenile.</p> <p>Summer 1999 Observations within the 175 that near Fort Lehigh in Fort Lehigh County need a mountain lion walking up the trail towards them.</p> <p>1997 deer season In the month of March for an hour to observe Deer residents outside Fort Allegany. Click here for the full story on this subject</p> <p>1996 deer season In the month of March for an hour to observe Deer residents outside Fort Allegany. Click here for the full story on this subject</p>

Table 28: Test Example for the task of GUI-VQA, showing BigDocs model failure. Phi3.5-V-4B+BigDocs was not able to give the correct output.

Component	Content
Input Image	
User Query	[If the user clicks [400, 770, 410, 780], what will they view?]
Ground Truth	Display the SAD.
Phi3.5-V-4B + BigDocs	Display the DRZAVA.

2970
2971
2972
2973
2974
2975
2976
2977
2978
2979
2980
2981
2982
2983
2984
2985
2986
2987
2988
2989
2990
2991
2992
2993
2994
2995
2996
2997
2998
2999
3000
3001
3002
3003
3004
3005
3006
3007
3008
3009
3010
3011
3012
3013
3014
3015
3016
3017
3018
3019
3020
3021
3022
3023

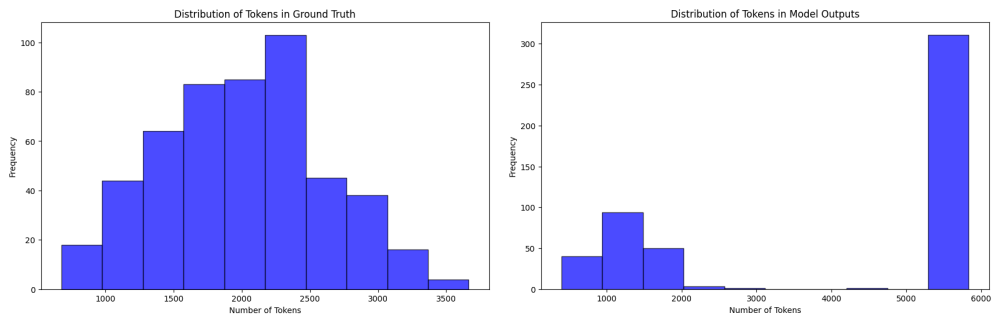


Figure 18: Comparison of token length histograms on the test set of Screenshot2HTML task, and the generated outputs of our model (Phi3.5-Vision+BigDocs)

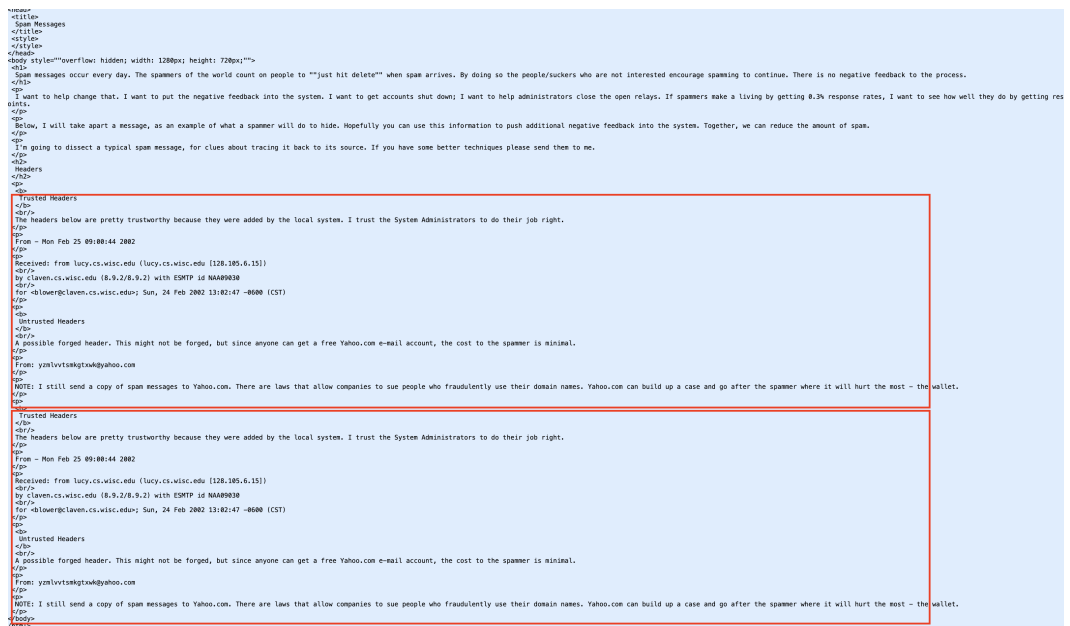


Figure 19: Failure case on the task of Screenshot2HTML. Output is generated by the Phi3.5-Vision + BigDocs model.

Context Length	HTML Score	HTML Score
	Greedy	Length penalty = -1
512	10.99	13.96
1,024	11.49	15.80
2,048	9.81	14.71
4,096	8.83	13.88
8,192	8.38	13.60
16,384	8.24	13.43

Table 29: HTML Scores for Phi3.5-Vision+BigDocs with varying context lengths. HTML Score defined as DOM Tree Edit Distance.

```
3024 <!DOCTYPE html PUBLIC "-//W3C//DTD XHTML 1.0 Transitional//EN" "http://www.w3.org/TR/xhtml1/DTD/xhtml1-transitional.dtd">
3025 <html style="overflow: hidden; width: 1280px; height: 720px;" xmlns="http://www.w3.org/1999/xhtml">
3026 <head>
3027 <meta content="text/html; charset=utf-8" http-equiv="Content-Type"/>
3028 <title>
3029 Washington state's Secretary of Health Mary Selecty: fraudulent, misquoted, or uninformed?
3030 </title>
3031 </style>
3032 </head>
3033 <body style="overflow: hidden; width: 1280px; height: 720px;">
3034 <h1>
3035 [back]
3036 </h1>
3037 <h1>
3038 Mercury and vaccines
3039 </h1>
3040 <h1>
3041 Washington state's Secretary of Health Mary Selecty: fraudulent, misquoted, or uninformed?
3042 </h1>
3043 <p>
3044 by Teresa Binstock
3045 </p>
3046 Sep 30, 2009
3047 </p>
3048 <p>
3049 Once again, a highly placed public figure has presented a misleading or inaccurate statement wherein thimerosal is erroneously described as harmless.
3050 </p>
3051 <p>
3052 In an article about thimerosal in swine flu shots, reporter Sandi Doughtton's summarized Washington Health Department's Secretary of Health Mary Selecty as having said, ""The p
3053 </p>
3054 Is Mary Selecty playing word games that differentiate between health problems and, in contrast, thimerosal-induced developmental delays? Is she not aware of peer-reviewed findi
3055 </p>
3056 <p>
3057 Conclusions in several studies prompt concern (a) for Sandi Daughton's reporting of what Mary Selecty said, or (b) for Mary Selecty said.
3058 </p>
3059 <p>
3060 Consider several studies. Male infants who received thimerosal-containing hepatitis-B vaccinations were nine times as likely to be receiving special education services (2) and w
3061 </p>
3062 primates injected with thimerosal-containing hepatitis B vaccines manifested developmental delays (4). A synopsis of the new study and delineation of other findings about thimerosa
3063 </p>
3064 Questions: Was Mary Selecty misquoted? If not, and if she is aware of thimerosal's adverse effects and was accurately quoted as saying ""no health effects"", ought she be remov
3065 </p>
3066 reported by Sandi Doughtton was rooted in Ms. Selecty's ignorance and a correction ought to be issued by Mary Selecty and the Health Department.
3067 </p>
3068 <p>
3069 Given various ""experts"" false assurances (eg, 6) about thimerosal's safety (when findings suggest quite the opposite) relevant questions include, Who profits from increased nu
3070 </p>
3071 </p>
3072 References:
3073 </p>
3074 <p>
3075 1. State lifts limit on mercury preservative in swine-flu shots
3076 <a href="http://www.seattletimes.com/cgi-bin/article.cgi?
3077 <!--[if IE]...</p>
```

Figure 20: Failure case on the task of Screenshot2HTML. Output is generated by the Phi3.5-Vision + BigDocs model.

```
3024 <!DOCTYPE html PUBLIC "-//W3C//DTD XHTML 1.0 Transitional//EN" "http://www.w3.org/TR/xhtml1/DTD/xhtml1-transitional.dtd">
3025 <html style="overflow: hidden; width: 1280px; height: 720px;" xmlns="http://www.w3.org/1999/xhtml">
3026 <head>
3027 <meta content="text/html; charset=utf-8" http-equiv="Content-Type"/>
3028 <title>
3029 Washington state's Secretary of Health Mary Selecty: fraudulent, misquoted, or uninformed?
3030 </title>
3031 </style>
3032 </head>
3033 <body style="overflow: hidden; width: 1280px; height: 720px;">
3034 <h1>
3035 [back]
3036 </h1>
3037 <h1>
3038 Mercury and vaccines
3039 </h1>
3040 <h1>
3041 Washington state's Secretary of Health Mary Selecty: fraudulent, misquoted, or uninformed?
3042 </h1>
3043 <p>
3044 by Teresa Binstock
3045 </p>
3046 Sep 30, 2009
3047 </p>
3048 <p>
3049 Once again, a highly placed public figure has presented a misleading or inaccurate statement wherein thimerosal is erroneously described as harmless.
3050 </p>
3051 <p>
3052 In an article about thimerosal in swine flu shots, reporter Sandi Doughtton's summarized Washington Health Department's Secretary of Health Mary Selecty as having said, ""The p
3053 </p>
3054 Is Mary Selecty playing word games that differentiate between health problems and, in contrast, thimerosal-induced developmental delays? Is she not aware of peer-reviewed findi
3055 </p>
3056 <p>
3057 Conclusions in several studies prompt concern (a) for Sandi Daughton's reporting of what Mary Selecty said, or (b) for Mary Selecty said.
3058 </p>
3059 <p>
3060 Consider several studies. Male infants who received thimerosal-containing hepatitis-B vaccinations were nine times as likely to be receiving special education services (2) and w
3061 </p>
3062 primates injected with thimerosal-containing hepatitis B vaccines manifested developmental delays (4). A synopsis of the new study and delineation of other findings about thimerosa
3063 </p>
3064 Questions: Was Mary Selecty misquoted? If not, and if she is aware of thimerosal's adverse effects and was accurately quoted as saying ""no health effects"", ought she be remov
3065 </p>
3066 reported by Sandi Doughtton was rooted in Ms. Selecty's ignorance and a correction ought to be issued by Mary Selecty and the Health Department.
3067 </p>
3068 <p>
3069 Given various ""experts"" false assurances (eg, 6) about thimerosal's safety (when findings suggest quite the opposite) relevant questions include, Who profits from increased nu
3070 </p>
3071 </p>
3072 References:
3073 </p>
3074 <p>
3075 1. State lifts limit on mercury preservative in swine-flu shots
3076 <a href="http://www.seattletimes.com/cgi-bin/article.cgi?
3077 <!--[if IE]...</p>
```

Figure 21: Failure case on the task of Screenshot2HTML. Output is generated by the Phi3.5-Vision + BigDocs model.

3078
3079
3080
3081
3082
3083
3084
3085
3086
3087
3088
3089
3090
3091
3092
3093
3094
3095
3096
3097
3098
3099
3100
3101
3102
3103
3104
3105
3106
3107
3108
3109
3110
3111
3112
3113
3114
3115
3116
3117
3118
3119
3120
3121
3122
3123
3124
3125
3126
3127
3128
3129
3130
3131

```
<html style="overflow: hidden; width: 1280px; height: 728px;">
<head>
<title>
Tennessee Highway 380
</title>
<style>
</style>
</head>
<body style="overflow: hidden; width: 1280px; height: 728px;">
<h1>
Tennessee Highway 380
</h1>
<p>
State Primary Route 380 is Tennessee's shortest freeway (and probably the state's shortest highway). Today, it connects I-40 in northwest Memphis with U.S. 51. There are no signs for TN 380; however, the route number is marked or
</p>
<h2>
Original Plans and a Third Bridge
</h2>
<p>
The original purpose of TN 380 was as the beginning of a riverfront freeway across Mud Island, to connect to I-40 and Riverside Drive at the Hernando Bridge (the "New Bridge").
</p>
<p>
Another plan was to connect the north loop of then-I-240 to a third bridge over the Mississippi River from Memphis into Arkansas. The Memphis-Arkansas Bridge (the "Old Bridge"), which serves I-55) is a four-lane bridge that pre
directly feed an I-40 route through central Memphis. Neither bridge was originally designed to be resistant to earthquakes, although the Hernando de Soto Bridge is currently being retrofitted to improve the situation due to concerns
</p>
<p>
Thus, the plan was to build a new bridge north of downtown. Most truck traffic would then be diverted over to the new bridge. When then-I-240's north was built, the current TN 380 was built as the first step in that route.
</p>
<p>
It is likely that the third bridge proposal was abandoned due to lack of funding. A new "third bridge" proposal has surfaced in 2001, but this proposal diverts I-55 over a bridge via Presidents Island or build a bridge near the
</p>
<p>
So, for now, TN 380 doesn't do very much. However, there are several unrelated projects that could make use of the route.
</p>
<h2>
North Second Street
</h2>
<p>
One plan being considered is the proposed "North Second Street" extension. Between Auction Street and the Wolf River, it would be a six-lane surface part of which would continue the one-way couplet of Second and Third streets,
interchange with I-40 in the downtown area.
</p>
<p>
The main purpose of this route is to get traffic heading for downtown to Memphis' central transit station at the north end of Main Street. It would also divert downtown-bound traffic away from the congested I-40/240 interchange c
</p>
<p>
There is no construction timetable for the route at present. The extension would probably be signed as TN 380, although TDOT might opt to not sign it as such.
</p>
</body>
</html>
```

Figure 22: Success case on the task of Screenshot2HTML. Output is generated by the Phi3.5-Vision + BigDocs model.